

Copyright  
by  
Xiaoxia Chen  
2004

**The Dissertation Committee for Xiaoxia Chen Certifies that this is the approved  
version of the following dissertation:**

**Nanoparticle Engineering Processes: Evaporative Precipitation into  
Aqueous Solution (EPAS) and Antisolvent Precipitation to Enhance the  
Dissolution Rates of Poorly Water Soluble Drugs**

**Committee:**

---

Johnston, Keith P., Supervisor

---

Williams III, Robert O., Co-Supervisor

---

Bonnecaze, Roger T.

---

Lloyd, Douglas R.

---

McGinity, James W.

**Nanoparticle Engineering Processes: Evaporative Precipitation into  
Aqueous Solution (EPAS) and Antisolvent Precipitation to Enhance the  
Dissolution Rates of Poorly Water Soluble Drugs**

**by**

**Xiaoxia Chen, B.S., M.S.**

**Dissertation**

Presented to the Faculty of the Graduate School of

The University of Texas at Austin

in Partial Fulfillment

of the Requirements

for the Degree of

**Doctor of Philosophy**

**The University of Texas at Austin**

**August, 2004**

## **Dedication**

To my dedicated Husband, Yu Ren

To my Father and Mother, Mr. Zhiyi Chen and Mrs. Jinfang Gao

## **Acknowledgements**

First, I would like to thank my advisor, Dr. Keith P. Johnston who guides me along the way, providing the intellectual and professional direction for this work and my development. I would also like to thank my co-advisor, Dr. Robert O. Williams, for his invaluable assistance and guidance throughout this effort. I would also like to thank Dr. Roger T. Bonnecaze, Dr. Douglas R. Lloyd, and Dr. James W. McGinity for their contributions as members of my dissertation committee.

I would like to thank the members of Dr. Keith P. Johnston's group, especially Timothy Young, Marazben Sarkari, Won Ryoo, Parag Shah, Jasper Dickson, Griffin Smith, Michal Matteucci, Dale Simpson and Todd Crispy. Your friendship and companionship was greatly appreciated. I would also like to thank members of other groups who provided support, contributions, and collaborations during my graduate studies: Jiahui Hu, Zhongshui Yu, True Rogers, Jason Vaughn, Kirk Overhoff, Prapasri Sinswart, Weijia Zheng and Chris Young. I would also like to thank Connie Lo and Zineb Benhayoune, who worked as undergraduates for me throughout my studies.

I would like to acknowledge support from The Dow Chemical Company and the National Science Foundation.

Finally, many thanks to my family: my husband Yu Ren, my parents, my sister and two brothers. Without your love and support, this would never have been possible.

# **Nanoparticle Engineering Processes: Evaporative Precipitation into Aqueous Solution (EPAS) and Antisolvent Precipitation to Enhance the Dissolution Rates of Poorly Water Soluble Drugs**

Publication No. \_\_\_\_\_

Xiaoxia Chen, Ph.D.

The University of Texas at Austin, 2004

Supervisors: Keith P. Johnston and Robert O. Williams

It is estimated that more than 1/3 of the compounds being developed by the pharmaceutical industry are poorly water soluble. The bioavailability of these drugs is limited by their low dissolution rates. Two nanoparticle engineering processes, evaporative precipitation into aqueous solution (EPAS) and antisolvent precipitation were developed to enhance the dissolution rate of poorly water soluble drugs.

EPAS is a process by which a drug solution in a water immiscible organic solvent is sprayed through an atomizer into an aqueous solution containing hydrophilic stabilizer (s) at high temperature. The rapid evaporation of the small organic droplets results in fast nucleation leading to submicron to micron particles suspensions. The adsorption of water soluble stabilizers on the drug particle surfaces facilitates the dissolution rates of the final powder after drying. The suspensions may be used in parenteral formulations to enhance bioavailability or may be dried to produce oral dosage forms with high dissolution rates due to small particle size and hydrophilic stabilizer that enhances wetting. The influence

of EPAS process parameters on the physicochemical properties of poorly water soluble drugs was determined. The influence of the dissociation of drug molecules on the stability of nanosuspensions at high suspension concentration, as high as 30 mg/ml with a drug-to-surfactant ratio of 3:1, was investigated. High-potency ( $\geq 90\%$ ) drug particles with high dissolution rates were produced by removing the non-adsorbed surfactant.

Antisolvent precipitation is a technique where a drug solution in a water miscible organic solvent is mixed with an aqueous solution containing a surfactant(s). Upon mixing, the supersaturated solution leads to nucleation and growth of drug particles, which may be stabilized by surfactants. Temperature was shown to have a large effect on the particle size distribution in the suspension. Crystalline drug particles with particle size of 300 nm were successfully recovered from the nanosuspensions by salt flocculation followed by filtration and vacuum drying with a drug yield higher than 92%. Upon redispersion, the average particle size was comparable to the value in the original aqueous suspension. The dissolution rate was correlated with the particle size after redispersion.

## Table of Contents

List of Tables .....	xiii
List of Figures .....	xv
Chapter 1 Introduction .....	1
1.1 The Bioavailability of Drugs .....	1
1.2 Micronization Processes to Enhance the Dissolution Rate of Poorly Water Soluble Drugs.....	3
1.2.1 Evaporative Precipitation into Aqueous Solution (EPAS) .....	6
1.2.2 Antisolvent Precipitation .....	11
1.2.3 Comparison between Micronization Processes .....	13
1.3 Objectives .....	14
1.4 References.....	17
Chapter 2 Preparation of Cyclosporine A Nanoparticles by Evaporative Precipitation into Aqueous Solution .....	21
2.1 Introduction.....	21
2.2 Experimental .....	23
2.2.1 Materials .....	23
2.2.2 High Performance Liquid Chromatography (HPLC) and Gas Chromatography (GC) .....	23
2.2.3 Calculation of Vapor-Liquid-Liquid Equilibrium for the Organic Solvent-Water System .....	24
2.2.4 Particle Size and Particle Size Distribution .....	24
2.2.5 Particle Crystallinity .....	24
2.2.6 Preparation of Phosphatidylcholine Vesicles.....	25
2.2.7 Evaporative Precipitation into Aqueous Solution (EPAS) .....	25
2.3 Results and Discussion .....	29
2.3.1 Particle Size with Phosphatidylcholine in the Aqueous Solution... ..	29
2.3.2 Effect of Solvents on Particle Size.....	31



2.3.3 Effect of Surfactant Type and Feeding Drug Concentration on Particle Size .....	33
2.3.4 Effect of Surfactant Concentration in the Aqueous Solution.....	34
2.3.5 Effect of Temperature on Particle Size.....	35
2.3.6 Effect of Drug Loading on Particle Size.....	37
2.3.7 Residual Solvent Concentration.....	38
2.3.8 X-ray Study.....	39
2.4 Conclusions.....	42
2.5 Reference .....	43
Chapter 3 Ketoprofen Nanoparticle Gels Formed by Evaporative Precipitation into Aqueous Solution (EPAS) .....	45
3.1 Introduction .....	45
3.2 Experimental .....	46
3.2.1 Materials .....	46
3.2.2 Determination of Ketoprofen Solubility in Pluronic F127 Micelles .....	47
3.2.3 Evaporative Precipitation into Aqueous Solution (EPAS) .....	47
3.2.4 Particle Size and Particle Size Distribution .....	47
3.2.5 Crystallinity and Surface Area Measurement.....	48
3.2.6 Dissolution Test .....	48
3.3 Results and Discussion .....	48
3.3.1 Ketoprofen Solubility in Pluronic F127 Aqueous Solutions .....	48
3.3.2 Appearance of Ketoprofen Dispersions in the Aqueous Suspensions Formed by EPAS.....	49
3.3.3 Effect of Surfactant Type and Temperature on Particle Size of Ketoprofen .....	53
3.3.4 Effect of Drug Feed Concentration and Concentration of the Ketoprofen Aqueous Suspension on the Particle Size.....	56
3.3.5 Effect of Surfactant Concentration, pH and Ionic Strength on Ketoprofen Particle Size .....	58
3.3.6 Ketoprofen-Pluronic F127 Gel Formation at High Pluronic Concentration in Aqueous Solution.....	61
3.3.7 The Crystallinity, Surface Area and Dissolution Rate of Dried Ketoprofen-Pluronic F127 Gel and Suspension .....	66



5.2.2 Antisolvent Precipitation .....	107
5.2.3 Recovery of Naproxen Nanoparticles by Salt Flocculation Followed by Filtration and Vacuum Drying` .....	109
5.2.4 Particle Size .....	110
5.2.5 Measurement of Residual Salt Concentration in Flocculated Samples by Conductivity .....	110
5.2.6 Morphology of the Floccs in the Suspension and after Drying .....	111
5.2.7 Dissolution Test .....	111
5.3 Results and Discussion .....	112
5.3.1 Effect of Temperature on Drug Particle Size in Antisolvent Precipitation .....	112
5.3.2 Compositions of the Formulations .....	114
5.3.3 Particle Size of Naproxen in Aqueous Suspensions .....	115
5.3.4 Polymer-Salt Cloud Point Concentrations and Flocculation of Naproxen Nanoparticles with Various Salts .....	119
5.3.5 Dissolution Test .....	121
5.3.6 Particle Redispersibility into Water after Flocculation Followed by Filtration and Vacuum Drying .....	126
5.3.7 Reproducibility of Salt Flocculation Process on Precipitate Weight, Drug Potency, Salt Concentration, Surfactant Concentration, Drug and Surfactant Yield .....	128
5.3.8 Morphology of Flocculated Naproxen Nanoparticles by Optical Microscope and SEM .....	132
5.3.9 X-ray Diffraction .....	132
5.4 Conclusions .....	135
5.5 References .....	137
Chapter 6 Conclusions and Recommendations for Further Study .....	140
6.1 Conclusions .....	140
6.1.1 Preparation of Cyclosporine A Nanoparticles by Evaporation Precipitation into Aqueous Solution (EPAS) .....	140
6.1.2 Ketoprofen Nanoparticle Gels Formed by Evaporative Precipitation into Aqueous Solution (EPAS) .....	141
6.1.3 Rapid Dissolution of High Potency Danazol Particles Produced by Evaporative Precipitation into Aqueous Solution .....	142

6.1.4 Flocculation of Suspensions Formed by Antisolvent Precipitation to Produce Redispersible Naproxen Nanocrystals .....	143
6.2 Recommendations.....	144
6.3 References.....	145
Appendix Rapid Dissolution of High Potency Itraconazole Particles Produced by Evaporative Precipitation into Aqueous Solution.....	146
A.1 Introduction.....	146
A.2 Experimental .....	149
A.2.1 Materials.....	149
A.2.2 Evaporative Precipitation into Aqueous Solution (EPAS) .....	149
A.2.3 High Potency Itraconazole Powder by Centrifugation .....	151
A.2.4 Crystallinity and Surface Area Measurement .....	152
A.2.5 Dissolution Test .....	152
A.2.6 Particle Size.....	152
A.3 Results and Discussion.....	153
A.3.1 Micrometering Valve Nozzle: Particle Size and Dissolution Rate ... .....	153
A.3.2 Conical Nozzle.....	157
A.3.2.1 Dissolution Test .....	157
A.3.2.2 Particle Size and Surface Area.....	158
A.3.2.3 Crystallinity.....	161
A.4 Conclusions.....	162
A.5 References.....	164
Bibliography .....	165
Vita .....	173

## List of Tables

Table 2.1	The chemical structure of drug and surfactants .....	27
Table 2.2	EPAS results for 10% w/v phosphatidylcholine in the aqueous solution.....	29
Table 2.3	Solvent effect on the particle size for 1% w/v Pluronic F127 in the aqueous phase for a drug/surfactant ratio: 0.93-1.07 .....	32
Table 2.4	Effect of surfactant type on particle size for a drug/surfactant ratio: 0.3-0.5 .....	34
Table 2.5	Effect of surfactant concentration on the particle size for a drug/surfactant ratio: 0.3-0.4.....	35
Table 2.6	Temperature effect on the particle size for a drug/surfactant ratio: 0.3-0.4.....	36
Table 2.7	Effect of drug/surfactant (drug loading) on particle size for 1% Tween 80 in the aqueous solution.....	37
Table 2.8	Concentration of residual dichloromethane in the aqueous suspension for a flow rate of 1 ml/min .....	39
Table 3.1	Effect of surfactant type and temperature on ketoprofen particle size .....	55
Table 3.2	Effect of feed drug concentration and suspension concentration on ketoprofen particle size at 80°C .....	57
Table 3.3	Effect of aqueous surfactant concentration and pH on ketoprofen particle size at 80°C .....	60
Table 3.4	Gel formation with 5% w/v Pluronic F127 in aqueous solution.....	65

Table 4.1	Adsorption ( $W_{\text{surf,ads}}/W_{\text{drug,ppt}}$ ) of surfactant onto danazol in EPAS suspension at 75°C .....	84
Table 4.2	Pluronic F127 adsorption on danazol particles after 3 days storage.....	85
Table 4.3	Characterization of high potency danazol powder produced by EPAS and centrifugation .....	87
Table 4.4	Particle size of danazol produced in an EPAS suspension at a concentration of 5 mg/ml with a surfactant concentration of 1% w/v and a drug-to-surfactant ratio of 1:2 .....	92
Table 5.1	System investigated .....	115
Table 5.2	Particle size of naproxen suspensions produced by antisolvent precipitation vs. time for system A without any added salt .....	117
Table 5.3	Particle size of naproxen in the original suspension before and after sonication, and after flocculation, filtration, vacuum drying and redispersion into pure water .....	118
Table 5.4	Properties of the precipitate after vacuum drying including selectivity for drug vs. surfactant.....	131
Table A.1	Mean particle size $D(v, 0.5)$ of itraconazole particles in the EPAS suspension for various organic phase flow rates with the micrometering valve nozzle .....	155
Table A.2	Mean particle size $D(v, 0.5)$ , and particle size distribution of itraconazole in EPAS suspension formed with the conical nozzle; and surface area and potency of itraconazole in dried EPAS powder ...	159

## List of Figures

Figure 1.1:	Apparatus of EPAS .....	9
Figure 1.2	Mechanism of EPAS particle formation and stabilization.....	10
Figure 1.3	Mechanism of antisolvent precipitation.....	12
Figure 2.1	Apparatus for EPAS.....	28
Figure 2.2	Spray of pure dichloromethane into aqueous solution at 80°C in the EPAS process for a flow rate of 1 ml/min .....	28
Figure 2.3	.....	40-41
(a)	The X-ray diffraction pattern of cyclosporine A+ PVP 40, 000 powder (drug/surfactant ratio= 0.4) .....	40
(b):	The X-ray diffraction pattern of cyclosporine A+ Myrj 52 powder (drug/surfactant ratio= 0.4) .....	41
Figure 3.1	Liquid ketoprofen dispersed in aqueous solution .....	52
(a):	In pH 1.5 KCl/HCl buffer solution .....	52
(b):	In pure water .....	52
Figure 3.2	Thermo reversible gel of ketoprofen-Pluronic F127 formed at room temperature .....	64
Figure 3.3	X-ray diffraction profiles of dried ketoprofen gels and suspensions by lyophilization or vacuum drying.....	68
Figure 3.4	Dissolution profiles of dried ketoprofen gels and suspensions by lyophilization or vacuum drying.....	69
Figure 4.1	The apparatus of EPAS.....	76
Figure 4.2	.....	90-91

(a):	Danazol systems with high dissolution rate.....	90
(b):	Danazol systems with low dissolution rate.....	91
Figure 4.3	X-ray diffraction profiles of danazol systems.....	98
Figure 4.4	ESEM picture of danazol precipitate stabilized with PVP K-15 after centrifugation and drying under 40°C and –30 in. Hg.....	98
Figure 4.5	Dissolution profile of system danazol +PVP 40T+SLS during 2-week thermal cycling stress test .....	100
Figure 5.1	Process for producing pharmaceutical powder by antisolvent precipitating, flocculation with salt, filtration and vacuum drying.	108
Figure 5.2	Temperature effect on particle size of naproxen suspensions produced by antisolvent precipitation. ....	113
Figure 5.3	Cloud point temperature of PVP and Pluronic F127 at various sodium sulfate concentrations in water.....	122
Figure 5.4	.....	123-125
(a):	Effect of salt concentration on dissolution rate of flocculated, filtered and vacuum dried naproxen nanoparticles produced by antisolvent precipitation (system B).....	123
(b):	Effect of stabilizers on dissolution rate of flocculated, filtered and vacuum dried naproxen nanoparticles produced by antisolvent precipitation. ....	124
(c):	Correlation between dissolution rate and specific surface area of flocculated, filtered and vacuum dried naproxen particles ( $R^2= 0.97$ ).....	125
Figure 5.5	.....	133
(a):	Microscopic pictures of naproxen flocs of system B in suspension	



	at salt concentration of 1.01M .....	133
(b):	SEM pictures of naproxen flocs after filtration and vacuum drying .....	133
Figure 5.6	X-ray diffraction of flocculated, filtered and vacuum dried naproxen particles produced by antisolvent precipitation. ....	134
Figure A.1	Apparatus for evaporative precipitation into aqueous solution (EPAS) .....	150
Figure A.2	Dissolution rates for dried EPAS itraconazole particles produced with the micrometering valve at various organic flow rates and aqueous surfactant concentration of 1% w/v .....	156
Figure A.3	Dissolution rates for dried EPAS itraconazole particles produced with conical nozzle for various aqueous surfactants at a concentration of 1 % w/v and organic flow rate of 1 ml/min .....	158
Figure A.4	X-ray diffraction pattern and $\alpha$ peak height, h, at $2\theta = 20.5^\circ$ of dried EAPS itraconazole powders produced with the conical nozzle .....	162

# CHAPTER 1

## Introduction

### 1.1 THE BIOAVAILABILITY OF DRUGS

It is estimated that more than 1/3 of compounds being developed by the pharmaceutical industry are poorly water soluble.<sup>1, 2</sup> The oral bioavailability of these poorly water soluble compounds is limited by their inadequate dissolution rate. Increasing the dissolution rate of poorly water soluble drugs has become a major challenge in pharmaceutical formulation development.

Drug dissolution is a prerequisite to drug absorption and clinical response for almost all drugs given orally. The drug flux ( $\text{mass} \cdot (\text{area} \cdot \text{time})^{-1}$ ) through the intestinal wall at any position and time can be expressed by Fick's First Law as<sup>3</sup>

$$J_w(x, y, z, t) = P_w(x, y, z, t) \cdot C_w(x, y, z, t) \quad (\text{Eq. 1.1})$$

where  $P_w(x, y, z, t)$  is the permeability of this membrane and  $C_w(x, y, z, t)$  is the drug concentration at the membrane (intestinal) surface. It is assumed that sink condition (drug concentration equals zero) exist for the drug inside this membrane and  $P_w$  is an effective permeability. The plasma may be assumed to be the physiological sink since concentration in the plasma is generally more than several orders of magnitude below that in the intestinal lumen in human.<sup>4</sup> The drug absorption rate assuming no luminal reactions, at any time is:

$$\text{Absorption rate} = dm/dt = \iint_A P_w C_w dA \quad (\text{Eq. 1.2})$$

where A is over the entire gastrointestinal surface. The total mass, M, of drug absorbed at time t is:

$$M(t) = \int_0^t \iint_A P_w C_w dA dt \quad (\text{Eq. 1.3})$$

The maximal absorption rate occurs when the drug concentration is at its solubility,  $C_s$ ,

$$J^{\max} = P_w C_{w,s} \quad (\text{Eq. 1.4})$$

$$\text{and } M^{\max}(t) = \int_0^t \iint_A P_w C_w dA dt \quad (\text{Eq. 1.5})$$

where  $C_w = C_s, C \geq C_s$  for permeability limited absorption;  $C_w = C, C \leq C_s$  for solubility limited absorption. For high solubility drugs that are dosed in solution or in dosage forms that dissolve very rapidly, a good correlation between drug absorption and intestinal membrane permeability is often obtained.<sup>5-7</sup> A drug with a permeability greater than  $2-4 \times 10^{-4}$  cm/sec or about 1 cm/hr would be well absorbed with the expected fraction absorbed being greater than 95%.<sup>8</sup>

Amidon et al.<sup>8</sup> divided drugs into four classes on the basis of their aqueous solubility and their ability to permeate the mucosa in the gut from the apical to the basolateral side. Class I drugs are defined as those with high permeability which are able to dissolve readily in aqueous media over the pH range 1 to 8. The drug is well absorbed (though its systemic availability may be low due to first pass extraction/metabolism) and the rate limiting step to drug absorption is drug dissolution or gastric emptying if dissolution is very rapid. Class II drugs are defined as those with high permeability but whose solubility in aqueous media is insufficient for the whole dose to be dissolved in the gastrointestinal (GI) contents under usual conditions. For these substances, dissolution is the rate limiting step to absorption. Class III drug are defined as those with high solubility but low permeability which is the rate limiting step in drug absorption. Class IV drugs are defined as those with low solubility and low permeability. Class II-IV drugs present significant problems for effective oral delivery. In this dissertation, two

nanoparticles engineering processes, evaporative precipitation in aqueous solution (EPAS) and antisolvent precipitation (AP) were applied to increase the dissolution rates of class II drugs which have low solubility in water but high permeability into intestinal membranes.

The dissolution rate of a drug into an aqueous solution is described by Noyes-Whitney equation,

$$\frac{dm}{dt} = \frac{DS}{h}(C_s - C) \quad (\text{Eq. 1.6})$$

The dissolution rate depends upon the diffusion coefficient of drug molecules in dissolution media,  $D$ ; the specific surface area of drug particles,  $S$ ; the local equilibrium concentration of the drug in the diffusion layer surrounding the particle,  $C_s$ ; the diffusion layer thickness,  $h$ ; and the concentration of the drug in dissolution media at time  $t$ ,  $C$ . In sink conditions, the dissolution rate may be increased by increasing surface area  $S$  and drug solubility in dissolution media  $C_s$ . The surface area  $S$  may be increased by reducing the particle size to sub-micro range,<sup>9</sup> by increasing the porosity and by enhancing wetting of the particles by the dissolution media. Wetting may be enhanced with hydrophilic excipients that are surface active at the API-aqueous interface.<sup>10</sup> The solubility of drugs,  $C_s$ , may be enhanced by trapping the API in metastable crystalline or amorphous states with higher free energies than the lowest energy equilibrium crystalline state.

## **1.2 MICRONIZATION PROCESSES TO ENHANCE THE DISSOLUTION RATE OF POOLY WATER SOLUBLE DRUGS**

The preparation of small drug particles is very challenging in pharmaceutical technologies since the formation of nanocrystalline organic particles is highly complex. Several techniques have been applied to convert generally coarse crystalline synthesis products into ultra fine particles. In general two strategies are utilized for this purpose:<sup>11</sup>

1) the mechanical milling of the raw material by wet or dry milling processes; 2)

precipitation of pharmaceuticals from solution. In the second case the undesirable solvent must nearly always be removed. Milling processes are subject to limitations in the production of nanodispersed systems with narrow size distribution.<sup>12</sup> With decreasing particle size it becomes increasingly more difficult to use the applied mechanical energy in the form of shearing and cavitation forces<sup>13</sup> for particle milling without simultaneously inducing particle agglomeration. Moreover, milling can be limited by unfavorable yields due to solid losses, high polydispersity in particle size, shear-induced particle denaturation, long processing time, high energy requirements and the need for separating the product and processing agent.<sup>12, 14-16</sup> In spite of these disadvantages milling processes do find widespread use in the formation of poorly water soluble active compounds since alternative technologies still are not as fully developed.<sup>9, 17</sup>

Nanometer to micrometer particles of poorly water soluble drugs can be produced by precipitation via various mechanisms. Finely dispersed naproxen can be prepared and precipitated by an acid-basic reaction. Aqueous solutions of naproxen were prepared in the presence of polyvinylpyrrolidone (PVP,  $M_w = 10,000$ ) and NaOH. The resulting pH was  $\sim 12$ . Aqueous HCl solutions were then added dropwise into naproxen aqueous solutions under agitation. At pH lower than 6, naproxen precipitates began to form. Aggregated particles with diameter of  $\sim 10 \mu\text{m}$  were formed that can be transferred into smaller rod-like, but rather uniform, particles which are  $\sim 1 \mu\text{m}$  long and  $\sim 0.3\text{-}0.4 \mu\text{m}$  wide when heated at a slightly acidic pH.<sup>18</sup> The disadvantage is the organic salt, sodium naproxen that is included in the product.

Precipitation in discrete emulsion droplets is a further way to produce small drug particles.<sup>11</sup> With lipophilic solvents, particle size control occurs through an emulsion step as an intermediate stage. The particle size distribution of an oil in water (o/w) emulsion is adjusted mechanically by homogenization<sup>19, 20</sup> or sonication.<sup>21-23</sup> The final droplet size

of the emulsion is smaller than 500 nm.<sup>20</sup> The conversion of the emulsion into a nanodispersion is then carried out by separation of the solvent by evaporation at a temperature lower than the boiling point of the organic solvent or at pressure higher than the vapor pressure of the organic solvent.<sup>19, 21-23</sup> The resulting particle size is determined by the size of the droplets in the o/w emulsion, stabilizer type, stabilizer and drug concentration, and the viscosity and volume of internal organic phase. This technique is used for the production of carotenoids,<sup>24</sup> indomethacin,<sup>19</sup> cyclosporine A,<sup>21</sup> U-86,<sup>22</sup> poly(MePEGCA-co-HDCA)<sup>23</sup> and cholesteryl acetate.<sup>20</sup> The solution of  $\beta$ -carotene in a lipophilic organic solvent or an oil<sup>24</sup> is emulsified in water containing a protective colloid. After removing the solvent by drying or distillation, each droplet forms solid nanoparticles.

Micron-sized particles may also be formed from solution in semi-continuous spray processes, for example spray drying. In these solution-based processes, the stabilizer is not likely to coat the surface of the drug particle as it forms during solvent evaporation, since the vapor surrounding the particle is highly hydrophobic.<sup>25, 26</sup> It is difficult to form submicron particles in the spray drying. Two important techniques have been developed to form small particles with compressed liquid and supercritical carbon dioxide, rapid expansion from supercritical solution and precipitation with a compressed fluid antisolvent (PCA), which is also referred to as the SAS or SEDS process.<sup>27-35</sup> The low solubility of water in carbon dioxide complicates the use of hydrophilic substances in both of these processes. RESS is often limited by the low solubility of drugs in supercritical fluids even when cosolvents are utilized. Since water is not very soluble in CO<sub>2</sub>, ethanol has been used to aid water dissolution in the PCA process by mixing three streams in a tri-axial nozzle.<sup>36</sup> The complicated nature of the resulting phase separation and particle formation can make it challenging to control the particle morphology.

Spray-freeze drying (SFD) is used to form nanostructured particles by atomizing solutions into droplets which then fall into liquid nitrogen.<sup>37-45</sup> Spray freezing into liquid (SFL) process is an alternative cryogenic particle engineering process that utilizes the atomization of a feed solution<sup>37-44</sup> or emulsion<sup>45</sup> containing drugs and/or surfactants directly into a cryogenic liquid to produce frozen nanostructured particles. The frozen particles are then lyophilized to obtain dry, freely flowing micronized powders. Advantages of the SFL process result from intense atomization in conjunction with rapid freezing rates.<sup>37-45</sup> Because liquid-liquid impingement occurs between the pressurized feed solution exiting the nozzle and the cryogenic liquid such as liquid nitrogen, a higher degree of atomization is achieved by spraying directly into the cryogenic liquid as opposed to spraying into the vapor phase above the cryogenic liquid in spray freeze drying. Ultra-rapid freezing rate prevent the phase separation of solutes within the feed solution and induce formation of amorphous structures. The intense atomization with rapid freezing rates have led to nanostructures aggregates composed of amorphous drug nanoparticles with high surface area and enhanced dissolution rates.<sup>37-45</sup>

### **1.2.1 Evaporative precipitation into aqueous solution (EPAS)**

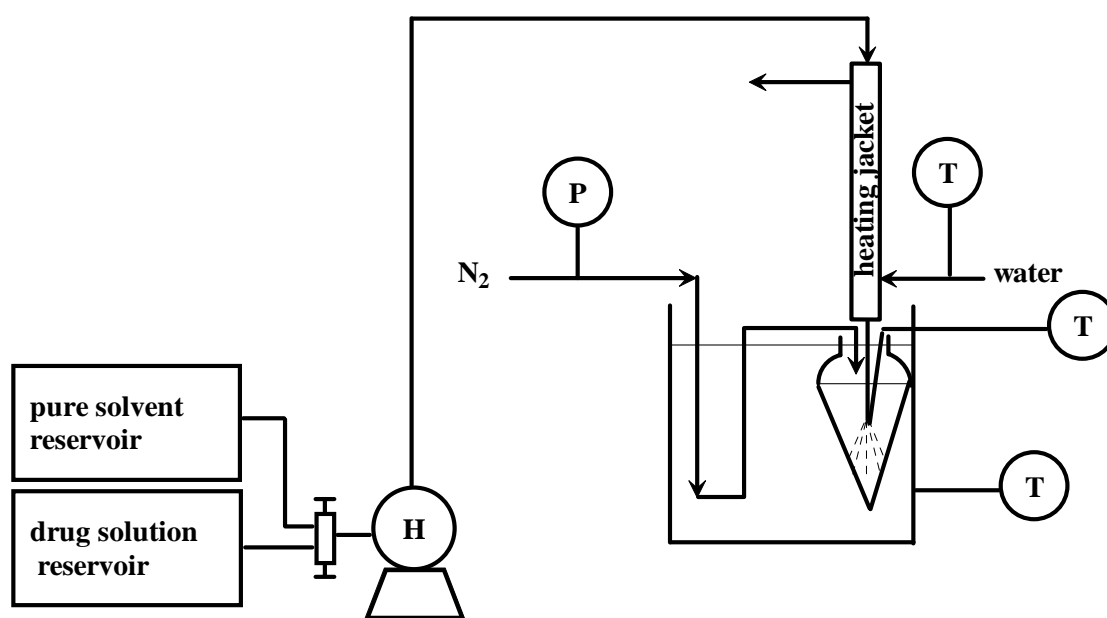
Evaporative precipitation into aqueous solution (EPAS) is a newly developed process for forming submicron to micron-sized particles of a poorly water-soluble drug coated with hydrophilic stabilizers. As shown in Figure 1.1, a drug dissolved in a water immiscible organic solvent is sprayed through an atomizer into an aqueous solution containing a hydrophilic stabilizer to produce an aqueous dispersion. Intense atomization leads to rapid evaporation of the small organic droplets in the aqueous solution. The rapid evaporation of the small organic droplets produces large supersaturation and rapid nucleation of the drug. Hydrophilic stabilizers in water surrounding the shrinking organic droplets diffuse to the surface of the growing particles to inhibit particle growth

and in some cases, crystallization. The diffusion is facilitated by the intensity of the spray. The temperature may be chosen to optimize the evaporation rates of organic solvent and water, solubility of the organic solvent in water, while minimizing thermal decomposition of the drug. The EPAS suspensions may be dried by spray drying, lyophilization, and centrifugation followed by vacuum drying etc. The stabilization of the drug particles with water soluble stabilizers in the aqueous suspensions facilitates dissolution rates of the final powder after drying. Since the particle formation stage is distinct from the stage in which the aqueous solution is dried, the drying step does not slow down the high dissolution rate of fine particles formed in the suspension.

The mechanism of particle formation and stabilization in EPAS is shown in Figure 1.2. After atomization, the droplet size of the organic solution containing poorly water soluble drugs decreases due to the evaporation of the organic solvent at high temperature. At the same time, the drug concentration increases with time. When the supersaturation of drugs in the shrinking droplet is high enough, the drug and in some cases, an excipient, nucleate. There are two mechanisms for the nuclei to form larger drug particles: 1) the drug molecules in the organic phase diffuse to the nuclei and condense; 2) the nuclei collide and coagulate together to form larger particles. A calculation on the moments of the size distribution in EPAS revealed that the drug particles grow predominantly by coagulation.<sup>46</sup> Surfactants in both organic and aqueous phases diffuse onto the growing particles. The hydrophobic moiety of the surfactants adsorbed onto drug particles and the hydrophilic moiety extend into water and form steric or electrostatic stabilization, if the surfactant is ionic. The adsorbed surfactants stabilize drug particles from particle growth and agglomeration. The particle growth and surfactant adsorption compete with each other. At high supersaturation or low particle growth rate, an aqueous suspension of drug particles may form with particle size smaller



than 1  $\mu\text{m}$ . Since the concentration of the organic solvent in water is extremely low,<sup>47</sup> the particle growth after suspension formation by Oswald ripening may be expected to be low relative to antisolvent precipitation where the organic solvent is much more soluble.



**T--thermocouple;**  
**P--pressure regulator;**  
**H--HPLC pump**

Figure 1.1. Apparatus for EPAS

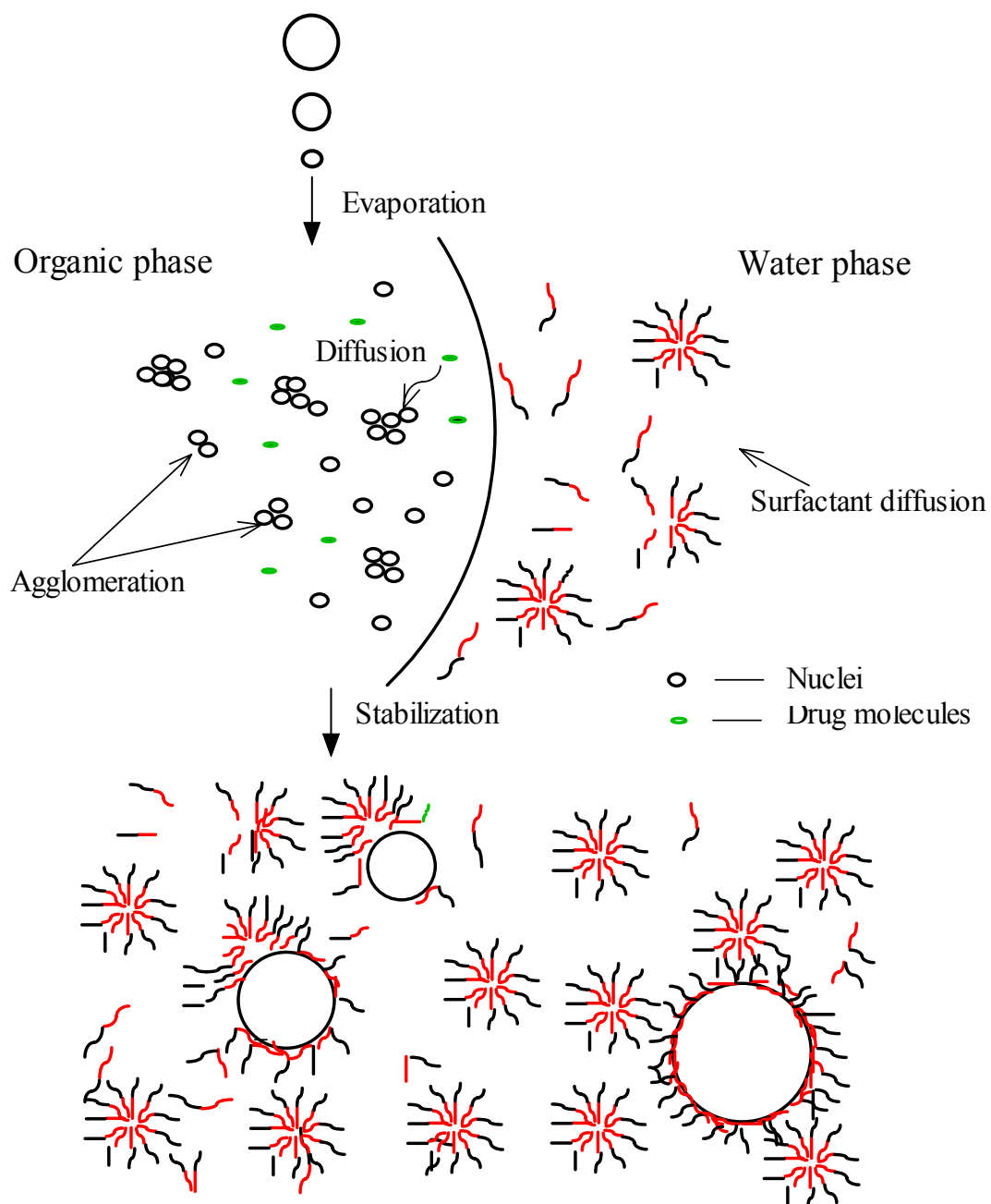


Figure 1.2. Mechanism of EPAS particle formation and stabilization

### 1.2.2 Antisolvent precipitation

Antisolvent precipitation is a widely used process to prepare inorganic and organic particles. A number of recent studies have utilized antisolvent precipitation to produce nanoparticles of poorly water soluble drugs.<sup>48-52</sup> In this process, a poorly water soluble drug with or without surfactant(s) is dissolved in a water miscible organic solvent, including methanol, ethanol, tetrahydrofuran (THF) and acetonitrile etc. The organic solution is then mixed with an “antisolvent”, usually an aqueous solution containing a surfactant (s) by a confined impinging jets (CIJ) mixer,<sup>50, 52</sup> sonication,<sup>49</sup> or just pouring the antisolvent into organic drug solution.<sup>48</sup> Upon mixing, the supersaturated solution leads to nucleation and growth of drug particles, which may be stabilized by surfactants. With sufficient supersaturation, and arrested growth by surfactant stabilization, it becomes possible to form suspensions of submicron particles in the aqueous solution.

The mechanism of antisolvent precipitation is shown in Figure 1.3.<sup>52</sup> A drug and a surfactant are dissolved in an organic solvent and mixed rapidly with an antisolvent to afford precipitation of the drug into nanoparticles. When water is the antisolvent, the hydrophobic drug and hydrophobic moiety of the surfactant precipitate simultaneously to form nanoparticles that are protected from aggregation and stabilized by the surfactant. The mixing time,  $\tau_{\text{mix}}$ , must be small compare to the process time,  $\tau_{\text{flash}}$ , in order to obtain a “homogenous kinetics” free of mixing effects and a narrow particle size distribution. The precipitation process can be further subdivided into the characteristic induction times for surfactant aggregation,  $\tau_{\text{agg}}$  and drug nucleation and growth,  $\tau_{\text{ng}}$ . The “reactions” compete and when times are matched, the surfactant can interact with the growing drug particle to alter nucleation and growth and offer colloidal stabilization.

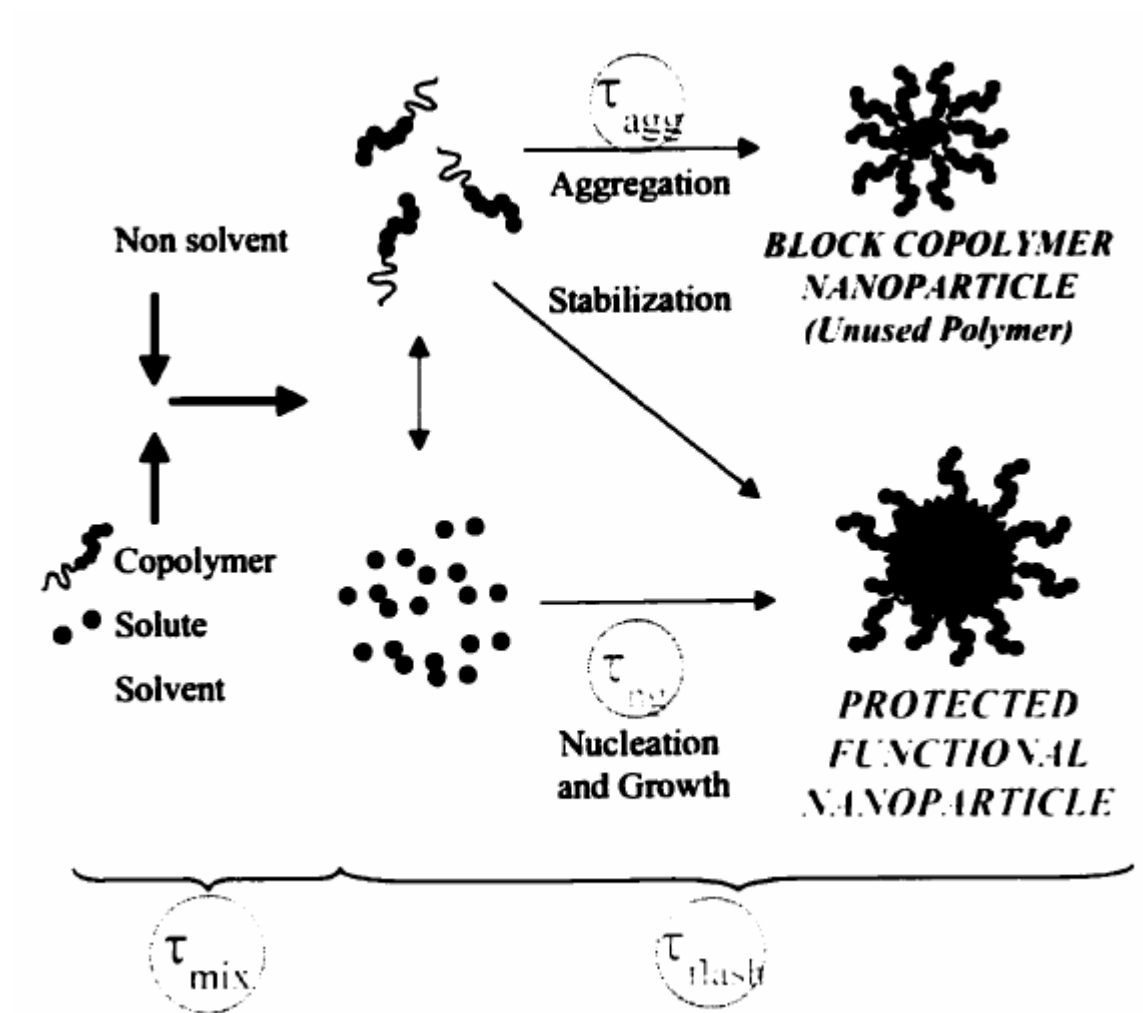


Figure 1.3. Mechanism of antisolvent precipitation

### **1.2.3 Comparison between micronization processes**

Evaporative precipitation into aqueous solution (EPAS) and antisolvent precipitation are two efficient processes to produce nanoparticles of poorly water soluble drugs based on two different mechanisms. The dried sample from EPAS or antisolvent precipitation yields nanometer to micrometer particle size, high dissolution rates, high surface areas and enhanced wettabilities. High shear, which is optional for antisolvent precipitation, is necessary for EPAS to atomize the organic solution to increase heat and mass transfer. Also, high interfacial tension between water immiscible organic solvent/vapor can hinder the mixing between drug nuclei and surfactant molecules, leading to micron size particles. Finally, the high temperature in EPAS favors particle growth which can lead to larger drug particles than in antisolvent precipitation.

On the other hand, since poorly water soluble drugs have higher solubility in water immiscible organic solvents such as dichloromethane, diethyl ether etc. but low solubility in water miscible organic solvents such as methanol, ethanol etc., EPAS is preferred process when the drug has a low solubility in water miscible solvents. Also, unlike antisolvent precipitation, the particle formation step in EPAS is separated from drying step with little amount of organic solvent left in the suspension. The suspension is more stable and easier to process due to the small amount of organic solvent.

As will be discussed in detail, nanoparticles of many poorly water soluble drugs can be produced with antisolvent precipitation at low temperature. But the recovery of nanoparticles needs more attention than in EPAS. The remaining of organic solvent in the suspension can lead to rapid particle growth by Oswald ripening. The removal of organic solvent from the suspension needs to be carefully controlled to prevent unnecessary particle growth, especially at high temperature.

### 1.3 Objectives

Two particle engineering technologies, evaporative precipitation into aqueous solution (EPAS) and antisolvent precipitation, were developed to micronize poorly water soluble drugs for the purpose of enhancing wetting and dissolution rates. The high surface area, enhanced wettability and even amorphous structure for some drugs of micronized particles enhanced dissolution. In this dissertation, Chapters 2-4 utilize the EPAS process and Chapter 5 utilizes antisolvent precipitation. Chapter 2 deals with the formation and stabilization of cyclosporine A nanoparticles. In Chapter 3, the effect of dissociation of ketoprofen in pure water, which adds ionic stabilization to steric stabilization is shown to lead nanosuspensions at extremely high suspension concentration and drug-to-surfactant ratio, as high as 30 mg/ml and 3:1; The interaction between ketoprofen and Pluronic F127 also leads to gels at low Pluronic F127 concentration with extremely small ketoprofen nanoparticles. In Chapter 4, high potency danazol formulations with high dissolution rates are formed by centrifugation to remove free surfactant. The dissolution rate of high potency drug formulations is correlated with surface area, crystallinity and particle size. Chapter 5 discusses nanoparticles formation by antisolvent precipitation. The nanoparticles are flocculated with salt and recovered by filtration to simplify solvent removal and to raise the drug potency.

In Chapter 2, amorphous nanoparticle suspensions of a poorly-water soluble drug, cyclosporine A, are produced by a new process, evaporative precipitation into aqueous solution (EPAS). The rapid evaporation of a heated organic solution of the drug, which is atomized into an aqueous solution, results in fast nucleation leading to nanoparticles suspensions. Hydrophilic stabilizers, introduced in the organic or aqueous phases, limit particle growth and inhibit crystallization for drug concentrations as high as 35 mg/ml, and drug-to-surfactant ratios up to 1.0. The suspensions may be used in parenteral

formulations to enhance bioavailability or may be dried to produce oral dosage forms with the potential for high dissolution rates due to the low crystallinity, small particle size and hydrophilic stabilizer that enhances wetting.

In Chapter 3, aqueous nanoparticle gels of a poorly-water soluble drug, ketoprofen, were produced by evaporative precipitation into aqueous solution (EPAS). Liquid droplets of coated ketoprofen were dispersed in water from 60 to 90°C, rather than solid particles, due to the freezing point depression from residual organic solvent. The dissociation of ketoprofen in pure water enhanced particle stabilization due to electrostatic repulsion to complement steric stabilization. Stable ketoprofen particles with a mean particle size of 135 nm, measured by dynamic light scattering, were formed with only 0.1% w/v Pluronic F127 and an exceptionally high drug-to-surfactant ratio of 10:1. With 5% w/v Pluronic F127, interactions between the polymer and ketoprofen produced a bluish, transparent gel of ~50 nm particles. The presence of the ketoprofen particles lowered the gellation concentration for the Pluronic F127 from 18 wt% all the way to 5.8 wt%. In 2 min, 98% ketoprofen in the gel nanoparticles dissolved, whereas the dissolution was slower if the gels were dried.

In Chapter 4, high-potency danazol particles with high dissolution rates were produced by evaporative precipitation into aqueous solution (EPAS). Aqueous suspensions formed by EPAS were centrifuged to remove the non-adsorbed surfactant. The resulting surfactant-coated drug particles had extremely high drug-to-surfactant ratios greater than 5, corresponding to potencies (wt drug/wt drug + wt surfactant) as high as 93%. The mechanism of the high dissolution rates was characterized as a function of surfactant adsorption, particle size and surface area, drug crystallinity, and the contact angle for water on the drug surface. For danazol stabilized by polyvinylpyrrolidone (PVP) alone or with sodium lauryl sulfate (SLS), small particle diameter and high surface



area led to high dissolution rates with ~90% drug dissolved in 2 min. The crystallinity of the danazol was typically 80%. The properties of the particles and the dissolution rates were mostly unchanged under a two-week thermal cycling stress test.

In Chapter 5, crystalline naproxen nanoparticle aqueous suspensions, formed by antisolvent precipitation, were flocculated with sodium sulfate, filtered and dried to form redispersible powders for oral delivery. The particles were stabilized with polyvinylpyrrolidone (PVP K-15) and poly(ethylene oxide-*b*-propylene oxide-*b*-ethylene oxide) (Pluronic F127) or both. The yield of the drug in the powder was typically 92 to 99%, and the drug potency varied by only 1 to 2%. The filtration process increased the drug potency by up to 61% relative to the initial value. Upon redispersion, the average particle size measured by light scattering, as low as 300 nm, was comparable to the value in the original aqueous suspension and consistent with primary particle sizes observed by SEM. The dissolution rate was correlated with the particle size after redispersion. Extremely rapid dissolution, up to 95% of the powder in two min, was achieved for 300 nm particles. The redispersibility of dried powders is examined as a function of the salt concentration used for flocculation and the surfactant composition and concentration. The residual sodium sulfate concentration in the dried powders was far below toxic limits.

#### 1.4 REFERENCES

- (1) Lipinski, C. *Am.Pharm. Rev.* 2002, 5, 82-85.
- (2) Radtke, M. *New Drugs* 2001, 3, 62-68.
- (3) Cussler, E. L. *Diffusion, Mass transfer in fluid systems*; Cambridge University Press: NY, 1986.
- (4) Lennernäs, H.; Ahrenstedt, O.; Hallgren, R.; Knutson, L.; Ryde, M.; Paalzow, L. K. *Pharm. Res* 1992, 9, 1243-1255.
- (5) Fagerholm, U.; Borgstrom, L.; Ahrenstedt, O.; Lennernas, H. J. *Drug Targeting* 1995, 3, 191-200.
- (6) Lennernas, H.; Ahrenstedt, O.; Ungell, A. L. *Br. J.Clin. Pharmacol.* 1994, 37, 589-596.
- (7) Lennernas, H.; Nilsson, D.; Aquilonius, S. M.; Ahrenstedt, O.; Knutson, L.; Paalzow, L. K. *Br. J.Clin. Pharmacol.* 1993, 35, 243-250.
- (8) Amidon, G. L.; Lennernäs, H.; Shah, V. P.; Crison, J. R. *Pharm. Res* 1995, 12, 413-420.
- (9) Liversidge, G., G.; Cundy, K. C. *Int J Pharm* 1995, 125, 91-97.
- (10) Reddy, R. K.; Khalil, S. A.; Gonda, M. W. *J Pharm Sci* 1976, 65, 115-118.
- (11) Horn, D.; Rieger, J. *Angew. Chem. Int. Ed.* 2001, 40, 4330-4361.
- (12) Byers, J. E.; Peck, G. E. *Drug Dev. Ind. Pharm.* 1990, 16, 1761-1779.
- (13) Peters, D. *Journal of Materials Chemistry* 1996, 6, 1605-1618.
- (14) Rubinstein, M. H.; Gould, P. *Drug Dev. Ind. Pharm.* 1987, 13, 81-92.
- (15) Aiache, J. M.; Beyssac, E. *Powder as dosage forms*; Marcel Dekker: New York, 1994.
- (16) Illig, K. J.; Mueller, R. L.; Ostrander, K. D.; Swanson, J. R. *Pharm. Technol.* 1996, 20, 78-88.
- (17) Müller, R. H.; Benita, S.; Böhm, B. *Emulsion and nanosuspensions for the formulation of poorly soluble drugs*; Medpharm: Stuttgart, 1998.

- (18) Pozarnsky, G. A.; Matjevic, E. *Colloids Surf. A Physico. Chem. Eng. Asp.* 1997, 125, 47-52.
- (19) Bodmeier, R.; Chen, H. *Journal of Controlled Release* 1990, 12, 223-233.
- (20) Sjöström, B.; Bergenstöhl, B.; Lindberg, M.; Rasmuson, A. C. J. *Dispersion Science and Technology* 1994, 15, 89-117.
- (21) Gref, R.; Quellec, P.; Sanchez, A.; Calvo, P.; Dellacherie, E.; Alonso, M. J. *European Journal of Pharmaceutical and Biopharmaceutics* 2001, 51, 111-118.
- (22) Labhasetwar, V.; Song, C.; Humphrey, W.; Shebuski, R.; Levy, R. J. *Journal of Pharmaceutical Science* 1998, 97, 1229-1234.
- (23) Peracchia, M. T.; Vauthier, C.; Desmaele, D.; Gulik, A.; Dedieu, J. C.; Demoy, M.; d'Angelo, J.; Couvreur, P. *Pharm. Res* 1998, 15, 550-556.
- (24) Cathrein, E.; Stein, H.; Stoller, H. J.; Viardot, K.: EP, 1991.
- (25) Masters, K. *Spray Drying Handbook*, 3rd ed.; New York: John Wiley and Sons, 1979.
- (26) Broadhead, J.; Rouan, S. K. E.; Rhodes, C. T. *Drug Dev. Ind. Pharm.* 1992, 18, 1169-1206.
- (27) Alessi, P.; Cortesi, A.; Kikic, I.; Foster, N. R.; Macnaughton, S. J.; Colombo, I. *Ind. Eng. Chem. Res.* 1996, 35, 4718-4726.
- (28) Subramaniam, B.; Rajewski, R. A.; Snavely, K. J. *Pharm. Sci.* 1997, 86, 885-890.
- (29) Ghaderi, R.; Artursson, P.; Carlfors, J. *Pharm. Res.* 1999, 16, 676-681.
- (30) Reverchon, E. J. *Supercritical Fluids* 1999, 15, 1-21.
- (31) Lengsfeld, C. S.; Delphanque, J. P.; Barocas, V. H.; Randolph, T. W. B. *J. Phys. Chem.* 2000, 104, 2725-2735.
- (32) Thiering, R.; Dehghani, F.; Dillow, A.; Foster, N. R. *J. Chem. Technol. Biotechnol.* 2000, 75, 42-53.
- (33) Chattopadhyay, P.; Gupta, R. B. *Ind. Eng. Chem. Res.* 2001, 40, 3530-3539.
- (34) Young, T. J.; Johnston, K. P.; Pace, G. W.; Mishra, A. K. *AAPS PharmSciTech* 2004, 5.
- (35) Young, T. J.; Mawson, S. M.; Johnston, K. P. *Biotechnol. Prog.* 2000, 402-407.

- (36) Palakodaty, S.; York, P. *Pharm. Res.* 1999, 16, 976-985.
- (37) Rogers, T. L.; Nelsen, A. C.; Sarkari, M.; Young, T. J.; Johnston, K. P.; Williams, R. O. *Pharmaceutical Research* 2003, 20, 485-493.
- (38) Hu, J.; Johnston, K. P.; Williams, R. O. *European Journal of Pharmaceutical Sciences* 2003, 20, 295-303.
- (39) Hu, J.; Johnston, K. P.; Williams, R. O. *Polymeric Materials: Science & Engineering* 2003, 89, 743.
- (40) Hu, J.; Johnston, K. P.; Williams, R. O. *International journal of pharmaceutics* 2004, 271, 145-154.
- (41) Hu, J.; Roger, T. L.; Brown, J.; Young, T. J.; Johnston, K. P.; Williams, R. O. *Pharmaceutical Research* 2002, 19, 1278-1284.
- (42) Rogers, T. L.; Hu, J.; Yu, Z.; Johnston, K. P.; Williams, R. O. *International Journal of Pharmaceutics* 2002, 242, 93-100.
- (43) Rogers, T. L.; Johnston, K. P.; Williams, R. O. *Pharmaceutical Development and Technology* 2003, 8, 187-197.
- (44) Rogers, T. L.; Nelsen, A. C.; Hu, J.; Brown, J. N.; Sarkari, M.; Young, T. J.; Johnston, K. P.; Williams, R. O. *European Journal of Pharmaceutics and Biopharmaceutics* 2002, 54, 271-280.
- (45) Rogers, T. L.; Overhoff, K. A.; Shah, P.; Santiago, P.; Yacaman, M. J.; Johnston, K. P.; Williams, R. O. *European Journal of Pharmaceutics and Biopharmaceutics* 2003, 55, 161-172.
- (46) Chen, X.; Vaughn, J. M.; Yacaman, M. J.; Williams, R. O.; Johnston, K. P. *J. Pharm. Sci.* 2004, 93, 1867-1878.
- (47) Chen, X.; Young, T. J.; Sarkari, M.; Williams, R. O.; Johnston, K. P. *Int J Pharm* 2002, 242, 3-14.
- (48) Rasenack, N.; Muller, B. W. *Pharm Res* 2002, 19, 1894-1900.
- (49) Ruch, F.; E., M. *Journal of Colloid and Interface Science* 2000, 229, 207-211.
- (50) Johnson, B. K.; Prud'homme, R. K. *Polymeric Materials: Science & Engineering* 2003, 89, 744-745.
- (51) Elder, E. J.; Hitt, J. E.; Rogers, T. L.; Tucker, C. J.; Saghir, S.; Svenson, S.; Evans, J. C. *Polymeric Materials Science and Engineering* 2003, 89, 741.

(52) Johnson, B. K., Princeton, 2003.

## **CHAPTER 2**

### **Preparation of Cyclosporine A Nanoparticles by Evaporation Precipitation into Aqueous Solution**

#### **2.1 INTRODUCTION**

The dissolution rate of many poorly water-soluble drugs limits their bioavailability via absorption into the gastrointestinal tract. Dissolution rates may be increased by reducing the particle size to increase the interfacial surface area and by inhibiting crystallization to form amorphous particles. Coating drug particles with polymeric and low molar mass hydrophilic stabilizers to enhance wetting and solvation by intestinal fluids may increase the rates further. The simultaneous application of all of these strategies would be desirable in attempting to achieve high dissolution rates; however, few existing micronization or particle formation techniques are capable of achieving such a goal.

Widely used mechanical techniques based on high shear or impaction, including microfluidization and milling can be limited by unfavorable yields due to solid losses, high polydispersity in particle size, shear-induced particle denaturation, long processing time, high energy requirements and the need for separating the product and processing agent.<sup>1-4</sup> To overcome many of these limitations, particles may be formed from solution in semi-continuous spray processes, for example spray drying. In these solution-based processes, it is often not possible to formulate a solvent that can dissolve both the poorly water-soluble drug and hydrophilic stabilizer. Even if such a solution may be formed, the stabilizer may not coat the surface of the drug particle as it forms during solvent evaporation, since the vapor surrounding the particle is highly hydrophobic.<sup>5, 6</sup> In

addition, it is difficult to form submicron particles in the above mechanical processes and spray drying.

Two important techniques have been developed to form small particles with compressed liquid and supercritical carbon dioxide, rapid expansion from supercritical solution and precipitation with a compressed fluid antisolvent (PCA), which is also referred to as the SAS or SEDS process.<sup>7-15</sup> The low solubility of water in carbon dioxide complicates the use of hydrophilic substances in both of these processes. RESS is often limited by the low solubility of drugs in supercritical fluids even when cosolvents are utilized. Since water is not very soluble in CO<sub>2</sub>, ethanol has been used to aid water dissolution in the PCA process by mixing three streams in a tri-axial nozzle.<sup>16</sup> The complicated nature of the resulting phase separation and particle formation can make it challenging to control the particle morphology.

The objective of this study is to develop a new process, evaporative precipitation into aqueous solution (EPAS), for forming submicron particles of a poorly water-soluble drug coated with hydrophilic stabilizers. As shown in Figure 2.1, a drug dissolved in an organic solvent is sprayed through an atomizer into an aqueous solution containing a hydrophilic stabilizer to produce an aqueous dispersion. Intense atomization leads to rapid evaporation of the small organic droplets in the aqueous solution. The rapid evaporation produces large supersaturation of the drug. The resulting rapid nucleation of the drug has the potential to produce amorphous instead of crystalline particles. Hydrophilic stabilizers in water diffuse to the surface of the growing particles to inhibit particle growth and crystallization. The diffusion is facilitated by the intensity of the spray. The temperature may be chosen to optimize the evaporation rates of organic solvent and water, solubility of the organic solvent in water, while minimizing thermal decomposition of the drug. The EPAS suspensions may be dried by spray drying,

lyophilization etc. The stabilization of the drug particles with water soluble stabilizers in the aqueous suspensions facilitates dissolution rates of the final powder after drying. Since the particle formation stage is distinct from the stage in which the aqueous solution is dried, EPAS has the potential to provide greater control over particle size and morphology than the above techniques. In this study, cyclosporine A, a water insoluble immunosuppressant for organ transplantation, was used as a model drug. The solvent, nature of the stabilizer, feed concentration of the drug, concentration of the stabilizer, temperature and drug-to-surfactant ratio were varied to control the particle size and morphology.

## **2.2 EXPERIMENTAL**

### **2.2.1 Materials**

Cyclosporine was obtained from North China Pharmaceutical Corporation and used without any further purification. L- $\alpha$ -phosphatidylcholine (Sigma), Myrj 52 (ICI Americas), Pluronic F127 (BASF), Polyvinylpyrrolidone (Sigma), Polyethylene glycol (Sigma), Brij 97 (Sigma) and Tween 80 (Aldrich) were used without further purification. The chemical structures of cyclosporine A and these surfactants are shown in Table 2.1. HPLC grade methanol was obtained from EM Science. Extra dry nitrogen was purchased from Matheson. Water was purified to Type I reagent grade by passing it through a Barnstead (NANOpure II) filtration system.

### **2.2.2 High performance liquid chromatography (HPLC) and gas chromatography (GC)**

HPLC was used to measure the drug concentration in the aqueous suspension with a 250 mm long C-18 column (SGE ODS, 5  $\mu$ m). The mobile phase was methanol and the detection wavelength was 210 nm. GC was used to measure the residual concentration of the organic solvent in the aqueous suspension. It was equipped with a fused silica



precolumn (i.d. = 0.53 mm, 0.5 m, methylated, Supelco) followed by a SPB-5 column (i.d. = 0.53 mm, 30 m, Supelco). To prepare the GC samples, 1 ml dimethylformamide was mixed with 1 ml EPAS suspension to dissolve the drug and then 1  $\mu$ l of the internal standard 1-butanol was added into the solution. The temperature program was: 35°C initial temperature for 1 min with a temperature ramp of 15°C/min and final temperature 200°C for 10 min. The injection volume was 1  $\mu$ l, and FID detection was used. The retention times were: 1-butanol, 0.68 min; dichloromethane, 1.36 min; DMF, 3.33 min.

### **2.2.3 Calculation of vapor-liquid-liquid equilibrium for the organic solvent-water system.**

For vapor-liquid-liquid equilibrium of an organic solvent and water binary system, there is only one degree of freedom. The equilibrium was calculated with the isothermal flash model at 1 atm (ASPEN, Cambridge, MA), utilizing UNIQUAC to calculate the activity coefficients, in order to determine the solubility of the organic in the aqueous phase.

### **2.2.4 Particle size and particle size distribution**

Particle size and particle size distribution were measured in aqueous suspensions by dynamic light scattering with a Brookhaven Zetaplus (Brookhaven Instruments Corporation, New York). To measure the particle size distribution, 0.5 ml suspension was diluted with distilled water to 8 ml before the measurement, and the results were based on the volume fraction distribution.

### **2.2.5 Particle crystallinity**

The suspensions were flash frozen with liquid nitrogen and lyophilized to produce dry powder. The crystallinity of the dry powders was examined with a PW1720 x-ray generator (PHILIPS).

### **2.2.6 Preparation of phosphatidylcholine vesicles**

Phosphatidylcholine was added into water to make a 10% w/v solution. The solution was stirred and sonicated to break up any large clumps. Then it was passed 30 times through a high-pressure homogenizer (Avestin Emulsiflex C-5) at a shear pressure drop of 15,000 psi to produce small unilamellar vesicles. The outlet of the homogenizer was submerged in an ice bath to keep the solution under 10°C. At the end of the run, 0.1 M NaOH solution was added to adjust the pH between 7.5 and 8.0. Prior to the experiments, the phosphatidylcholine solution was filtered through a 0.2 µm filter.

### **2.2.7 Evaporative precipitation into aqueous solution (EPAS)**

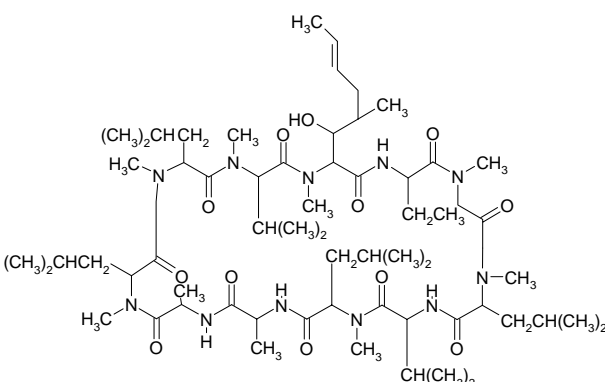
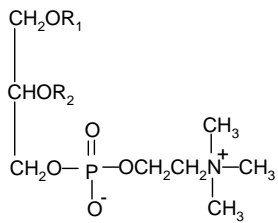
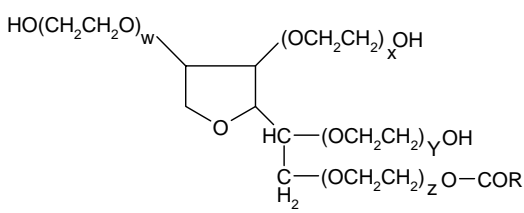
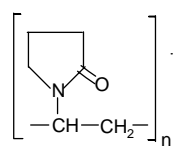
The EPAS apparatus is shown in Figure 2.1. Either the drug solution or pure solvent could be fed to the HPLC pump. The organic cyclosporine A solution was fed through a 3 m long 1/16 in. o.d. × 0.030 in. i.d. stainless steel coiled tube contained within a 1-1/2" OD × 24" long plastic water jacket (Alltech). Water was circulated through the jacket with a Julabo MP temperature controller. The organic solution was atomized through a crimped nozzle into hot water. The nozzle was made from a 10 in. long, 1/16 in. o.d. × 0.030 in. i.d. stainless steel tube. The tube was cut with a wire cutter to produce a crimped thin slit orifice. The tapered section of the tube was only 0.5 mm long. The tip was filed until the desired pressure drop was achieved for a given flow rate.<sup>13, 15</sup> The flow rate of the solution was checked by spraying drug solution in pure methanol, which would dissolve the drug completely, and the sample was analyzed by HPLC.

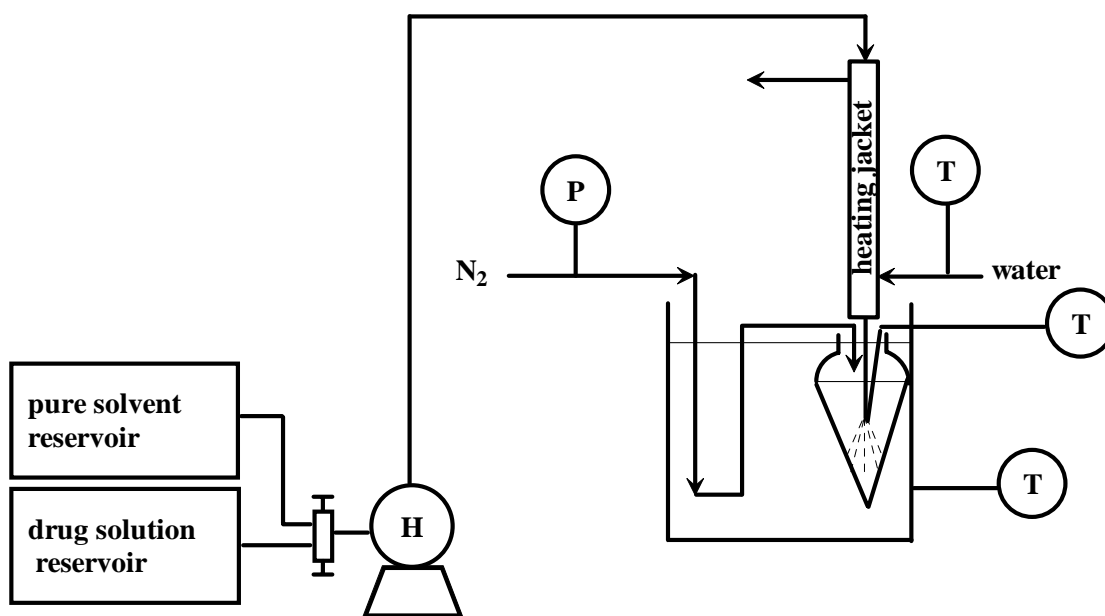
The aqueous stabilizing solution was contained in a 125 ml separatory funnel that was submerged in a temperature-controlled water bath. The nozzle was submerged approximately 2 cm under the surface of the aqueous solution. As shown in Figure 2.2, the turbulence of the spray mixed the precipitated drug and the surfactant solution

vigorously. To suppress and drain the foam produced by the organic vapor, nitrogen was blown downwards on top of the foam at 20 psi into the funnel through three 1/16 in. o.d.  $\times$  0.030 in. i.d. stainless steel tubes. A thermocouple was submerged next to the nozzle in the stabilizing aqueous solution to measure the actual temperature of the aqueous solution. About a 6°C temperature drop resulted from the evaporation of organic solution at the thermocouple tip. Unless indicated otherwise, the stabilizer was added in the aqueous phase and was not present in the organic feed solution. After spraying for a required time to produce the desired drug/surfactant ratio, the suspension was recovered and analyzed within 1 h to determine the particle size by DLS. The suspensions were flash frozen in liquid nitrogen and lyophilized into dry powders for characterization by X-ray diffraction.

After the spray, the stabilizing solution was replaced by pure water and feed was switched to pure solvent to flush the remaining drug out of the tube. Without this pure solvent flush, the drug would precipitate and plug up the nozzle.

Table 2.1. The chemical structures of drug and surfactants

Drug/surfactant	Chemical structure
Cyclosporine A	
L- $\alpha$ -phosphatidylcholine	 <p><math>R_1, R_2 = \text{Fatty Acid Residues}</math></p>
Tween 80	 <p><math>W+X+Y+Z=20</math>  <math>R=\text{CH}_3(\text{CH}_2)_7\text{CH}=\text{CH}(\text{CH}_2)_7</math></p>
Polyvinylpyrrolidone	



**T--thermocouple;**  
**P--pressure regulator;**  
**H--HPLC pump**

Figure 2.1. Apparatus for EPAS

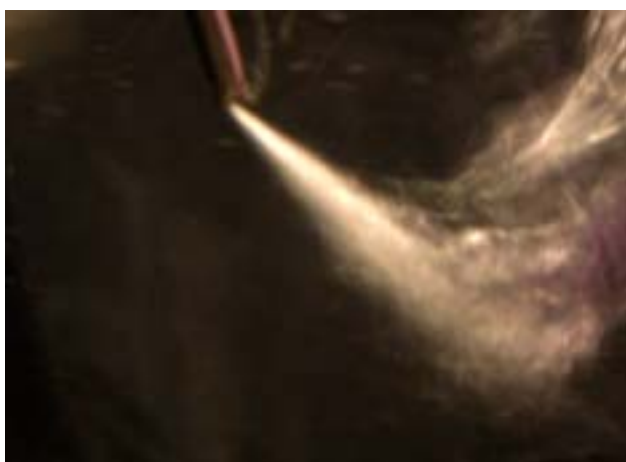


Figure 2.2. Spray of pure dichloromethane into aqueous solution at 80°C in the EPAS process for a flow rate of 1 ml/min.

## 2.3 RESULTS AND DISCUSSION

### 2.3.1 Particle sizes with phosphatidylcholine in the aqueous solution

The organic solutions were sprayed into small unilamellar vesicles composed of phosphatidylcholine. All EPAS experiments in this section were performed with a surfactant concentration of 10% w/v, a temperature of 75°C for the aqueous solution and the preheater and a flow rate of 1 ml/min. The final concentration of drug in suspension was measured by HPLC and used to determine the drug/surfactant ratio. The yield was determined by comparing the measured drug concentration and the amount sprayed into the aqueous solution. The experiments with dichloromethane were unsuccessful as this solvent modified the vesicles such that the phosphatidylcholine phase separated from the water during the spray.

Table 2.2. EPAS results for 10% w/v phosphatidylcholine in the aqueous solution.

C <sub>soln.</sub>	D <sub>avg</sub>	Particle size distribution	C <sub>aq.</sub>	Yield	Drug/surf. ratio
(% w/v)	(nm)	(nm)	(mg/ml)	(%)	(w/w)
0	131	53-66 (65%); 225-323 (35%)	0	/	0
1	253	134-160 (48%); 324-386 (52%)	14.4	96	0.14
2	526	120-212 (13%); 375-663 (87%)	30.8	87	0.30
5	477	217-253 (20%); 507-615 (80%)	37.1	100	0.37
5	408	96-166 (19%); 287-496 (79%)	34.6	98	0.35
5	446	53-73 (44%); 188-414 (39%); 1252-2357 (17%)	31.8	90	0.32
36.0 <sup>a</sup>	460	123-642 (97%)	35.2	83	0.35
36.0 <sup>a</sup>	466	267-327 (61%); 653-801 (39%)	34.9	79	0.35

a: phosphatidylcholine in organic solution

The initial size of the SUVs produced during the homogenization process was only 48.7 nm. As shown in Table 2.2, when pure diethyl ether was sprayed into the surfactant solution without drug, the vesicle size increased modestly to 130 nm, with 65% by volume of the vesicles still smaller than 65 nm. This result indicates that the vesicles are still intact after exposure to the diethyl ether and would be available to stabilize a drug. Upon spraying drug solution into the vesicles, stable turbid suspensions were formed. The mean size of the drug particles increased with the concentration of drug in the aqueous suspension  $C_{aq}$ , which was a function of the drug concentration in the organic feed  $C_{soln}$ , and the spray time. As  $C_{aq}$  increased from 14 mg/ml to values over 30, a significant increase in particle size was observed. At a drug concentration of ~14 mg/ml, the dispersed particles had a mean size of 253 nm with a size range of 134-386 nm. At a concentration of ~35 mg/ml, the mean size increased to 526 nm with a very broad size distribution, including some particles larger than 1  $\mu$ m. The particle size did not change significantly with a change in  $C_{soln}$  from 2 to 5% w/v, as long as  $C_{aq}$  was constant. The three experiments with a drug concentration of 5% w/v in diethyl ether showed that the experimental reproducibility in particle size was 7.5% and in yield was 4.2%. Several factors may contribute to this particle growth with an increase in  $C_{aq}$ . The collision frequency increases, which may increase aggregation. As the drug/surfactant ratio increases during the spray, surfactant is transferred from the empty vesicles to the surface of the drug particles. Fewer empty vesicles are available to stabilize the drug particles and prevent growth. Also, the coverage of the drug by surfactant is lower when the drug/surfactant ratio increases, leading to less effective stabilization against aggregation. Finally, the longer the spray, the longer the time for aggregation. Shear induced collisions during the spray and an increase in exposure time to organic solvent residues could lead to particle growth. However, this effect of shear was not observed as

$C_{\text{soln}}$  was increased from 2 to 5% w/v, as this lowered the spray time from 18 to 7 min for a constant  $C_{\text{aq}}$  of 35 mg/ml.

To further explore the mechanism of surfactant stabilization, phosphatidylcholine was dissolved in diethyl ether with cyclosporine and sprayed into pure water, as shown in the last two entries in Table 2.2. Despite the lack of vesicles in the aqueous solution at the start of the process, the mean size and size distribution of the drug particles were similar to the case above where vesicles were already present in the water at the start of the spray. This comparison may be made in Table 2.2 at a nearly constant drug to surfactant ratio of 0.35. It is possible that the high shear in the spray produced vesicles. The particle sizes at the low end of the distribution were not as small as in the case where the vesicles were made in water prior to the EPAS spray. Thus, the vesicles formed during the EPAS spray appeared to be larger than those formed by homogenization. Regardless of the size of the vesicles, the surfactant was available to coat and stabilize the growing drug particles.

Heavy foam was formed in the aqueous solution when the organic drug-surfactant solution was sprayed into water. The shear from the evaporating organic jet created vapor bubbles that were stabilized by the phosphatidylcholine. In the earlier experiments where the phosphatidylcholine was present only in the aqueous solution, much less foam was produced. In this case the surfactant did not diffuse as quickly to the organic vapor-water interface to stabilize the foam. Despite the large degree of foam generation, the foam did not leave the top of the vessel containing the aqueous solution due to the downward flow of nitrogen.

### **2.3.2 Effect of solvents on particle size.**

Two solvents were compared in EPAS experiments, diethyl ether and dichloromethane. They have similar boiling points, vapor pressures and heats of



vaporization.<sup>17</sup> At a temperature of 75°C, the liquid phase concentration of dichloromethane in water is 0.004 g/ml for the equilibrium flash calculation described above. The corresponding value for diethyl ether is 0.012 g/ml due to a lower value of the activity coefficient resulting from polar interactions and hydrogen bonding with water. In each spray, the solvent evaporated, and a layer of organic solvent was not observed in the precipitation vessel. As shown in Table 2.3, the size of drug particles was much smaller when the organic solvent was dichloromethane versus diethyl ether for Pluronic F127 ( $\text{HO}(\text{CH}_2\text{CH}_2\text{O})_{98}(\text{CH}_2\text{C}(\text{CH}_3)\text{HO})_{67}(\text{CH}_2\text{CH}_2\text{O})_{98}\text{H}$ , HLB =18-23) as a stabilizer. Additional experiments were performed by spraying pure diethyl ether at 75°C into a stable suspension formed by EPAS with dichloromethane, which had an average particle size of 423 nm. After spraying diethyl ether for 10 min at 1 ml/min, large particles several microns in diameter formed and settled. This experiment indicates that the large particles formed with diethyl ether are influenced by the stability of the aqueous suspensions, and not just the particle formation stage. Given that the two solvents have similar volatilities and heats of vaporization, it is likely that the difference in size is related to the much different solubility of the solvents in water and the influence of the solvent on Oswald ripening and/or steric interactions between surfactant coated drug particles.

Table 2.3. Solvent effect on the particle size for 1% w/v Pluronic F127 in the aqueous phase for a drug/surfactant ratio: 0.93-1.07

Solvent	D <sub>avg</sub>	Size distribution	Yield
	(nm)	(nm)	(%)
Diethyl ether	1218	316-1000 (91%)	86
Dichloromethane	423	358-424 (96%); 909-990 (4%)	96
Dichloromethane	499	263-303 (38%); 576-689 (62%)	93

### 2.3.3 Effect of surfactant type and feeding drug concentration on particle size.

In addition to phosphatidylcholine, a variety of other surfactants and polymers were used in the aqueous solution to stabilize the drug particles, as shown in Table 2.4. All of the experiments were done with preheater and aqueous solution temperatures of 75°C, a flow rate of 1 ml/min, dichloromethane as the solvent, a drug concentration of 1% w/v, and a surfactant concentration of 1% w/v. In these experiments, concentrations of cyclosporine were significantly higher than typical solubility levels in micelles composed of these surfactants.<sup>13, 15</sup> Unlike the case for the other surfactants, dichloromethane/water emulsions were formed with Brij 97 ( $C_{18}H_{35}(OCH_2CH_2)_nOH$ ,  $n=1-10$ , HLB = 12.4) due to its low HLB value. Much of the drug was lost to the emulsion droplets which settled, leaving an aqueous suspension with unusually low turbidity. For a feed concentration of 5% w/v, the results were similar for the Tween 80 (HLB = 15.0) and Myrj 52 ( $CH_3(CH_2)_{16}(OCH_2CH_2)_{40}OH$ , HLB = 16.9) nonionic ethoxylated surfactants, which had similar HLB values. However, the particle sizes were much larger for the homopolymer stabilizers, which had much higher molecular weights. These particles may have had more time to grow due to slower diffusion of stabilizer to the particle surface. However, the steric stabilization provided by the high molecular weight of the adsorbed PVP molecules led to suspensions that were stable overnight. The suspensions for the other surfactants were only stable for 1-2 h.

As shown in Table 2.4, increasing the feed drug concentration to 5% w/v decreased the particle size even though the suspension concentration  $C_{aq}$  and drug/surfactant ratios were approximately the same for Myrj 52, Tween 80, and PVP. With an increase in the feed drug concentration,  $C_{soln}$ , the supersaturation increases during evaporation, leading to smaller particles, if the steric stabilization is sufficient. Furthermore, the shorter spray time for the higher  $C_{soln}$  may produce less shear induced

aggregation. For a given homopolymer, steric stabilization increased with molecular weight, as is evident in comparing particle sizes for PVP and PEG.

Table 2.4. Effect of surfactant type on particle size for a drug/surfactant ratio: 0.3-0.5

Aqueous surfactants	C <sub>soln</sub> (% w/v)	D <sub>avg</sub> (nm)	Size distribution (nm)	Yield (%)
1% Brij 97 <sup>a</sup>	1	1177	664-1038 (90%); 3962-5663 (10%)	87
1% Myrj 52	1	625	512-738 (100%)	86
1% Myrj 52	5	339	324-349 (100%)	93
1% Tween 80	1	532	151-191 (19%); 529-713 (81%)	91
1% Tween 80	5	338	78-571 (100 %)	96
1% PEG 8, 000	5	1365	1343-1387 (100%)	88
1% PEG 18, 500	5	1018	77-437 (45%); 876-2091 (55%)	95
1% PVP 40, 000	1	1076	909-1374 (100%)	95
1% PVP 40, 000	5	595	577-741 (100%)	89
1% PVP K-15	5	1115	932-1222 (100%)	98

a: suspension concentration: 10 mg/ml water and drug/surfactant ratio =1.0.

#### 2.3.4 Effect of surfactant concentration in the aqueous solution

All of the experiments in Table 2.5 were conducted under the same conditions in Table 2.4 unless otherwise denoted. The drug to surfactant ratio was chosen to be approximately 0.35 at the end of each spray. As the surfactant concentration was doubled, the particle size decreased, even though the drug concentration in the suspension increased. Early in the sprays, the drug to surfactant ratio was lower in the case where the surfactant concentration was higher. This difference may be expected to lead to smaller particles, if the particles are well stabilized. It would not be expected to occur if

the particles were not well stabilized, due to enhanced particle collisions with higher suspension concentrations. Thus surfactant concentration may have a large effect on the particle formation mechanism.

Table 2.5. Effect of surfactant concentration on the particle size for a drug/surfactant ratio: 0.3-0.4

Aqueous surfactants	D <sub>avg</sub>	Size distribution	Suspension concentration	Yield
	(nm)	(nm)	(mg/ml)	(%)
1% PVP 40, 000	1076	909-1374 (100%)	3.3	95
2% PVP 40, 000	861	719-1136 (100%)	6.8	94
1% Tween 80	559	492-644 (100%)	3.7	101
2% Tween 80	361	226-435(100%)	6.6	103
5% Tween 80	122	33-47 (23%); 124-177 (77%)	20.0	97

### 2.3.5 Effect of temperature on particle size.

The temperature affects the equilibrium concentration of the organic solvent in water markedly. For example, the solubility of dichloromethane in water without surfactant in vapor-liquid-liquid equilibrium is 0.0081 g/ml at a temperature of 55°C but only 0.0023 g/ml at 85.0°C. As shown in Table 2.6, the particle size increased with temperature for Tween 80 as a stabilizer, but decreased with temperature for PVP 40, 000. The other experimental conditions were the same as in Table 2.4. As temperature increases, more rapid evaporation of the organic solvent enhances nucleation favoring smaller particles. Higher temperature also increases the rate of diffusion of the PVP. These two factors may explain the decrease in particle size for the PVP data. For Tween

80 other factors were dominant. The hydrogen bonding between the EO group of Tween 80 and water is well known to become much weaker over this temperature range. In fact, this reduction of hydrogen bonding often leads to precipitation of EO based surfactants in water.<sup>18</sup> The steric stabilization from the EO tails in Tween 80 becomes weaker with this loss in hydration, and this may lead to particle growth, as observed experimentally.

Table 2.6. Temperature effect on the particle size for a drug/surfactant ratio: 0.3-0.4

Surfactant		1% w/v Tween 80		1% w/v PVP 40, 000	
T	D <sub>avg</sub>	Size Distribution		D <sub>avg</sub>	Size Distribution
(°C)	(nm)	(nm)		(nm)	(nm)
55	308	37-68 (68%); 168-308 (6%) 765-1632 (26%)		1354	577-741 (38%); 1570-2017 (62%)
65	438	204-233 (3%); 400-473 (97%)		1144	503-563 (11%); 1149-1335 (89%)
75	559	492-644 (100%)		1076	909-1374 (100%)
85	774	622-925 (100%)		803	594-938 (100%)

### 2.3.6 Effect of drug loading on particle size.

The drug loading, as reflected in the drug/surfactant ratio, increased linearly with the spray time. As shown in Table 2.7, with an increase in drug loading, and consequently, the concentration of the suspension, the mean particle size and polydispersity increased. When the drug to surfactant was above 0.7, very large particles were formed, some as large as 3.6  $\mu\text{m}$ . As the drug/surfactant ratio and the drug concentration in the suspension increased, less surfactant was available to stabilize the growing drug particles. Also, the coverage of surfactant on the drug particles decreased providing less stability to flocculation and agglomeration. Both of these reasons may contribute to the larger particle size at high drug loading.

Table 2.7. Effect of drug/surfactant ratio (drug loading) on particle size for 1% Tween 80 in the aqueous solution

$C_{\text{soln}}$	Drug/surf. ratio	Suspension concentration	$D_{\text{avg}}$	Size distribution
(% w/v)		(mg/ml)	(nm)	(nm)
1 <sup>a</sup>	0.37	3.7	559	492-644 (100%)
1 <sup>a</sup>	1.16	11.6	518	211-409 (76%); 695-1180 (24%)
5 <sup>a</sup>	0.33	3.3	338	78-571 (100%)
5 <sup>a</sup>	0.72	7.2	523	168-301 (89%); 2687-3598 (11%)
5 <sup>b</sup>	2.50	25.0	921	563-691 (80%); 1740-2249 (20%)

a: Q=1 ml/min; b: Q=2.5 ml/min

### 2.3.7 Residual solvent concentration

The residual solvent concentration was measured by gas chromatography (HP 5890A). As shown in Table 2.8, the residual concentration of dichloromethane did not change significantly with spray time, but did change slightly with surfactant type. In Pluronic F127 aqueous solution, some dichloromethane will be dissolved in the micelles. This factor may contribute to higher residual concentration than for PVP, which does not form micelles. The residual concentrations of dichloromethane in the suspension at 75°C are slightly smaller than the equilibrium value for the binary system, which is 0.0039 g/ml. When the temperature increased from 75 to 85°C, the residual solvent decreased from 0.0041 to 0.0021 g/ml, consistent with the decrease in solubility (binary system) from 0.0039 to 0.0023 g/ml. In a single experiment a new nozzle was formed that required a higher pressure drop of 4000 psi for the same flow rate to produce more intense atomization. However, the residual solvent was not changed. Dichloromethane is a class 2 solvent with a permitted daily exposure of 6 mg/day.<sup>19</sup>

Table 2.8. Concentration of residual dichloromethane in the aqueous suspension for a flow rate of 1 ml/min

Aqueous surfactants	t (min)	Residual DCM concentration (g/ml)
1% PVP 40, 000	10	0.0031
1% PVP 40, 000	20	0.0029
1% PVP 40, 000	30	0.0035
1% Pluronic F127	10	0.0041
1% Pluronic F127 <sup>a</sup>	10	0.0044
1% Pluronic F127 <sup>b</sup>	10	0.0021

a: Pressure drop = 4000 psi; b: Temperature = 85°C

### 2.3.8 X-ray study.

The drug particle suspensions were flash frozen with liquid nitrogen and lyophilized to dry powder. The x-ray diffraction patterns of several samples are shown in Figure 2.3 (a) and (b). Originally, cyclosporine A was crystalline with sharp peaks in the diffraction pattern. After the EPAS process, these sharp peaks disappeared indicating a large loss in crystallinity. The crystalline peaks of the samples with Myrj 52 come from the bulk Myrj 52 and not the drug. The large loss in crystallinity may be expected to enhance the bioavailability of this water-insoluble drug.



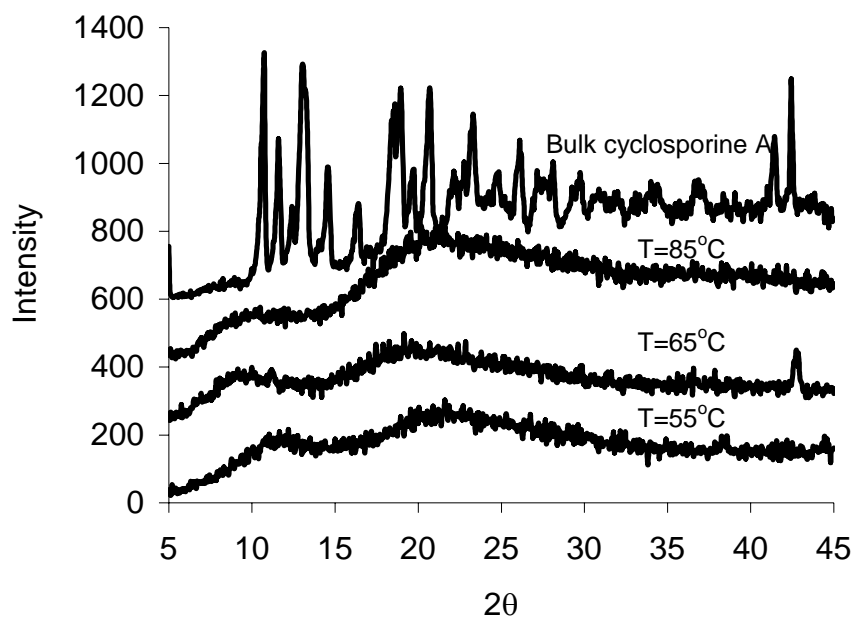


Figure 2.3 (a). The X-ray diffraction pattern of cyclosporine A+PVP 40, 000 powder (drug/surfactant ratio= 0.4).

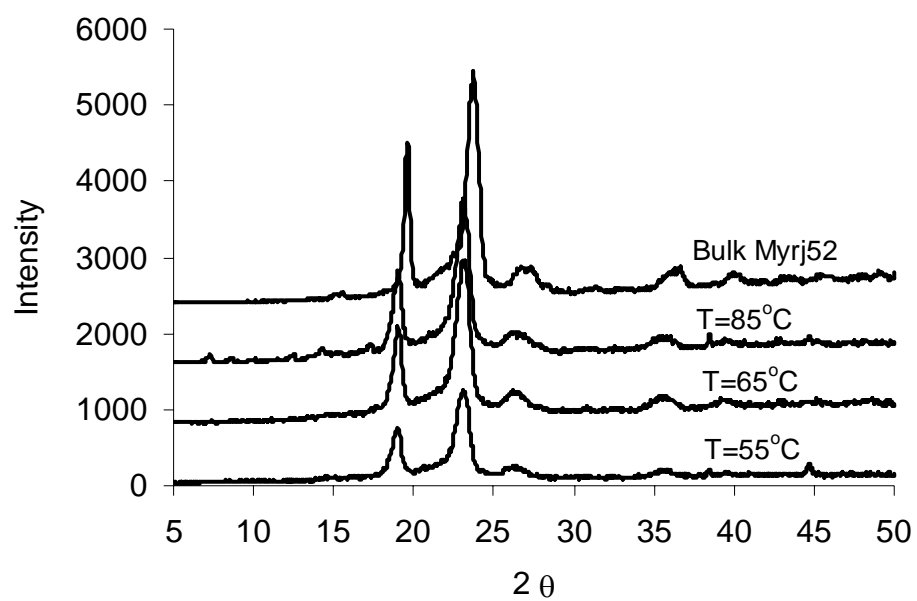


Figure 2.3 (b). The X-ray diffraction pattern of cyclosporine A + Myrj 52 powder (drug/surfactant ratio= 0.4).

## 2.4 CONCLUSIONS

The rapid evaporation of the heated organic solution in EPAS results in fast nucleation leading to amorphous nanoparticle suspensions. A variety of hydrophilic stabilizers were found to diffuse to the surface of the growing particles rapidly enough to prevent growth of the nanoparticles. Nanoparticle suspensions with low drug crystallinity were formed for cyclosporine A with L- $\alpha$ -phosphatidylcholine vesicles, low molecular weight ethoxylated nonionic surfactants, and high molecular weight homopolymers. The drug concentrations were as high as 35 mg/ml, and drug/surfactant ratios reached unity. Both of these values are far in excess of the values obtained for solvation of this drug in micelles or vesicle bilayers.<sup>13, 15</sup> For the two solvents studied, diethyl ether and dichloromethane, the difference in particle size is related to Oswald ripening and/or steric interactions between surfactant coated drug particles, and in the case of L- $\alpha$ -phosphatidylcholine, to the effect of solvent on the vesicle stability. The particle sizes were larger for the high molecular weight homopolymer stabilizers versus the low molecular weight ethoxylated surfactants. It is likely that the slower diffusion for the former allowed more time for particle growth. For a given drug/surfactant ratio, particle size decreased with increasing surfactant concentration, despite the increase in the concentration of the suspension. An increase in temperature speeds up evaporation and nucleation leading to smaller particles, except in the cases where it is detrimental to steric stabilization, as was found for ethoxylated surfactants.

## 2.5 REFERENCES

- (1) Rubinstein, M. H.; Gould, P. *Drug Dev. Ind. Pharm.* 1987, 13, 81-92.
- (2) Byers, J. E.; Peck, G. E. *Drug Dev. Ind. Pharm.* 1990, 16, 1761-1779.
- (3) Aiache, J. M.; Beyssac, E. *Powder as dosage forms*; Marcel Dekker: New York, 1994.
- (4) Illig, K. J.; Mueller, R. L.; Ostrander, K. D.; Swanson, J. R. *Pharm. Technol.* 1996, 20, 78-88.
- (5) Masters, K. *Spray Drying Handbook*, 3rd ed.; New York: John Wiley and Sons, 1979.
- (6) Broadhead, J.; Rouan, S. K. E.; Rhodes, C. T. *Drug Dev. Ind. Pharm.* 1992, 18, 1169-1206.
- (7) Alessi, P.; Cortesi, A.; Kikic, I.; Foster, N. R.; Macnaughton, S. J.; Colombo, I. *Ind. Eng. Chem. Res.* 1996, 35, 4718-4726.
- (8) Subramaniam, B.; Rajewski, R. A.; Snavely, K. *J. Pharm. Sci.* 1997, 86, 885-890.
- (9) Ghaderi, R.; Artursson, P.; Carlfors, J. *Pharm. Res.* 1999, 16, 676-681.
- (10) Reverchon, E. *J. Supercritical Fluids* 1999, 15, 1-21.
- (11) Lengsfeld, C. S.; Delphanque, J. P.; Barocas, V. H.; Randolph, T. W. B. *J. Phys. Chem.* 2000, 104, 2725-2735.
- (12) Thiering, R.; Dehghani, F.; Dillow, A.; Foster, N. R. *J. Chem. Technol. Biotechnol.* 2000, 75, 42-53.
- (13) Young, T. J.; Johnston, K. P.; Pace, G. W.; Mishra, A. K. *AAPS PharmSciTech* 2004, 5.
- (14) Chattopadhyay, P.; Gupta, R. B. *Ind. Eng. Chem. Res.* 2001, 40, 3530-3539.
- (15) Young, T. J.; Mawson, S. M.; Johnston, K. P. *Biotechnol. Prog.* 2000, 16, 402-407.
- (16) Palakodaty, S.; York, P. *Pharm. Res.* 1999, 16, 976-985.
- (17) Yaws, C. L. *Chemical properties handbook: physical, thermodynamic, environmental, transport, safety, and health related properties for organic and inorganic chemicals*; New York: McGraw-Hill, 1999.

- (18) Blankschtein, D.; Thurston, G. M.; Benedek, G. B. *J. Chem. Phys.* 1986, 85, 7268-7288.
- (19) Federal Register: International Committee on Harmonization, Quality Guidance Q3C, 1997.

## CHAPTER 3

### **Ketoprofen Nanoparticle Gels Formed by Evaporative Precipitation into Aqueous Solution (EPAS)**

#### **3.1 INTRODUCTION**

The bioavailability of many class II poorly water-soluble drugs is dissolution-rate limited as their high lipophilicity leads to rapid permeation of biomembranes.<sup>1</sup> According to Noyes-Whitney equation,<sup>2</sup> dissolution rates may be increased by reducing the particle size to increase the interfacial surface area. Coating drug particles with polymeric and low molar mass hydrophilic stabilizers enhances wetting of this interfacial surface area by intestinal fluids to increase the rates further. Recently a new process, evaporative precipitation into aqueous solution (EPAS), was introduced to form rapidly dissolving poorly water-soluble drug coated with hydrophilic stabilizers.<sup>3-6</sup> A drug dissolved in an organic solvent is sprayed through an atomizer into an aqueous solution to produce an aqueous dispersion. Amphiphilic stabilizers diffuse to the surface of the growing particles to inhibit particle growth and in some cases, crystallization. Although nanoparticles have been produced for cyclosporine A,<sup>3</sup> particle aggregates several microns in diameter composed of smaller primary particles have been reported for other drugs such as danazol and itraconazole.<sup>4,5</sup> However the relatively high surface areas on the order of 5 m<sup>2</sup>/g led to rapid dissolution, which is desirable for oral delivery formulations. However, for parenteral, pulmonary and transdermal applications, it would be desirable to produce aqueous dispersions in which the particle size is well below 1 micron.<sup>7-9</sup>

The primary objective of this study was to develop an understanding of how to produce nanoparticles by EPAS rather than the typically reported micron-sized particles.<sup>4-6</sup> Ketoprofen, a nonsteroidal anti-inflammatory drug, was chosen as a model drug due to its tendency to ionize in neutral water. The particle size was studied as a function of the drug concentration in the organic feed solution, to influence the supersaturation, the surfactant structure, the suspension concentration, typically 10 to 30 mg/ml, and the surfactant concentration in the aqueous suspension. A polyethylene oxide-*b*-polypropylene oxide-*b*-polyethylene oxide triblock copolymer, Pluronic F127, was used to form viscous hydrogels in the aqueous phase with ketoprofen upon cooling to prevent particle growth. Ketoprofen is shown to interact with the polymer to lower the polymer concentration needed for gelation markedly. Amorphous ketoprofen particles were formed, whereas EPAS produces crystalline drugs in most cases,<sup>4, 10</sup> with some exceptions.<sup>3</sup> Electrostatic repulsion is shown to stabilize the aqueous suspensions, as the particles coalesced upon lowering the pH to protonate the ketoprofen or with the addition of salt. The dissolution rate of the ketoprofen in the original hydrogels and in dried hydrogels and suspensions is reported and the stability of the particle size in the gel after one month is investigated.

## **3.2. EXPERIMENTAL**

### **3.2.1 Materials**

Ketoprofen, Pluronic F127, Pluronic F68, polyvinylpyrrolidone (PVP K-15,  $M_w$  = 10, 000) and hydrolyzed polyvinyl alcohol (PVA,  $M_w$  = 22, 000) were purchased from Spectrum Chemicals & Laboratory Products Corporation (Gardena, CA). Myrj 52 (Sigma) was used as received. Spectral grade dichloromethane was from Fisher Scientific Co. (NJ, USA).

### **3.2.2 Determination of ketoprofen solubility in Pluronic F127 micelles**

Excess ketoprofen was added into 50 ml 1%, 2% and 5% w/v Pluronic F127 aqueous solutions, respectively, and stirred with a magnetic stir bar for 24 h to achieve equilibrium. 10 ml suspensions were filtered with 0.45  $\mu$ m syringe filters and then 2 ml of the filtrates were mixed with 0.2 ml of methanol/water mixture (v:v= 57:40). All samples were then filtered through 0.45  $\mu$ m filters and ketoprofen concentrations were measured by HPLC (Shimadzu, LC-10AT VP, Japan) with a 250 mm long C-18 column (SGE ODS, 5  $\mu$ m).

### **3.2.3 Evaporative precipitation into aqueous solution (EPAS)**

The EPAS apparatus is described in elsewhere.<sup>3-6</sup> The organic ketoprofen with or without surfactant solution in dichloromethane was atomized through an elliptical conical nozzle into hot water at flow rate of 1 ml/min and pressure drop of 3500-5000 psi. 100 ml aqueous stabilizing solution was added to a graduated cylinder that was submerged in a temperature-controlled water bath. The nozzle was submerged approximately 4 cm under the surface of the aqueous solution. Unless indicated otherwise, the stabilizer was added in the aqueous phase and was not present in the organic feed solution. After spraying for a required time, typically less than 20 min, to produce the desired drug/surfactant ratio, the suspension was recovered and analyzed within 2 h to determine the particle size by dynamic light scattering (DLS).

### **3.2.4 Particle size and particle size distribution**

The particle size distribution was measured in the aqueous suspensions by dynamic light scanning (Brookhaven Zetaplus, Brookhaven Instruments Corporation, New York). The EPAS suspension was diluted with distilled water until the count rate of the suspension in DLS ranged in 5-250 kcps. For example, for a suspension



concentration of 30 mg/ml, 0.2 ml of the EPAS suspension was added to 10 ml of water. The particle size distributions were based on intensity. The EPAS suspensions were measured in 2 h while the gels were analyzed overnight. The particle size did not change overnight for the ketoprofen suspension. The particle size of the ketoprofen gel increased only slightly over one month, as discussed below.

### **3.2.5 Crystallinity and surface area measurement**

The crystallinity of the dry powders was examined by x-ray diffraction with a Philips PW 1720 X-ray generator (Philips Analytical Inc., Natick, MA). The reflected intensity of EPAS sample was measured between 5° to 45° with a step size of 0.05° and a dwell time of 1 s. The surface area of the dry powders was measured with a high-speed surface area BET analyzer (NOVA 2000, Quantachrome Instruments, Boynton Beach, FL) with nitrogen as adsorbate.

### **3.2.6 Dissolution test**

After freeze drying or vacuum drying, dry powder containing ~5 mg ketoprofen was placed into a USP basket assembly and stirred at 50 rpm in pure water. 5 ml aliquots of the dissolution medium were sampled at 2, 5, 10, 20, 30, 60 min. The aliquots were filtered through 0.45 µm syringe filters and 2 ml of each sample were diluted with 0.1 ml methanol before analysis. Ketoprofen concentrations were measured using HPLC (Shimadzu, LC-10AT VP, Japan).

## **3.3 RESULTS AND DISCUSSION**

### **3.3.1 Ketoprofen solubility in Pluronic F127 aqueous solutions**

The solubility of ketoprofen in water containing various concentrations of Pluronic F127, the primary surfactant in this study, was measured by HPLC. The solubility measurements were repeated three times for each surfactant concentration. The

solubilities of ketoprofen in 1, 2, 5% w/v Pluronic F127 solutions were  $0.34 \pm 0.01$ ,  $0.81 \pm 0.03$ , and  $2.67 \pm 0.02$  mg/ml, respectively, much higher than its solubility in pure water, 0.05 mg/ml. The solubility of ketoprofen in the micelles increased linearly with the concentration of Pluronic F127. In each case, the Pluronic F127 concentration was well above the cmc,  $4 \times 10^{-3}\%$  w/v.<sup>11</sup> In EPAS experiments, the drug concentration in suspension was much higher than its micellar solubility in Pluronic F127 aqueous solutions, indicating the drug particles were stabilized by surfactant and not merely dissolved in the cores of micelles.

### **3.3.2 Appearance of ketoprofen dispersions in the aqueous suspensions formed by EPAS**

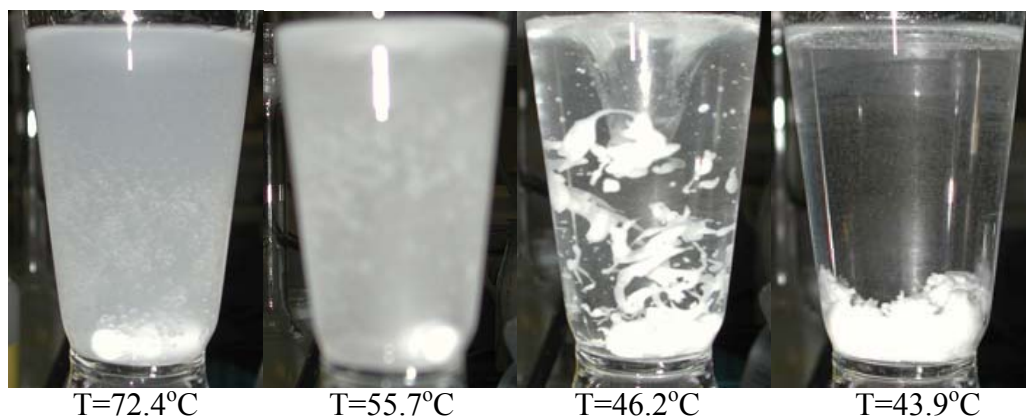
Ketoprofen, with a carboxylic acid group, has a pKa of 4.45. Relative to other commonly studied water insoluble drugs such as danazol and itraconazole etc., ketoprofen has a rather high water solubility, 51 mg/L. In water at the pH of 7 in this study, ketoprofen dissociates and has the potential to function as an anionic surfactant itself in water, as it contains a hydrophobic moiety. Another key property of ketoprofen is its low melting point, 94°C.<sup>12</sup> The temperature of EPAS experiments in this paper ranged from 60 to 90°C. With residual dichloromethane ( $T_m = -96.7^\circ\text{C}$ )<sup>13</sup> and the surfactants in the suspension, ketoprofen was likely dispersed in water as a liquid droplet instead of as solid particles, as discussed below.

To investigate the ketoprofen dispersion produced in EPAS, 20% w/v ketoprofen in dichloromethane was sprayed into pH 1.5, pH 2.0 KCl/HCl buffer solutions and into pure pH neutral water without any surfactant at temperature of 60, 70, 80, and 90°C for 10 min. The ketoprofen concentration in the final dispersion was 20 mg/ml. The dispersions were cooled down after spray while stirring at room temperature and photographed to characterize the state of ketoprofen. For example, pictures of ketoprofen

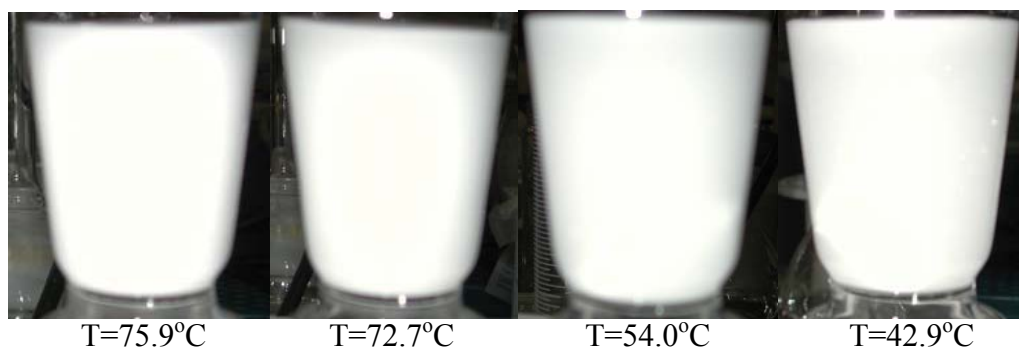
dispersions formed in pH 1.5 buffer solution and pure water at 80°C are shown in Figure 3.1 (a) and (b). The white object at the bottom of the container was a magnetic stir bar. At pH 1.5, individual liquid droplets were visible with the naked eye. It is easy to tell that these were liquid droplets and not solid particles as they were transparent. When the dispersions were cooled down, ketoprofen changed from liquid (72.4, 55.7°C), to semisolid (46.2°C) and to its solid state (43.9°C) as the particles became progressively more opaque. The same behavior was observed with pH 2.0 buffer solutions (not shown). When ketoprofen was sprayed into pure water at neutral pH, the liquid emulsion was much milkier and the droplet size appeared to be significantly smaller than in pH 1.5 buffer solution. Single droplets of ketoprofen in this fine emulsion were not present to the naked eye, as shown Figure 3.1 (b).

For a poorly water soluble drug, drug solubility in water increases significantly as the pH crosses the pKa.<sup>14</sup> In pH 1.5 or 2.0 buffer solution below the pKa of 4.45, ketoprofen does not dissociate. In neutral water (pH= 7), it is dissociated and the solubility becomes significant, 51 mg/L. Here ketoprofen contains an anionic moiety and a hydrophobic residue. This amphiphilic character will lower the interfacial tension between ketoprofen droplets and water. For a given shear produced by the nozzle, much smaller droplets were produced in neutral water where ketoprofen ionized, in the form of a milky white emulsion, than in the low pH buffer solutions. The same change in emulsion morphology was observed at other temperatures, 60, 70, and 90°C. Since the melting point of ketoprofen is 94°C, the formation of ketoprofen liquid droplets rather than solid, indicated the presence of residual dichloromethane, which has a low melting point of -96.7°C. At lower temperatures the amount of residual dichloromethane may increase due to the decrease in its volatility. In the results presented below, the

dispersion formed in EPAS was cooled down to room temperature and the particle size of the solid ketoprofen was then measured by DLS.



(a): In pH 1.5 KCl/HCl buffer solution



(b): In pure water

Figure 3.1. Liquid ketoprofen dispersed in aqueous solution. 20% w/v ketoprofen in dichloromethane was sprayed into a pH 1.5 KCl/HCl buffer solution and pure water without any surfactant at 80°C for 10 min. Ketoprofen concentration in the final dispersion was 20 mg/ml. The dispersion was cooled down at room temperature.

### 3.3.3 Effect of surfactant type and temperature on particle size of ketoprofen

5% w/v ketoprofen in dichloromethane solution was sprayed into 1% w/v aqueous solutions containing various surfactants at 90°C for 20 min. The suspension concentration of ketoprofen was 10 mg/ml. The particle sizes of ketoprofen with various stabilizers are shown in Table 3.1. Some experiments were repeated to check experimental reproducibility and shown as (a), (b) and (c). Stable nanosuspensions of ketoprofen with mean particle size smaller than 400 nm were formed with all three surfactants, Pluronic F127 ( $\text{HO}(\text{CH}_2\text{CH}_2\text{O})_{\sim 101}\text{-}b\text{-(CH}_2\text{CH(CH}_3\text{)O})_{\sim 56}\text{-}b\text{-(CH}_2\text{CH}_2\text{O})_{\sim 101}\text{H}$ ), Pluronic F68 ( $\text{HO}(\text{CH}_2\text{CH}_2\text{O})_{\sim 80}\text{-}b\text{-(CH}_2\text{CH(CH}_3\text{)O})_{\sim 27}\text{-}b\text{-(CH}_2\text{CH}_2\text{O})_{\sim 80}\text{H}$ ) and Myrj 52 ( $\text{CH}_3(\text{CH}_2)_{\sim 16}(\text{OCH}_2\text{CH}_2)_{\sim 40}\text{OH}$ ). For Pluronic F127, Pluronic F68 and Myrj 52, ketoprofen nanoparticles with mean particle size of 230, 383, and 381 nm, respectively, were formed in EPAS. Among these three copolymers, the hydrophilic EO moieties of Pluronic F127 were the longest. Greater steric stabilization with longer hydrophilic blocks would yield smaller particles if the other factors were equal, for example the level of surfactant adsorption. Even though the lowest molecular weight surfactant Myrj 52 may be expected to diffuse the fastest, it produced larger particles than Pluronic F127. Perhaps the shorter stabilizing PEO chain provided weaker steric stabilization. Another possibility is that a single PEO chain provides less stabilization than dual PEO end segments. The adsorption of Pluronic F127 on the particles may be expected to be higher than for Pluronic F68 since it has higher weight fraction of hydrophobic moieties. Differences in solubilities of ketoprofen in the three different types of micelles could also influence the particle size. Both surfactant micelles and free surfactant diffuse to the growing particle surface. The micelle diffusion and the

deposition of surfactant from the micellar surface will depend upon the micelle size and surfactant mobility in the micelles.

With the homopolymer PVA in aqueous solution, the particle size was much larger than with the various copolymers in the aqueous phase. A dispersion was not formed with PVP K-15 in the aqueous phase. An oily ketoprofen liquid layer floated on the top of aqueous phase. It is well known that a homopolymer is often a less effective stabilizer than a properly designed copolymer, since the copolymer has both hydrophilic and hydrophobic moieties. The hydrophobic moieties attach to the particle/droplet surface and hydrophilic moieties extend to water, stabilizing the particles/droplet from agglomeration, flocculation and coalescence.

To determine the effect of temperature on ketoprofen particle size, experiments were conducted at various temperatures from 60 to 90°C with 1% w/v Pluronic F127 in aqueous solution. As the temperature was decreased from 80 to 70°C, the particle size distribution shifted significantly to smaller particles. This decrease can be influenced by several factors. Decreasing temperature may increase the steric repulsion between the EO blocks due to better solvation by water.<sup>15</sup> At lower temperature, particle growth by diffusion of ketoprofen molecules in the organic phase is slower. The lower evaporation rate will slow down nucleation of the ketoprofen droplets. This slower production of nuclei may give the surfactant more time to diffuse from the water phase and coat the particles to lower growth. However, the evaporation was fast enough to prevent the buildup of large organic droplets in the water phase. As the temperature was lowered further, the average particle size increased slightly and some much larger particles were formed. The large particles may reflect too much time for growth in large slowly evaporating organic droplets.

Table 3.1. Effect of surfactant type and temperature on ketoprofen particle size. Organic phase: 5% w/v ketoprofen in dichloromethane; aqueous phase: 1% w/v surfactant solution; t= 20 min; suspension concentration: 10 mg/ml.

Aqueous surfactant	T <sub>bath</sub> (°C)	T <sub>thermo</sub> (°C)	D <sub>mean</sub> (nm)	Particle size distribution (nm)
Pluronic F127	90	81.4	230	16-25 (3%); 48-139 (50%); 214-626 (47%)
Pluronic F68	90	81.4	381	212-251 (51%); 485-597 (49%)
Myrj 52	90	81.4	383	224-264 (57%); 509-625 (43%)
PVA	90	81.4	2551	13-32 (14%); 56-237 (54%); >5 µm (32%)
PVP K-15			Did not form suspension	
Pluronic F127	80	75.3	184	17-22 (4%); 79-159 (67%); 278-487 (29%)
Pluronic F127	70	64.4	114	27-39 (25%); 123-164 (75%)
Pluronic F127 (a)	60	55.1	133	12-25 (5%); 53-135 (91%); 729-879 (1%); 1279-1860 (3%)
Pluronic F127 (b)	60	54.9	126	17-24 (2%); 49-121 (95%); 1056-1266 (1%); 1816-2607 (2%)

(a), (b): experiment reproducibility



### **3.3.4 Effect of drug feed concentration and concentration of the ketoprofen aqueous suspension on the particle size**

To investigate the effect of feed concentration, ketoprofen solutions were sprayed into 1% w/v Pluronic F127 at a temperature of 80°C. As summarized in Table 3.2, increasing in the ketoprofen concentration in the aqueous suspension increases the particle size. At a given drug feed concentration, 20% w/v, the particle size of ketoprofen increased from 136 nm to 401 nm when the suspension concentration increased from 10 to 30 mg/ml. The higher particle concentration in the suspension increases the collision rate and increases the drug-to-surfactant ratio. The higher ratio may lead to reduced surfactant adsorption and thus weaker steric stabilization. Both of these factors would be consistent with the observed larger particles.

At a given ketoprofen suspension concentration, the ketoprofen particle size decreased with increasing drug feed concentration. For a 10 mg/ml aqueous suspension, when the drug feed concentration increased, the mean particle size of ketoprofen decreased slightly from 183 nm to 152 nm and the percentage of the largest particles also decreased. At 1% w/v drug in the feed, 2% of the particles were larger than 2  $\mu$ m, but at 20% w/v drug in the feed, all the particles were smaller than 300 nm. At a suspension concentration of 30 mg/ml, when the feed concentration increased from 20% w/v to 70% w/v, the mean particle size of ketoprofen decreased by a factor of more than three with all particles smaller than 200 nm. With an increase in the drug feed concentration, the supersaturation increases during evaporation, leading to faster nucleation resulting in smaller particles. Furthermore, the shorter spray time for the higher feed drug concentration provided less time for particle growth. The formation of stable nanosuspensions of ketoprofen, despite the very high drug-to-surfactant ratio of 3, is unique relative to other drugs such as cyclosporine A, danazol and itraconazole etc.<sup>3-6</sup>

Table 3.2. Effect of feed drug concentration and suspension concentration on ketoprofen particle size at 80°C. Aqueous phase: 1% w/v Pluronic F127 solution.

C <sub>drug</sub> in organic phase (% w/v)	C <sub>susp.</sub> (mg/ml)	t (min)	D/S ratio	D <sub>mean</sub> (nm)	Particle size distribution (nm)
1	10	100	1	183	25-51 (15%); 104-253 (83%); 2129-3037 (2%)
5	10	20	1	184	17-22 (4%); 79-159 (67%); 278-487 (29%)
20 (a)	10	5	1	136	10-13 (2%); 47-94 (56%); 163-327 (42%)
20 (b)	10	5	1	147	35-46 (21%); 144-206 (79%)
20 (c)	10	5	1	152	13-18 (3%); 46-73 (29%); 144-255 (68%)
20	20	10	2	169	27-51 (12%); 95-210 (80%); 395-635 (8%)
20	30	15	3	401	27-41 (6%); 95-222 (88%); 3474-5303 (6%)
70 (a)	30	4.3	3	122	29-37 (16%); 118-163 (84%)
70 (b)	30	4.3	3	122	30-40 (19%); 122-174 (81%)

(a), (b), (c): experiment reproducibility for separate sprays

### **3.3.5 Effect of surfactant concentration, pH and ionic strength on ketoprofen particle size**

The negative charge due to dissociation of the carboxylic acid groups may enhance the stability of the ketoprofen suspension in the aqueous phase by adding electrostatic stabilization to complement the steric stabilization from the nonionic surfactant. To study the influence of ketoprofen dissociation on the stabilization, 20% w/v ketoprofen solution in dichloromethane was sprayed into various concentrations of Pluronic F127 at two different values of pH for 5 or 10 min. The concentration of Pluronic F127 in the aqueous phase ranged from 0 to 1% w/v. The temperature was 80°C. As shown in Table 3.4, with no surfactant in the aqueous phase, ketoprofen did not float to the top of the suspension, unlike the case for other drugs tested in EPAS including danazol, itraconazole and carbamazepine.<sup>3-6</sup> A milky suspension with a mean particle size of 4.0  $\mu\text{m}$  formed. At 0.1% w/v Pluronic F127, the mean particle size of ketoprofen was 135 nm and only 5% of the particles were larger than 500 nm. When the Pluronic F127 concentration was increased to 1% w/v, the mean particle size changed only slightly, but all particles were smaller than 210 nm.

To examine the effect of pH, the same ketoprofen organic solution was sprayed into 1% w/v Pluronic F127 dissolved in pH 2.0 KCl/HCl buffer solution. At a suspension concentration of 10 mg/ml, stable ketoprofen suspensions were still formed with a mean particle size of 151 nm. But after 5 min where the suspension concentration reached 10 mg/ml, further spray would cause phase separation of liquid ketoprofen and water. The milky dispersion would suddenly become much clearer due to coalescence of ketoprofen droplets. In contrast, stable nanosuspensions of ketoprofen were formed in pH neutral pure water at suspension concentrations of even 30 mg/ml, as shown in Table 3.3. It is apparent that electrostatic stabilization due to the negative charge on the ketoprofen

droplets retarded emulsion flocculation and coalescence. Steric stabilization requires time for the surfactant to be adsorbed, whereas electrostatic stabilization is extremely rapid once the particles are surrounded by a sufficient amount of water. At low pH below the  $pK_a$ , 1% Pluronic F127 was not sufficient to stabilize concentrated ketoprofen particles/droplets without the electrostatic stabilization, as the droplets coalesced and phase separated. The effect of drug-to-surfactant ratio has been characterized for the steric stabilization of drug particles during Young et al.<sup>16</sup> in a related process, rapid expansion from supercritical to aqueous solution (RESAS).

The effect of ionic strength on the ketoprofen suspension was also investigated. A 20% w/v ketoprofen solution in dichloromethane was sprayed into 1% w/v Pluronic F127 dissolved in 1% w/v NaCl aqueous solution, which had an ionic strength of 0.17 M. At a suspension concentration of 10 mg/ml, a milky but unstable ketoprofen suspension was formed which coalesced after 1.3 min stirring at 80°C after the spray. This experiment further confirmed that electrostatic stabilization due to the negative charge on the ketoprofen droplets retarded emulsion flocculation and coalescence. The high ionic strength screened the electrostatic stabilization, and the emulsion coalesced whereas it was very stable at zero ionic strength.

Table 3.3. Effect of aqueous surfactant concentration and pH on ketoprofen particle size at 80°C. Organic phase: 20% w/v ketoprofen solution in dichloromethane; t= 5 min; suspension concentration: 10 mg/ml.

C <sub>surf.</sub> in aqueous phase (% w/v)	pH	C <sub>susp.</sub> (mg/ml)	D/S ratio	D <sub>mean</sub> (nm)	Particle size distribution (nm)
0	7	10	∞	3986	192-332 (38%); 861-1296 (20%); >5 µm (42%)
0.01	7	10	100:1	1378	42-178 (50%); 422-1778 (38%); >5 µm (12%)
0.1	7	10	10:1	135	89-136 (95%); 578-746 (5%)
1 (a)	7	10	1:1	147	35-46 (21%); 144-206 (79%)
1 (b)	7	10	1:1	163	20-30 (8%); 78-133 (50%); 203-345 (42%)
1	2	10	1:1	151	19-27 (3%); 57-85 (27%); 154-252 (70%)
1	2	14	1.4:1	Phase separation	

(a), (b): experiment reproducibility for separate sprays

### **3.3.6 Ketoprofen-Pluronic F127 Gel formation at high Pluronic concentration in aqueous phase.**

For certain PPO-PEO-PPO block polymers (Pluronic) in water, a gel region appears at high concentration (typically >20 wt%) and intermediate temperatures.<sup>17-20</sup> Due to the possibility of solubilization of both water-soluble and water-insoluble solutes in these gels, they are of great interest in drug delivery.<sup>20-22</sup> For the Pluronic F127-water system,<sup>17</sup> the gel region occurs at polymer concentration above approximately 18 wt%, but only at intermediate temperatures, e.g. between 20 and 85°C for a concentration of 25 wt%. The viscosity becomes small, even in concentrated solutions at temperatures above or below the gelation temperature. According to Wanka et al.<sup>11</sup> and Mortensen et al.,<sup>23</sup> gels of Pluronic consist of a close-packed array of block copolymer micelles.

Gel formation was investigated in EPAS experiments. Either 20 or 70% w/v ketoprofen with or without 5% Pluronic F127 in the organic phase was sprayed into Pluronic F127 aqueous solution. The temperatures ranged from 60 to 90°C. Figure 3.2 shows a photograph of ketoprofen-Pluronic F127 gel formed at room temperature after cooling from the spray temperature of 90°C. When the gel was heated in hot water (80°C) for 3 min, the gel was converted to a turbid suspension. Upon recooling to room temperature, the translucent gel reformed. Thus the gelation was thermally reversible. The particle size of ketoprofen did not change during the heating and recooling. It was found that if the stirring was too strong and a lot of air was trapped in the gel, ketoprofen would crystallize along the air cavities. In the air cavities, the unprotected ketoprofen that was not complexed with the gel began to crystallize and form large particles.

The conditions where the gel formed and the resulting particle sizes at various conditions are shown in Table 3.4. Either with or without Pluronic 127 in the organic feed, when the Pluronic F127 concentration in the aqueous phase was 5% w/v, the

sprayed suspension was as milky as in the above experiments with less Pluronic F127, except more viscous. When the suspension was cooled down at room temperature with gentle magnetic stirring, a bluish, transparent ketoprofen-Pluronic gel formed. The ketoprofen particles in the gel were much smaller than those formed in suspensions with lower Pluronic F127 concentrations, where a gel did not form upon cooling. At least 90% particles were smaller than 50 nm, while the samples with lower Pluronic F127 concentrations contained particles larger than 150 nm. For surfactant concentrations lower than 5% w/v, no gel was formed. Compared to the Pluronic F127-water binary system, a gel was formed at a much lower Pluronic concentration (5.75-6.61 wt% including the water evaporation during EPAS spray) with ketoprofen than without ketoprofen (>18 wt%). In the presence of 1 M NaCl, the gel concentration of Pluronic F127 only shifted from 18 wt% at 50°C to 17 wt% at 30°C.<sup>17</sup> Since the solubility of ketoprofen is only 0.05 mg/ml or  $1.97 \times 10^{-4}$  M at room temperature, it would not be expected to shift the Pluronic F127 gel concentration due to a general effect based on ionic strength. Ketoprofen particles may be distributed both inside the PPO core of Pluronic F127 micelles and in the PEO corona. The polar and ionic carboxylate groups will interact favorably with the EO moieties of Pluronic F127 to provide order and enhance gel formation. Also, since the size of the coated drug particles (50 nm) is larger than that of the Pluronic micelles (15-20 nm),<sup>24</sup> the Hamaker interaction between ketoprofen particles may also be expected to aid. At high temperature, the lattice of the Pluronic F127 gel was disrupted by contraction of the micelles as the average polyethylene oxide hydrodynamic radius ( $R_H$ ) decreased with temperature.<sup>17</sup>

The viscosity of the ketoprofen-Pluronic F127 gel was measured with a Brookfield digital viscometer (model DV-I+, Brookfield Engineering Laboratories, Inc. Middleboro, MA) at room temperature. A spindle (LV 2 with a LV guardleg) was

rotated at various speeds in a 500 ml gel sample contained in a 600 ml beaker. The viscosity was measured at 6 min after rotation of the spindle. The gel yielded a non-Newtonian rheology; the viscosity decreased from 1185 cp at 2 rpm shear rate to 294 cp at 10 rpm and leveled off to 85 cp at 100 rpm. Gels in this viscosity range are appropriate for parenteral injection.<sup>25</sup> Because of high viscosity of the gel, the ketoprofen diffused slowly in the gel and particle aggregation and Ostwald ripening were very slow. A gel formed at 80°C was stable for 1 month with a slight increase in mean particle size from 78 nm to 115 nm.





Gel formed at 90°C  
 $D_{\text{mean}} = 71 \text{ nm}$   
 21-39 nm (90%);  
 353-576 nm (10%)

Gel heated in 80°C  
 water bath for 3  
 min.

Gel formed again with  
 cool it down  
 $D_{\text{mean}} = 80 \text{ nm}$   
 23-39 nm (84%);  
 475-595 nm (16%)

Figure 3.2. Thermo reversible gel of ketoprofen-Pluronic F127 formed at room temperature

Table 3.4. Gel formation with 5% w/v Pluronic F127 in aqueous phase. Organic phase: 20% or 70% w/v ketoprofen solution in dichloromethane; suspension concentration: 30 mg/ml.

C <sub>F127</sub> in organic phase (% w/v)	C <sub>F127</sub> in aqueous phase (% w/v)	C <sub>drug</sub> in organic phase (% w/v)	t (min)	T (°C)	Gel formation	D <sub>mean</sub> (nm)	Particle size distribution (nm)
0	1	70	4.3	80	N	122	29-37 (16%); 118-163 (84%)
0	2	70	4.3	80	N	136	18-27 (14%); 45-76 (29%); 157-264 (57%)
0 (a)	5	70	4.3	80	Y	95	18-32 (28%); 59-96 (58%); 251-408 (14%)
0 (b)	5	70	4.3	80	Y	81	26-37 (50%); 104-165 (50%)
5	1	20	15	90	N	139	37-49 (21%); 140-198 (79%)
5	2	20	15	90	N	120	18-39 (23%); 85-185 (73%)
5	5	20	15	90	Y	71	21-39 (90%); 353-576 (10%)
5	5	20	15	80	Y	76	18-45 (98%); 2570 (2%)
5	5	20	15	70	Y	108	29-47 (41%); 123-222 (59%)
5	5	20	15	60	Y	50	24-32 (78%); 104-151 (22%)

(a), (b): experiment reproducibility; Y: gel formed; N: no gel formed.

### **3.3.7 The crystallinity, surface area and dissolution rate of dried ketoprofen-Pluronic F127 gel and suspension**

A ketoprofen gel was formed by spraying 20% w/v ketoprofen + 5% w/v Pluronic F127 in dichloromethane into 5% w/v Pluronic 127 for 15 min at 80°C and cooling the suspension to room temperature with magnetic stirring. The ketoprofen concentration in the suspension was 30 mg/ml. A ketoprofen suspension was also formed by spraying 20% w/v ketoprofen in dichloromethane into 1% w/v Pluronic F127 for 5 min at 80°C. The ketoprofen concentration in the suspension was 10 mg/ml and the drug-to-surfactant ratio was 1:1. The gel was dried with two different methods. One gel sample was vacuum dried at room temperature and -30 in. Hg. 100 ml of the gel was poured into three 500 ml beakers to form a thin gel layer. It took more than three days to dry the gel at room temperature due to slow diffusion of water from the gel. The other sample was dried by slowly injecting the gel into liquid nitrogen with a syringe and then lyophilizing the frozen mixture for 3 days. The suspension was also dried by flash freezing in liquid nitrogen and was lyophilized for 3 days.

The BET method was used to measure the surface area of the dried ketoprofen gels. The surface area of the ketoprofen gel dried by lyophilization was 9.7 m<sup>2</sup>/g, while that of the gel dried with vacuum was 8.3 m<sup>2</sup>/g. The surface area for the 50 nm particles in the gel that was not dried would be much larger. The x-ray diffraction patterns for the dried gel and suspension are shown in Figure 3.3. Whereas ketoprofen in the suspension remained amorphous after lyophilization, the ketoprofen in the gel crystallized during the drying step. The highest ketoprofen peaks coincided with those of bulk Pluronic F127. The ketoprofen peaks were much smaller and broader in EPAS samples as well as in the physical mixture. However, the ketoprofen peaks at  $2\theta = 18.4^\circ$  were evident for the gels dried by vacuum or lyophilization. Thus, ketoprofen crystallized during drying by either

technique, lyophilization or vacuum drying. As observed in the above experiments with the trapped air, it is likely that any vapor bubbles formed during drying may have caused crystallization. Another possibility is that the ketoprofen at the surface of the thin film of the gel crystallized. Finally as the gel dried out, the residual water may have added mobility to the ketoprofen and caused crystallization. The dried gel was redispersed into water by magnetic stirring and the particle size was measured. The mean particle size of ketoprofen gel after drying by vacuum and lyophilization was 12.7 and 12.2  $\mu\text{m}$  respectively, as measured with a Mastersizer-S (Malvern Instruments Ltd., U. K.) since the particle size was too large for DLS. The particles from Mastersizer were somewhat aggregated based on the BET surface areas.

The dissolution rates of the wet ketoprofen gel, the gels dried by vacuum and by lyophilization, the suspension dried by lyophilization (formed with dilute Pluronic F127), and a physical mixture of ketoprofen and Pluronic F127, with the same composition as the gel, are shown in Figure 3.4. The ketoprofen release from the wet gel or lyophilized suspension, 98% and 94%, respectively, in 2 minutes was extremely rapid. However, when the gel was dried by vacuum or lyophilization, the dissolution rate of ketoprofen was much slower than for the wet gel. There are two reasons for the slower dissolution rates. One is due to the large particle size and smaller surface area after drying. The other is due to slow hydration and swelling of ketoprofen-Pluronic F127 complex which was observed during dissolution test. The slow hydration rate of this complex slowed down the dissolution. In all cases, the release rate of ketoprofen gel was much higher than that of bulk ketoprofen and a physical mixture with Pluronic F127.

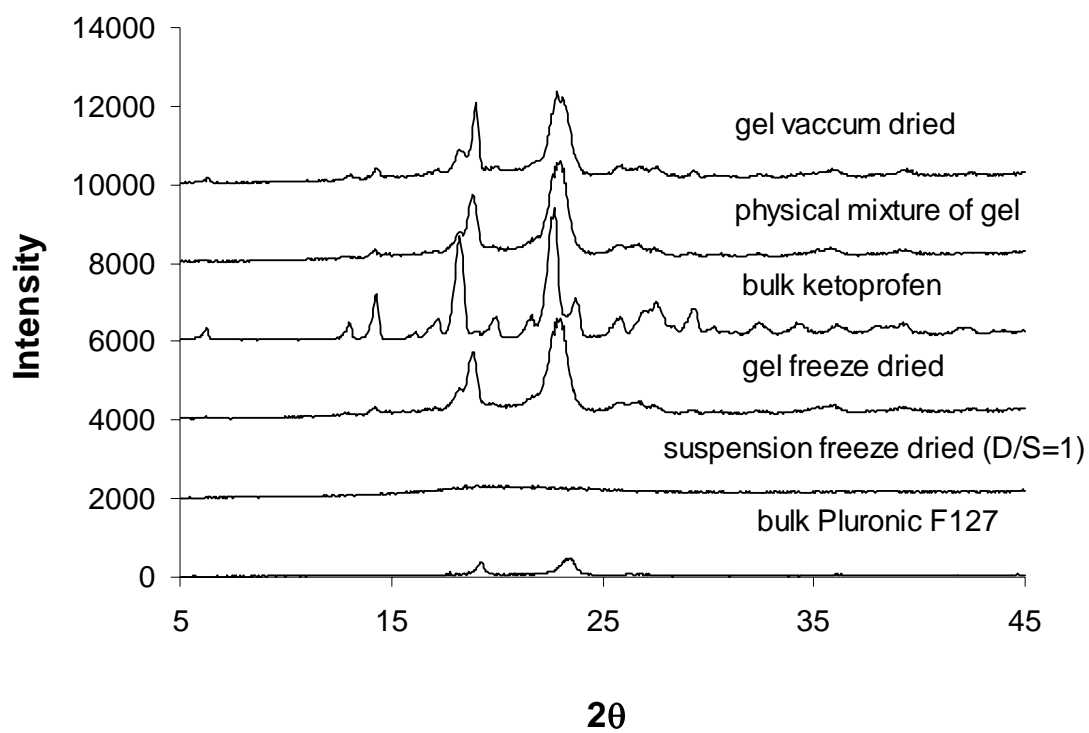


Figure 3.3. X-ray diffraction profiles of dried ketoprofen gels and suspensions by lyophilization or vacuum drying

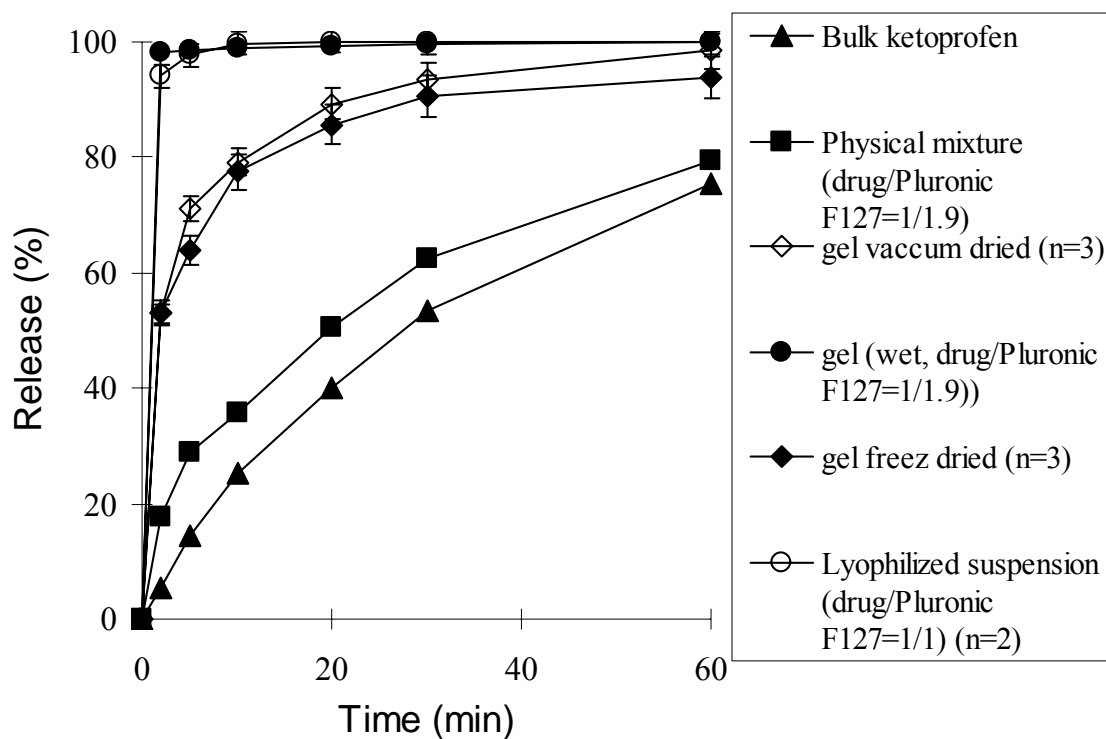


Figure 3.4. Dissolution profiles of dried ketoprofen gels and suspensions by lyophilization or vacuum drying

### 3.4 CONCLUSIONS

Aqueous ~50 nm gels of a poorly-water soluble drug, ketoprofen, were produced by evaporative precipitation into aqueous solution (EPAS) followed by cooling. In only two minutes, 98% of this wet gel dissolved. In addition, 94% of the ketoprofen dissolved from suspensions with lower surfactant concentration, which were dried by lyophilization. The size of the particles in the gel changed only a small amount over one month reaching only 115 nm. The addition of electrostatic repulsion, due to ketoprofen ionization, to complement steric stabilization led to much smaller particles than normally produced by EPAS. Furthermore, the particles were amorphous, whereas crystalline particles are normally formed. The favorable interactions between ketoprofen and Pluronic F127 led to amorphous particles for low Pluronic F127 concentrations. Stable ketoprofen particles with a mean particle size of 135 nm, measured by dynamic light scattering, were formed with only 0.1% w/v Pluronic F127 and with an exceptionally high drug-to-surfactant ratio of 10:1. Here the concentration was well below the gellation concentration. For higher Pluronic concentrations, these interactions induced gellation and produced unusually smaller particles, as small as 50 nm. When the drug concentration in the organic phase increased from 20% to 70% w/v, the particle size of ketoprofen decreased from 401 to 122 nm at suspension concentration of 30 mg/ml due to higher supersaturation. The rapidly dissolving wet gels, with relatively low viscosities, are of interest in transdermal and parenteral delivery; furthermore, the gels may be dried for oral delivery.

### 3.5 REFERENCE

- (1) Oh D, C., RL, Amidon GL Pharm Res 1993, 10, 264-270.
- (2) Ansel, H. C.; Allen, L. V.; Popovich, N. G. Pharmaceutical dosage forms and drug delivery systems, 7th ed. ed.; Lippincott-Williams & Wilkins: Philadelphia, PA, 1999.
- (3) Chen, X.; Young, T. J.; Sarkari, M.; Williams, R. O.; Johnston, K. P. Int J Pharm 2002, 242, 3-14.
- (4) Chen, X. Drug. Del. Sci. Techn. to appear.
- (5) Chen, X.; Vaughn, J. M.; Yacaman, M. J.; Williams, R. O.; Johnston, K. P. J. Pharm. Sci 2004, 93, 1867-1878.
- (6) Sarkari, M.; Brown, J.; Chen, X.; Swinnea, S.; Williams, R. O.; Johnston, K. P. Int J Pharm 2002, 243, 17-31.
- (7) Cevc, G. Advanced Drug Delivery Reviews 2004, 56, 675-711.
- (8) Shama, J. O.; Zhang, Y.; Finlay, W. H.; Roaa, W. H.; Lobenberg, R. International Journal of Pharmaceutics 2004, 269, 457-467.
- (9) Couvreur, P.; Puisieux, F. Advanced Drug Delivery Reviews 1993, 10, 141-162.
- (10) Chen, X.; Vaughn, J. M.; Yacaman, M. J.; Williams, R. O.; Johnston, K. P. J. Pharm. Sci. 2004, 93, 1867-1878.
- (11) Wanka, G.; Hoffmann, H.; Ulbricht, W. Colloid polymer science 1990, 268, 101-117.
- (12) The Merck Index: an encyclopedia of chemicals, drugs, and biologicals; Merck & CO., Inc.: Rahway, 1996.
- (13) Yaws, C. L. Chemical properties handbook: physical, thermodynamic, environmental, transport, safety, and health related properties for organic and inorganic chemicals; McGraw-Hill: New York, 1999.
- (14) Martin, A. N. Physical pharmacy: physical chemical principles in the pharmaceutical sciences, 4th ed.; Lea & Febiger: Philadelphia, 1993.
- (15) de Bruijn, V. G.; van den Broeke, J. P.; Leermakers, F. A. M.; Keurentjes, J. T. F. Langmuir 2002, 18, 10467-10474.



- (16) Young, T. J.; Mawson, S. M.; Johnston, K. P. *Biotechnol. Prog.* 2000, 402-407.
- (17) Malmsten, M.; Lindman, B. *Macromolecules* 1992, 25, 5440-5446.
- (18) Malmsten, M.; Lindman, B. *Macromolecules* 1993, 26, 1282-1286.
- (19) Brown, W.; Schillen, K.; Almgren, M. *Jornal of physical chemistry* 1991, 95, 1850-1858.
- (20) Gilbert, J. C.; Hadgraft, J.; Bye, A.; Brookes, L. G. *International Journal of Pharmaceutics* 1986, 32, 223-228.
- (21) Wei, G.; Xu, H.; Ding, P. T.; Li, S. M.; Zheng, J. M. *Journal of controlled release* 2002, 83, 65-74.
- (22) Miyazaki, S.; Tobiyama, T.; Takada, M.; Attwood, D. *Jornal of pharmacy and pharmacology* 1995, 47, 455-457.
- (23) Mortensen, K.; Brown, W.; Norden, B. *Physical Review Letters* 1992, 68, 2340-2343.
- (24) Cohn, D.; Sosnik, A.; Levy, A. *Biomaterials* 2003, 24, 3707-3714.
- (25) Paavola, A.; Yliruusi, J.; Rosenberg, P. *Journal of Controlled Release* 1998, 52, 169-178.

## CHAPTER 4

### **Rapid Dissolution of High Potency Danazol Particles Produced by Evaporative Precipitation into Aqueous Solution**

#### **4.1 INTRODUCTION**

From a therapeutic and biological point of view, a drug delivery system with a high drug-to-surfactant ratio or payload has many advantages. This will allow an effective dose to be administered and consequently produce high blood levels with less potential interactions from the excipients. A major challenge for water insoluble drugs is to achieve rapid release with a high drug-to-surfactant ratio or payload. Typically, the ratio of drug-to-surfactant ranges from 1:10 to 1:1.<sup>1-3</sup> For these compounds, permeability of biological membranes is often not an obstacle to absorption since the lipophilicity of a drug, which facilitates permeation, generally increases as the solubility decreases.<sup>4</sup>

Oral bioavailability of water insoluble drugs is often dependent upon the rate of dissolution of the drug in the gastrointestinal tract.<sup>5</sup> The dissolution rate of an active pharmaceutical ingredient (API) into an aqueous solution depends upon the diffusion coefficient,  $D$ , the surface area,  $S$ , the local equilibrium concentration of API in the diffusion layer surrounding the particle,  $C_s$ , and the diffusion layer thickness,  $h$ , as follows:

$$\frac{dm}{dt} = \frac{DS}{h}(C_s - C) \quad (\text{Eq. 4.1})$$

where  $C$  is the concentration of the API in bulk solution. The surface area  $S$  may be increased by reducing the particle size,<sup>6</sup> by increasing the porosity and by enhancing wetting of the particles by the dissolution media. Wetting may be enhanced with hydrophilic excipients that are surface active at the API-aqueous interface.<sup>7</sup> The value of

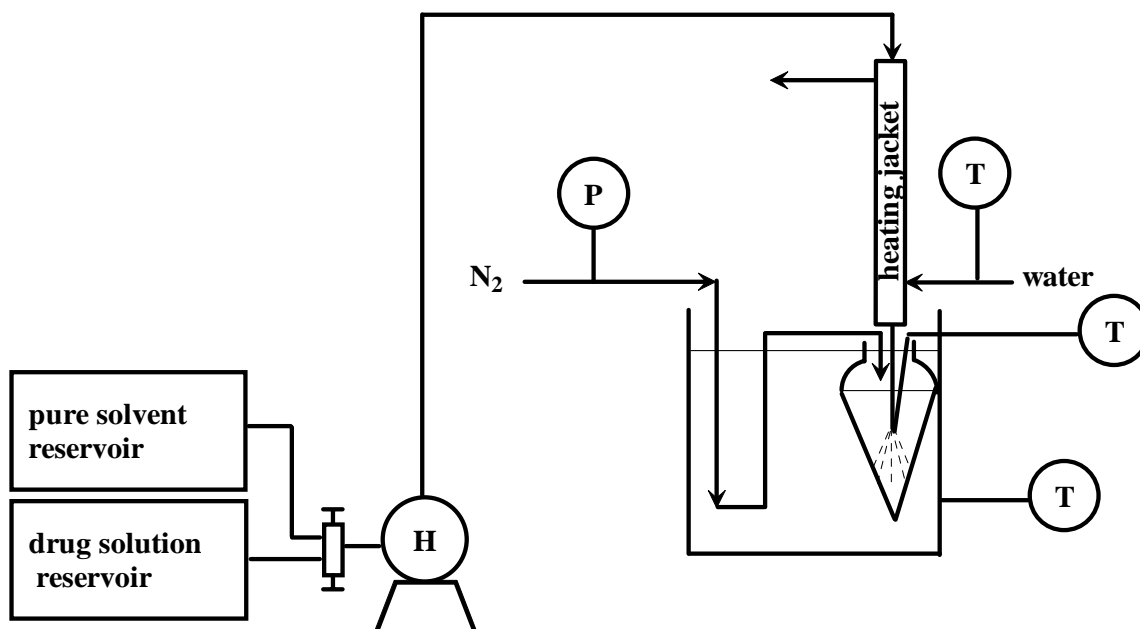
$C_s$  may also be enhanced by trapping the API in metastable crystalline or amorphous states with higher free energies than the lowest energy equilibrium crystalline state.

Although APIs may be dissolved in micelles, vesicles or microemulsions, the drug-to-surfactant ratios are typically well below 1:1.<sup>8-10</sup> An alternative approach is to stabilize drug particles formed by mechanical milling.<sup>11,12</sup> Widely used batch mechanical techniques based on high shear or impactation, including microfluidization and milling can be limited by unfavorable yields due to solid losses, high polydispersity in particle size, shear-induced particle denaturation, long processing time, high energy requirements and the need for separating the product and processing agent.<sup>13, 14</sup> To attempt to overcome many of these limitations, particles may be formed from solution in spray processes. However, drug-to-surfactant ratios are still typically below 1:1. It has been highly challenging to raise the potency further due to incomplete coating of particles by surfactant that leads to poor wetting, particle aggregation, and low surface area. Amorphous cyclosporine particles coated with various surfactants have been produced by rapid expansion from supercritical to aqueous solution (RESAS) utilizing CO<sub>2</sub> as the supercritical fluid.<sup>15</sup> The average particle size increased from below 1 micron to well over 1 micron at a threshold drug/surfactant ratio of about 0.6-0.7.

Another approach is to use solid dispersions to increase effective surface area. However, the dissolution rate of triamterene from melted and spray-dried solid dispersions containing D-mannitol decreased significantly as the drug loading increased from 5% to 40%.<sup>16</sup> Similar behavior was observed with ketoprofen-PEG 6000 dispersions.<sup>17</sup> Rowley et al.<sup>18</sup> and Brown et al.<sup>19</sup> showed that adsorption of a surfactant at a solid drug particle surface, by equilibrating drug particles with surfactant aqueous solution, improved wetting, as indicated by the contact angle, and dissolution rates. Reduction in contact angle from 91° for untreated danazol to 62° was achieved at a high

drug/surfactant ratio of 99:1, with a corresponding increase in drug dissolution from 35 to 65% in 10 minutes.

Evaporative precipitation into aqueous solution (EPAS) is a new process to produce submicron to micron-sized hydrophobic drug particle dispersions stabilized by surfactants.<sup>20, 21</sup> As shown in Figure 4.1, a drug dissolved in an organic solvent is sprayed through an atomizer into an aqueous solution containing a hydrophilic stabilizer to produce an aqueous dispersion. Rapid evaporation of the small organic droplets produces large supersaturation and rapid nucleation of the API. Hydrophilic stabilizers in water surrounding the shrinking organic droplets diffuse to the surface of the growing particles to inhibit particle growth and in some cases, crystallization. In previous studies, EPAS suspensions were dried by spray drying or lyophilization. All of the surfactant stabilizer remained with the product after drying leading to a moderate drug-to-surfactant ratio ranging from 1:4 to 1:1. Here we show that only a fraction of the surfactant utilized to stabilize the aqueous suspension formed during the EPAS process is needed in the final powder to achieve high dissolution rates.



**T--thermocouple;**  
**P--pressure regulator;**  
**H--HPLC pump**

Figure 4.1. The apparatus of EPAS

The primary objective of this study is to produce danazol particles by EPAS with high dissolution rates and extremely high drug-to-surfactant ratios greater than 5, corresponding to a potency (wt drug/wt drug + wt surfactant) above 80%. An aqueous suspension is produced by EPAS as done earlier<sup>20, 21</sup> to produce surfactant coated particles. The suspension is then centrifuged and the supernatant is decanted to remove the free surfactant in order to raise the potency in the precipitate. Also, this centrifugation process is utilized to determine the adsorption of the surfactant on the drug surface. We hypothesize that the free surfactant is not needed for high dissolution rates

once the particles are coated with adsorbed surfactant. It will be shown that the adsorbed surfactant is sufficient to prevent aggregation and enhance wetting to maintain a high S. The dissolution rate is analyzed as a function of the surfactant adsorption, particle size, surface area, contact angle, particle morphology and crystallinity to provide an understanding of the mechanism of enhanced dissolution rates. From a processing point of view, removal of water by centrifugation followed by vacuum drying is faster and more economical than lyophilization. Also, the yields can be improved relative to spray drying due to ease of particle recovery. Danazol was chosen as the model drug given its low water solubility of 0.6 µg/ml.

## **4.2 EXPERIMENTAL**

### **4.2.1 Materials**

Danazol was purchased from Spectrum Chemicals& Laboratory Products Corporation (Gardena, CA). Pluronic F127 (BASF, Mount Olive, NJ), polyvinyl pyrrolidone (PVP K-15,  $M_w = 10,000$  and PVP 40T,  $M_w = 40,000$ ) (Sigma, St. Louis, MO), sodium lauryl sulfate (Sigma) and sodium deoxycholic acid (Sigma) were used as received. HPLC grade acetonitrile was from EM Science (NJ) and spectro grade dichloromethane was from Fisher Scientific Co. (NJ).

### **4.2.2 Evaporative precipitation into aqueous solution (EPAS)**

The EPAS apparatus is shown in Figure 4.1. The danazol solution in dichloromethane was fed by an HPLC pump through a 3 m long 1/16 in. o.d. × 0.030 in. i.d. stainless steel coiled tube contained within a 1-1/2 in. o.d. × 24 in. long plastic water jacket (Alltech). Water was circulated through the jacket with a Julabo MP temperature controller. The organic solution was atomized through an unheated insulated adjustable restrictor (5 mm dia. × 136 mm long, ISCO, USA) into hot water. The angle of the stem

was 30°, and the diameter was tapered from 0.038 in. down to 0.022 in. The angle of the seat was 60°. Atomization was achieved by adjusting the nozzle valve manually to maintain a pressure drop to about 3500 psi. The aqueous stabilizing solution was contained in a 250 ml plastic cylinder submerged in a temperature-controlled water bath. The nozzle was submerged approximately 4 cm under the surface of the aqueous solution. To suppress and drain the foam produced by the organic vapor, nitrogen was blown downwards on top of the foam at 20 psi into the cylinder through three 1/16 in. o.d. × 0.030 in. i.d. stainless steel tubes. Unless indicated otherwise, the stabilizer was added in the aqueous phase and was not present in the organic feed solution. After spraying for a required time to produce the desired drug/surfactant ratio, the suspension was recovered and analyzed within 30 min to determine the particle size by light scattering with a Malvern Mastersizer-S (Malvern Instruments Ltd., U. K.).

#### **4.2.3 Surfactant adsorption measurement**

To quantify surfactant stabilization of the danazol particles in the EPAS suspension, surfactant adsorption was measured based on a mass balance between the supernatant and precipitate. In these measurements,  $W_{\text{sup,wet}}$  was the weight of the supernatant before drying, which included danazol, which may dissolve in micelles or surfactant complexes if formed.  $W_{\text{sup,dry}}$  was the weight of the supernatant after drying to remove water.  $W_{\text{ppt,wet}}$  was the weight of the precipitate before drying, which includes danazol, adsorbed surfactant and a small amount of supernatant with the same composition as the bulk supernatant.  $W_{\text{ppt,dry}}$  was the weight of the precipitate after drying.  $W_{\text{drug,ppt}}$  was the amount of danazol in the precipitate measured by HPLC.  $W_{\text{surf,ads}}$  was the amount of adsorbed surfactant on danazol. Since the composition of the small amount of supernatant left on the precipitate was assumed to be the same as that in the bulk supernatant

$$\frac{W_{sup,dry}}{W_{sup,wet} - W_{sup,dry}} = \frac{W_{ppt,dry} - W_{drug,ppt} - W_{surf,ads}}{W_{ppt,wet} - W_{ppt,dry}} \quad (\text{Eq. 4.2})$$

where it has been assumed that the amount of danazol in the precipitate was at least 50 times more than danazol dissolved in micelles. From this equation, the amount of adsorbed surfactant on danazol is given by

$$W_{surf,ads} = W_{ppt,dry} - W_{drug,ppt} - (W_{ppt,wet} - W_{ppt,dry}) \times \left( \frac{W_{sup,dry}}{W_{sup,wet} - W_{sup,dry}} \right) \quad (\text{Eq. 4.3})$$

To measure the amount of surfactant adsorbed on the particles, 1% w/v danazol solution in dichloromethane was sprayed into 15 ml aqueous solution containing 1% w/v surfactant at a flow rate of 1 ml/min for 7.5 min to produce a suspension with a drug-to-surfactant ratio of 0.5:1. The pressure drop was 3000-4000 psi and the temperature was 75°C. 4 ml of the suspension was centrifuged. After centrifugation, the supernatant and the precipitate were weighed before and after vacuum drying at 40°C and –30 in. Hg to determine surfactant adsorption.

#### 4.2.4 High potency danazol powder by centrifugation

2% w/v danazol solution in dichloromethane was sprayed at a flow rate of 1 ml/min into 100 ml aqueous solution containing 1% w/v surfactant or a surfactant mixture at 1:1 w/w ratio, if two surfactants were used, to stabilize the drug particles. The temperatures of both heating jacket and water bath were 80°C and the pressure drop was 3500-4000 psi. After 25 min of spray, a suspension with a drug-to-surfactant ratio of 0.5 was recovered and the particle size of the danazol particles was measured with Malvern. The suspensions were centrifuged (Beckman, Model TJ-6, USA) at 3000 rpm for 30 min. The supernatants were decanted and the precipitates were placed into a vacuum oven and dried at 40°C, and -30 in. Hg overnight. The potency was determined by dissolving a known amount, about 10 mg, dry powder into 50 ml danazol mobile phase



(acetonitrile/water mixture, v:v = 70:30) and measuring danazol concentration by HPLC (Shimadzu, LC-600, Japan). The crystallinity of the dry powders was examined by x-ray diffraction (PW1720, Philips). The surface area of the dry powders was measured with a high-speed surface area BET analyzer (NOVA 2000, Quantachrome Instruments, USA).

#### **4.2.5 Dissolution test**

The dissolution media of danazol in USP 25 is 0.75% SLS aqueous solution. In this article, pH = 9.0 SLS/tris buffer, which contained 0.75% w/v sodium lauryl sulfate and 1.21% w/v tris (hydroxymethyl) aminomethane PD 2960 in aqueous solution was used. According to experimental measurements, pH of 0.75% SLS aqueous solution is 8.5. Also, results showed that the solubility of danazol (0.44 mg/ml vs. 0.40 mg/ml in 0.75% SLS and pH 9 SLS/tris buffer, respectively) and the dissolution rate of bulk danazol in both dissolution media were very close, almost identical. With the same concentration of SLS, very close pH values, almost identical danazol solubility and release rate, pH 9 SLS/tris buffer is a better dissolution media than 0.75% SLS aqueous solution, minimizing a possible pH change of the dissolution media by the surfactants from EPAS process.

After centrifugation and vacuum drying, ~ 20 mg dry powder was placed into a USP basket assembly and stirred at 50 rpm for 30 min in SLS/tris buffer. Aliquots of the dissolution medium (5 ml) were sampled at 2, 5, 10, 20, 30 minutes. The aliquots were filtered through 0.45  $\mu$ m syringe filters and 2 ml of each sample was diluted with 0.1 ml acetonitrile before analysis. Danazol concentrations were measured using HPLC (Shimadzu, LC-600, Japan). Dissolutions were repeated for three times and the statistics was shown in the dissolution figures.

#### **4.2.6 Particle size**

Particle size distributions, based on volume fraction, of the original EPAS suspension and redispersed dry powder were measured by static light scattering with a Malvern Mastersizer-S. To measure the particle size distribution, 5 ml suspension with 5 mg drug/ml water concentration, was diluted with 500 ml distilled water, to produce a light obscuration in the range of 10-30% for accurate measurement. To study the redispersibility of the dry powders after centrifugation and vacuum drying, about 25 mg dry powder were suspended into 500 ml distilled water to produce an obscuration in the range 10-30%. After 1 min, the particle size distribution was measured. In a control experiment, bulk danazol was dispersed in 500 ml 0.02% w/v non micelle-forming PVP 40T aqueous solution, since it is very hydrophobic and difficult to disperse in pure water. Ultrasound was used in the measurement to break up the agglomerated particles.

#### **4.2.7 Contact angle**

Dry powder (100 mg) was loaded into a 0.7 cm diameter flat faced die and compressed with a Carver Laboratory Press (Model M, Fred S. Carver Inc, WIS, USA) at 1500 kg<sub>f</sub> into a tablet. A 5 µl drop of distilled water was placed on the surface of the tablet and contact angle was measured from the tangential angle of the water drop with help of a camera (Panasonic WV-1410, Philippines).

#### **4.2.8 Thermal cycling stress test**

Dry powders were placed in 60 ml Qorpak® glass bottles, sealed with sodium calcium aluminosilicate hydrate desiccant containing cobaltous chloride indicator (VWR International, West Chester, PA) in a temperature controlled oven. The temperature cycle was: increase temperature from –5°C to 40°C over 30 minutes, hold at 40°C for 2.5 hours and then decrease temperature from 40°C to – 5°C over 30 minutes. The cycle was

repeated 6 times per day. The duration of the stability study was 2 weeks. The characteristics of the dry powders were studied over two weeks.

### **4.3 RESULTS AND DISCUSSION**

#### **4.3.1 Surfactant adsorption study**

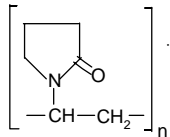
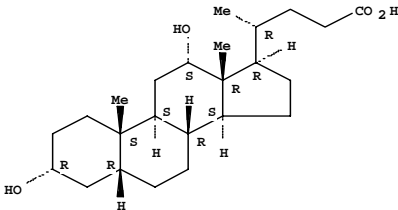
The adsorption of various surfactants onto drug particle surfaces formed during the EPAS process is listed in Table 4.1 and 4.2. For this short spray time of 7.5 min, the adsorption of PVP K-15 was 30% larger than that of PVP 40T. At equilibrium, the adsorption of the higher molecular weight PVP 40T may be expected to be larger due to its higher molecular weight than PVP K-15. The equilibrium adsorption of a polymer often increases with molecular weight, since the adsorbed chains form a thicker layer, as predicted by the Scheutjens-Fleer model.<sup>22</sup> Since thermodynamics would favor higher adsorption for the higher molecular weight PVP 40T for a given surface area, it is likely that mass transfer and kinetic factors may also contribute to the difference observed in the adsorption. Part of this higher adsorption for PVP K-15 may result from generally larger surface area for the PVP K-15 samples relative to the PVP 40T samples, as shown in Table 4.3.

The rate of adsorption depends upon the diffusion rate to the surface and the kinetics of adsorption at the surface. The kinetics of polyethylene oxide (PEO) adsorption on a flat silica surface has been studied in a stagnation-point flow cell with a fixed angle reflectometer.<sup>23, 24</sup> The rate of adsorption decreased with increasing polymer molecular weight because of a lowering of the diffusion constant, indicating that the adsorption rate is mass transfer rate limited up to at least 70% of the plateau. From the scaling theory of polymer solutions,<sup>25</sup> in a good solvent, the diffusion coefficient  $D$  of a polymer is correlated with its molecular weight  $M$  as  $D \sim M^{-\gamma}$  with  $\gamma = 0.5$  for low  $M$  and

0.588 for high M. The diffusion coefficient of PVP 40T is expected to be about 40% lower than PVP K-15 due to its higher molecular weight. Both slower diffusion and slower adsorption kinetics at the surface would lower the amount of adsorbed PVP 40T relative to the lower molecular weight homopolymer PVP K-15.

For the copolymer Pluronic F127 in the aqueous solution, only 3.87% w/w surfactant to drug was adsorbed during the EPAS spray in contrast with much larger values for both PVP polymers. After storage at ambient temperature without stirring for 3 days, the molecules of the adsorbed surfactant may rearrange on the drug particle surface providing space for much more surfactant to adsorb as shown in Table 4.1 and 4.2. The adsorption of Pluronic F127 increased from 3.87 to 11.21% w/w drug. These dynamics are consistent with fundamental studies of block copolymer adsorption by FTIR spectroscopy.<sup>26</sup> In the adsorption dynamics of PS-*b*-PEO on hydrophilic silica, three distinct zones were observed. In the first 5 minutes, the polymer adsorbs on many vacant sites with little rearrangement as a function of the differential sticking enthalpies and geometric sizes of the blocks. In the next two time zones, PEO interactions with the silica displace PS interactions to produce a polymer brush. The kinetics of rearrangement of PS-*b*-PEO on the surface to accommodate more polymer on progressively fewer surface sites takes several hours, as was observed in the present study for Pluronic F 127.

Table 4.1. Adsorption ( $W_{\text{surf,ads}}/W_{\text{drug,ppt}}$ ) of surfactant onto danazol in EPAS suspension at 75°C.

Aqueous surfactant	Properties	Chemical structure of surfactants	$M_w$ of surfactants	$W_{\text{surf,ads}}/W_{\text{drug,ppt}}$ (w/w, %)
PVP K-15	homopolymer		10, 000	$13.0 \pm 2.43$
PVP 40T	homopolymer		40, 000	$10.0 \pm 1.01$
Pluronic F127	triblock copolymer	$\text{HO}(\text{CH}_2\text{CH}_2\text{O})_{98}(\text{CH}_2\text{CH}(\text{CH}_3)\text{CHO})_{67}(\text{CH}_2\text{CH}_2\text{O})_{98}\text{H}$	12,500	$3.87 \pm 1.43$
Pluronic F127 <sup>a</sup>				$11.2 \pm 0.72^a$
DCA	anionic surfactant		414	$5.79 \pm 1.61$
SLS	anionic surfactant	$\text{CH}_3(\text{CH}_2)_{10}\text{CH}_2\text{O}-\text{SO}_2-\text{ONa}$	288	$5.44 \pm 0.46$

a: Adsorption measurement after 3 days

Table 4.2. Pluronic F127 adsorption on danazol particles after 3 days storage. The two entries indicate the reproducibility of the experiment for 4 ml samples of the suspension described in text.

$W_{\text{sup,wet}}$ (g)	$W_{\text{sup,dry}}$ (g)	$W_{\text{ppt,wet}}$ (g)	$W_{\text{ppt,dry}}$ (g)	$W_{\text{drug,ppt}}$ (mg)	$W_{\text{surf,ads}}$ (mg)	$W_{\text{surf,ads}}/W_{\text{drug,ppt}}$ (w/w, %)
1.8987	0.0414	0.1276	0.0200	15.820	1.888	11.9
1.5594	0.0373	0.0901	0.0213	17.753	1.862	10.5

The difference in adsorption dynamics for PVP homopolymer and Pluronic F127 copolymer may be examined in terms of the different conformations on the drug particle surface. For the Pluronic F127, the PEO blocks favor water. It is likely that significant rearrangement on the surface is needed for the central hydrophobic PPO blocks to displace the more prevalent PEO blocks in order to adsorb on the drug surface. For PVP homopolymers, these rearrangements between two types of blocks are not needed leading to faster adsorption. Attachment of only a fraction of the homopolymer segments on the surface of drug particles can lead to adsorption, with loops and dangling ends of homopolymer protruding into water and providing steric stabilization.

As shown in Table 4.1, the adsorption ( $W_{\text{surf,ads}}/W_{\text{drug,ppt}}$ ) of the anionic surfactants SLS and DCA was significantly smaller than that of PVP. For a given area per surfactant on the surface, the lower molecular weight of these surfactants will lead to a thinner adsorbed layer and thus a smaller number of grams of adsorbed surfactant at equilibrium. The kinetics of adsorption is rapid as the number of rearrangements of the low molecular weight tails are much smaller than for polymeric surfactants.

#### **4.3.2 The recovery of danazol in the precipitate and its potency**

In the aqueous suspensions produced by EPAS, certain surfactant stabilizers form micelles that dissolve a small fraction of the API. This small amount of soluble API will be lost to the supernatant after centrifugation. As shown in Table 4.3, the concentration of danazol in the supernatant is strongly dependent on the surfactant type. For PVP 40T and PVP K-15, which do not form micelles in water, the concentration of danazol in the supernatant solution was expected to be its solubility in water, 0.6 µg/ml, which was too low to be measured reproducibly with HPLC used in the experiments (Shimadzu, LC-600). The danazol recovery is defined as the fraction not found in the supernatant after centrifugation. It is not the overall yield from the EPAS process as some of the drug may be lost to other places such as the side of the collection vessel. The fraction of danazol in the aqueous suspension recovered in the precipitate after centrifugation was above 99%. For the micelle-forming surfactants, Pluronic F127, SLS and DCA, the recoveries decreased, but were still greater than 96.2% for each surfactant except for SLS. The recovery was high in all cases except SLS since the concentration of drug in the suspension was far above the micellar solubility of the drug. After centrifugation and vacuum drying, the potency of danazol in the dry powders was higher than 83.2%, as shown in Table 4.3. Drug-to-surfactant ratios varied from 5:1 to 13:1. These values are much higher than typical values of 1:4 to 1:1 observed for milling and spray processes including earlier EPAS studies.<sup>21, 27</sup> The high potencies result from the removal of a large amount of the surfactant with the supernatant.

Table 4.3. Characterization of high potency danazol powder produced by EPAS and centrifugation

Aqueous surfactant	Danazol concentration in supernatant (mg/ml)	Danazol recovery (%)	Potency of danazol (%)	X-ray peak height at $2\theta = 15.9^\circ$ (counts)	S ( $\text{m}^2/\text{g}$ )	Contact angle ( $^\circ$ )
Bulk danazol	/	/	/	3182	0.52	61.3
PVP K-15	X <sup>a</sup>	100	88.5	2358	5.55	41.1
PVP 40T	X <sup>a</sup>	100	92.3	1942	4.89	47.9
Pluronic F127	0.035	99.3	89.3	2843	3.13	34.0
DCA	0.084	98.3	85.1	2413	3.72	18.9
SLS	0.804	82.1	83.2	2867	3.07	7.0
PVP40T +Pluronic F127	0.009	99.8	91.5	2546	3.28	39.8
PVP 40T+DCA	0.020	99.6	86.4	2371	3.22	35.1
PVP 40T+SLS	0.191	96.2	92.9	2465	4.98	13.9

a: Too low to be measured reproducibly by HPLC



### 4.3.3 Dissolution rate

As shown in Figures 4.2 (a) and (b), the dissolution rate was strongly dependent on the type of surfactant. It was much higher for PVP K-15, PVP 40T or PVP 40T + SLS than the other stabilizers. In 2 min, 78, 88 and 90% danazol dissolved with PVP 40T, PVP K-15 or PVP 40T+ SLS as the surfactants, respectively. For the other systems, the dissolution rates were much lower, closer to that of bulk danazol. We will show below that these systems with low dissolution rates had larger particle sizes and lower surface areas.

Pure PVP 40T powder was added to a sample of high potency powder already stabilized by PVP 40T in EPAS. The high potency powder was produced by centrifugation. The objective was to determine if the addition of free surfactant would raise the dissolution rate even further, relative to the high potency EPAS powder without free surfactant. The free surfactant lowered the overall drug-to-surfactant ratio from 12:1 to 1:2. As shown in Figure 4.2 (a), the dissolution rate did not change. Apparently, the changes in *S* from the EPAS spray and adsorbed surfactant were sufficient to produce high dissolution rates, without any need for mixing in additional stabilizer.

Notice the dissolution rate is higher for PVP 40T+ SLS than for PVP 40T even though the surface areas were similar. Perhaps the SLS was able to coat danazol particle surface not covered by the high molecular weight polymer to enhance wetting.

As a control experiment, 0.5 g bulk danazol was dispersed into 100 ml 1% w/v PVP K-15 under magnetic stirring for 25 min (same composition and adsorption time as EPAS). The dispersion was then centrifuged and the precipitate was vacuum dried at 40°C and -30 in. Hg. The potency of danazol in this dried powder was 93.0%; ~20 mg dried powder was put in the dissolution media, and the drug release rate of danazol was

measured by HPLC. The release rate of danazol was higher than bulk danazol but much slower than EPAS high potency danazol dry particles stabilized by PVP K-15, PVP 40T, or PVP 40T and SLS binary mixture, as shown in Figure 4.2 (a). The enhancement of dissolution rate of EPAS samples came from a much smaller particle size and higher surface area, as discussed later in the article.

#### **4.3.4 Particle size distribution and redispersibility of the dry powders**

The mean particle sizes of the EPAS suspensions, EPAS suspensions after sonication, and suspensions of dry powders after centrifugation, vacuum drying and redispersion are shown in Table 4.4. The particle sizes for the EPAS suspensions dropped by a factor of 2 or more in most cases upon sonication for 30 s, as the shear broke particle aggregates. The particle sizes were larger than those produced in the previous EPAS studies.<sup>20</sup> The atomization for the ISCO variable nozzle with a stem angle of 30° tapered from 0.038 to 0.022 in. and a seat angle of 60°, was observed to be less intense than for the crimped nozzles with a 675 × 12 µm slit. However, the atomization generated by the ISCO variable nozzle was sufficient to produce high dissolution rates in this study.

For particles with high dissolution rates in Table 4.4 and Figure 4.2 (a), the mean particle size was less than 15 µm in the EPAS suspension after sonication. Conversely, low dissolution rates were observed for particle sizes larger than 20 µm. The particle sizes of danazol coated with the better excipients for high dissolution rates, PVP K-15, PVP 40T or PVP 40T +SLS, were much smaller than those stabilized with the less effective excipients. After sonication, the reduction in particle size was greater for the less effective excipients than for the more effective excipients. This result suggests that aggregation was greater for the less effective excipients.

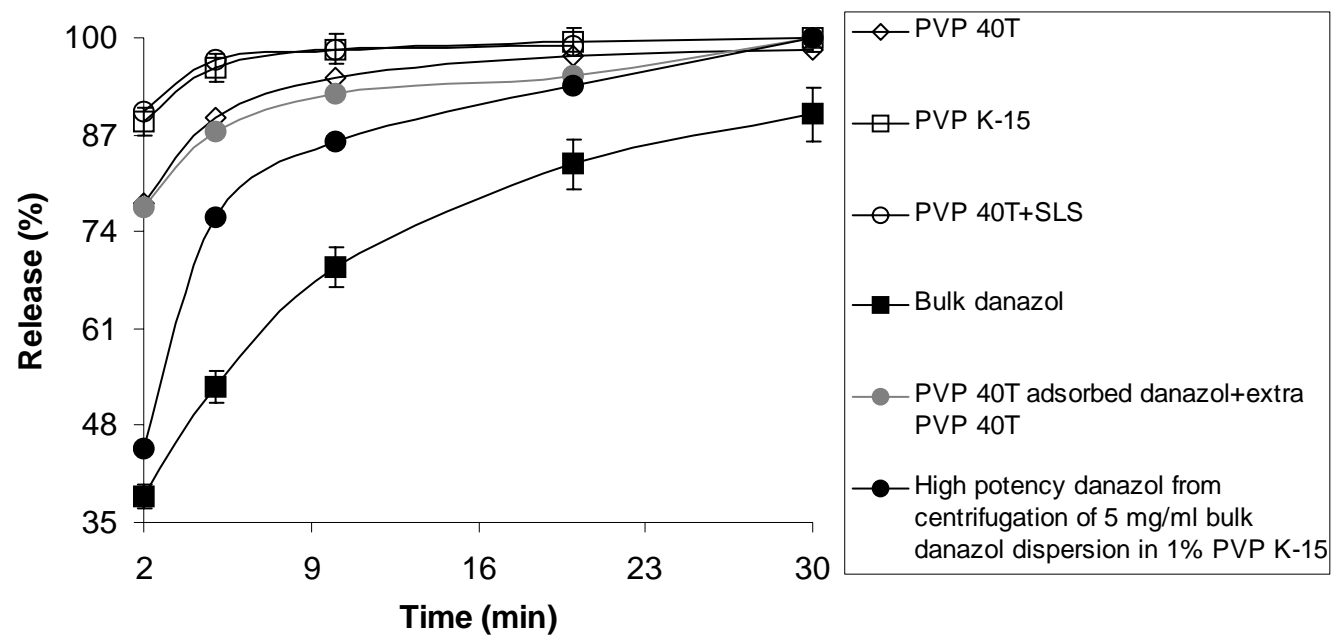


Figure 4.2 (a). Danazol systems with high dissolution rate (conditions were the same as in Table 4.3).

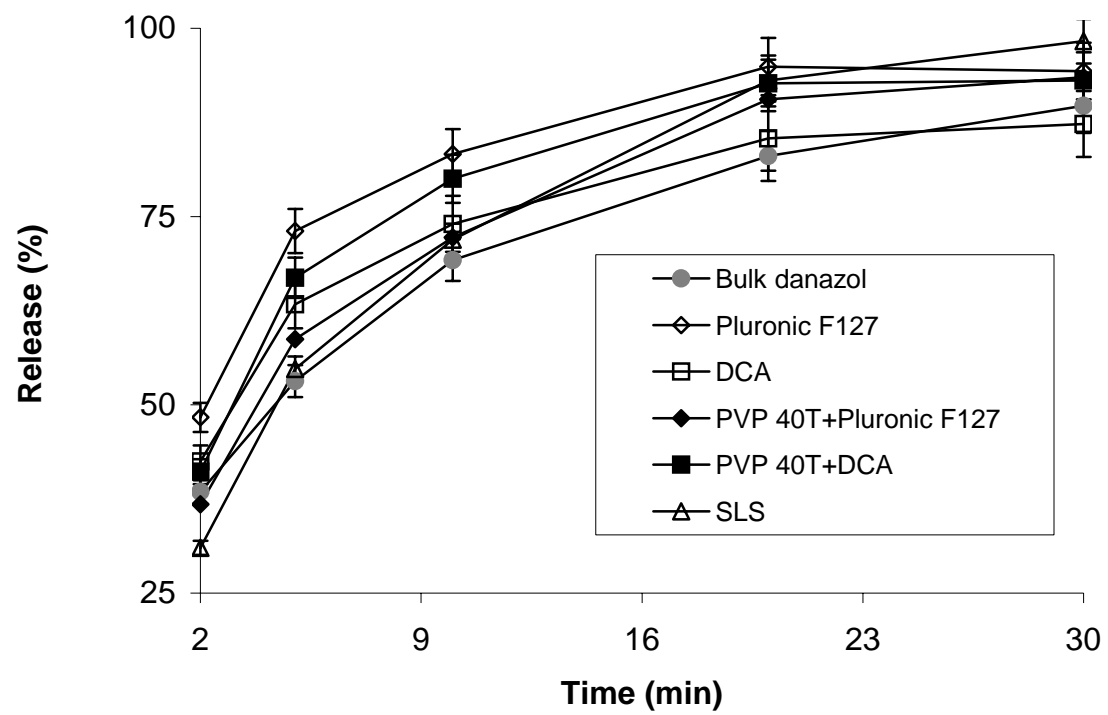


Figure 4.2 (b). Danazol systems with low dissolution rate (conditions were the same as in Table 4.3).

Table 4.4. Particle size of danazol produced in an EPAS suspension at a concentration of 5 mg/ml with a surfactant concentration of 1% w/v and a drug-to-surfactant ratio of 1:2.

Aqueous surfactants	D (v, 0.5)				
	(μm)				
	Suspension w/o sonication	Suspension 15 s sonication	Suspension 30 s sonication	Redispersed w/o sonication	Redispersed 30 s sonication
Bulk danazol				29.6	21.1
PVP K-15	29.5	15.3	12.5	14.2	7.60
PVP 40T	49.3	17.6	13.8	14.1	10.5
PVP 40T+SLS (1:1)	16.8		13.8	18.0	12.1
Pluronic F127	80.4	32.3	25.1	39.7	22.2
DCA	100.1		24.6	56.9	23.9
SLS	70.6	31.7	27.5	61.1	29.3
PVP 40T +Pluronic F127 (1:1)	126		28.8	71.7	26.2
PVP 40T+DCA (1:1)	122	28.0	23.6	52.9	23.2

The particle sizes, both with and without sonication, are correlated with the adsorption during the EPAS spray given in Table 4.1 and 4.2. The adsorption for the PVP K-15 and PVP 40T systems above, that produced the smaller particles, was far greater than for the other surfactants that led to the larger particles. The high level of surfactant adsorption was needed to prevent agglomeration of growing crystals. The smaller particle size for the EPAS suspensions stabilized with PVP K-15 versus PVP 40T is also consistent with the higher adsorption for PVP K-15. However, the particle sizes became the same after sonication suggesting breakup of the large agglomerates. The agglomerates may have been produced by polymer bridging flocculation, which is more prevalent for the higher molecular weight PVP 40T.<sup>28</sup> The smallest particles were produced when SLS was combined with PVP 40T in the aqueous solution. Small linear SLS molecules bind onto PVP macromolecules<sup>29</sup> and add electrostatic stabilization to the steric stabilization. The presence of both stabilization mechanisms led to the smallest particles.

For Pluronic F127, the surfactant adsorption was low, as shown in Table 4.1. The thickness and surface coverage of the surfactant layer was not sufficient to provide enough steric repulsion to overcome the attractive van der Waals forces between growing particles. Agglomeration led to large particles. The combination of Pluronic F127 and PVP 40T at a ratio of 1:1 led to very large particles, 126  $\mu\text{m}$  without sonication. Perhaps interactions between the polymers and Pluronic F127 micelles impeded diffusion to the surface and the adsorption kinetics. Yet another possibility is that Pluronic micelles in the solution about the particles produced depletion flocculation.

The particle sizes produced with the low molecular weight ionic surfactants were large. Several factors may contribute to this unsuccessful stabilization. First, the adsorption for these surfactants was only about half that for the PVP stabilizers. Also,

the ionic surfactant molecules are not long enough to provide significant steric stabilization to prevent the van der Waals attraction between particles. As the solvent in the organic droplets evaporates, the drug particles nucleate and grow. The surfactant must diffuse across the dichloromethane-water interface to begin to adsorb on the particles. The driving force is small for SLS because it is insoluble in dichloromethane.

Drug particles size distribution can be used to characterize the particle growth mechanism. Particle growth can generally occur through two mechanisms: condensation of free molecules onto nucleated cores and coagulation of cores into larger crystals. The moments of the size distribution indicate that the drug particles grow through coagulation and not condensation.

It was very easy to redisperse each of the dry powders in water after the particles were dried after centrifugation. Without sonication, the particle sizes of redispersed dry powder were comparable or even smaller than those of the original EPAS suspension, as shown in Table 4.4. After 30 s sonication, the particle sizes of redispersed dry powder were in most cases smaller than those of the original EPAS suspensions after the same amount of sonication. For the PVP systems, the particle size for the redispersed suspensions without sonication were about the same as those in the original EPAS suspension after 30 s sonication. Thus the redispersion appeared to reduce the amount of aggregation. In the redispersed samples, the free polymer had been removed after centrifugation leaving only the adsorbed polymer. Bridging flocculation would be expected to decrease with the removal of this large amount of excess surfactant. With less bridging flocculation in the redispersed suspensions, ultrasound did not appear to be needed to produce the small particle sizes. All of these effects will be beneficial in enhancing dissolution rates.

#### 4.3.5 X-ray diffraction

X-ray diffraction was used to analyze the crystallinity of the dry powders. As shown in Figure 4.3, the crystallinity of danazol was lower for the vacuum dried precipitates from EPAS relative to bulk danazol. The  $\alpha$ -peak heights of danazol in different surfactant systems at  $2\theta = 15.9^\circ$  are listed in Table 4.3. It was assumed that the crystallinity was linear in danazol peak height, corrected for the potency. The reduction in crystallinity was less than 20%, and was similar for each of the excipients except for PVP 40T. Thus enhanced dissolution rates are possible even with only a small reduction in crystallinity.

#### 4.3.6 Surface area

As shown in Table 4.3, systems with small particle size and high dissolution rates, that is, danazol with PVP K-15, PVP 40T or PVP 40T +SLS, had higher surface areas, on the order of  $5 \text{ m}^2/\text{g}$ . Surface areas were higher for drug particles stabilized with PVP K-15 than with PVP 40T, consistent with the smaller particle sizes. Systems with larger particles and lower dissolution rates had significantly lower surface areas, about  $3 \text{ m}^2/\text{g}$  as expected. Thus surface area is a primary factor for predicting dissolution rate.

The surface areas for danazol with PVP K-15, PVP 40T or PVP 40T +SLS were an order of magnitude higher than that of the bulk danazol. However, the particle diameters in the EPAS suspension after 30 s sonication were only modestly smaller than that of the bulk particles. The calculated surface area for monodisperse sphere with a similar particle diameter would be  $1.36 \text{ m}^2/\text{g}$ . The much larger surface area for the powders in Table 4.3 suggests that the particles were not uniform spheres, but were aggregates composed with smaller primary particles, which was confirmed with an ESEM micrograph of dried high potency danazol precipitate stabilized with PVP K-15. As shown in Figure 4.4, the primary particle size of danazol was smaller than  $1 \text{ }\mu\text{m}$ .



These small primary particles contributed to the high surface area and high dissolution rate for EPAS samples stabilized with PVP or PVP and SLS binary system. The light scattering measurements indicated the size of the aggregates composed of these nanoparticles. In the dissolution rate experiments, not only is the surface area,  $S$ , much higher for these nanostructured particle aggregates, but this much larger surface area is accessible to water given the hydrophilic surfactant coating on the particle surface.

#### 4.3.7 Contact angle

The contact angle results are shown in Table 4.3. Although each surfactant reduced the contact angle indicating improved wettability, there was no apparent correlation between dissolution rate and contact angle. For systems with high dissolution rates, contact angles were close to the value of pure PVP, which is  $43^\circ$ , indicating high surface coverage by PVP. For the anionic surfactant systems, the contact angles were very low due to high wetting of a surface covered with the anionic charges. However, the surface areas and particle sizes for these systems were unfavorable for high dissolution rates. The overall contact angle may be written as

$$\cos \theta = f_1 \cos \theta_1 + f_2 \cos \theta_2 \quad (\text{Eq. 4.4})$$

where  $f_1$  and  $f_2$  are the fractions of the surface occupied by surface types having contact angles  $\theta_1$  and  $\theta_2$ . This equation has been shown to be accurate for the contact angle of a mixed monolayer of OH and  $\text{CH}_3$  terminated alkyl thiols as a function of alkylthiol ratio.<sup>30</sup> The contact angles in Table 4.3 are below the values expected from this equation, based on the pure component values  $\theta_1$  and  $\theta_2$ , indicating that the surface is enriched by the hydrophilic excipient. This enrichment may be expected to be generated during the EPAS spray, as the surfactant hydrophobic moieties prefer the surface of the drug particles and hydrophilic moieties orient outward to interact with water. This orientation of the surfactant to the drug-water interface produces a hydrophilic surface that enhances

dissolution rates. This driving force for orientation of the surfactant at the surface is not present in nonaqueous particle formation processes, such as spray drying and precipitation with a compressed fluid antisolvent, PCA.<sup>31</sup>

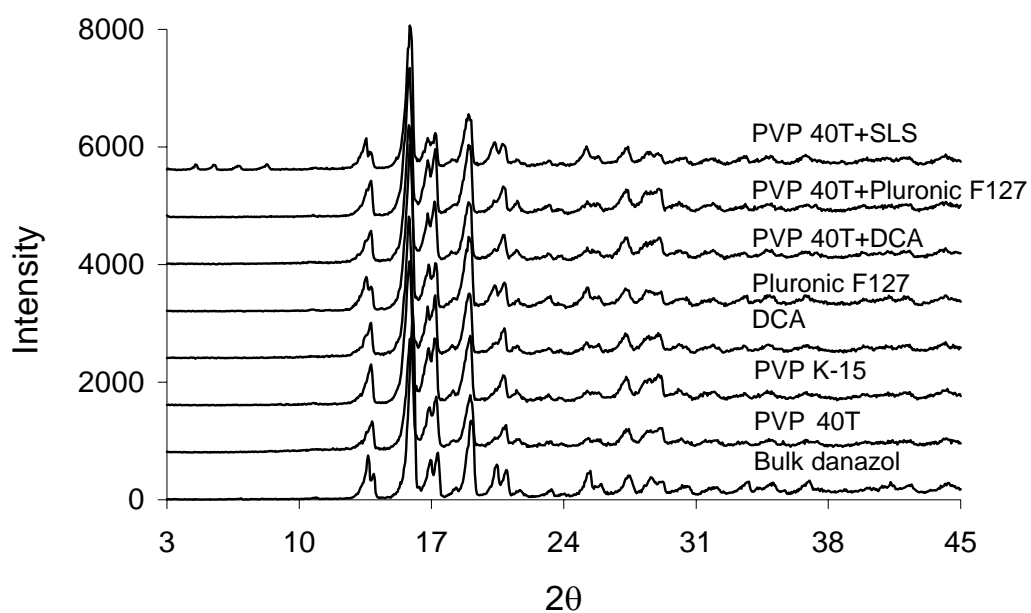


Figure 4.3. X-ray diffraction profiles of danazol systems (conditions were the same as in Table 4.3)

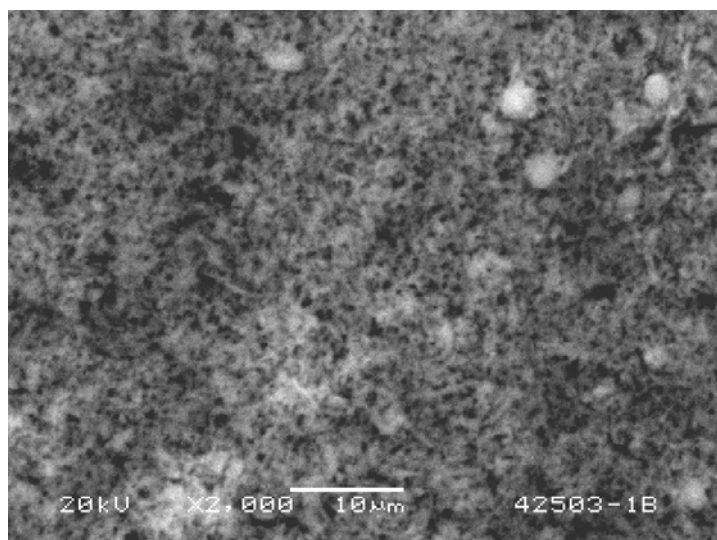


Figure 4.4. ESEM picture of danazol precipitate stabilized with PVP K-15 after centrifugation and drying under 40°C and –30 in. Hg

#### **4.3.8 Thermal cycling stress test on high potency danazol EPAS particles**

Two-week thermal cycling stress tests were undertaken under harsh storage conditions for the three systems with the highest dissolution rates. This short time thermal cycling stress test was used to determine the stability of EPAS danazol particles with small amounts of stabilizer, as an indicator for long term and accelerated stability studies. Samples were analyzed each week to determine if the particle size, crystallinity, surface area and dissolution rate had changed with time. The potencies of danazol in the three systems were: 88.9% with SD (standard deviation) of 2.9% in PVP K-15 +Danazol, 93.6% with SD of 1.4% in PVP 40T +Danazol and 89.6% with SD of 5.0% in PVP 40T +SLS +Danazol.

The particle size, crystallinity, surface area, and dissolution rate of these three EPAS samples changed slightly in 2-week thermal cycling stress test. After 2 weeks, the redispersed particle size of danazol measured by Malvern with 15 s of sonication changed from original value of 8.20 to 8.09  $\mu\text{m}$  for the PVP K-15 system, 8.89 to 9.30  $\mu\text{m}$  for PVP 40T, and 6.38 to 6.37  $\mu\text{m}$  for the PVP 40T + SLS system. The  $\alpha$ -peak height of danazol at  $2\theta = 15.9^\circ$  change from 2275 to 2210, 2297 to 2612, and 1899 to 2209 counts for the PVP K-15, PVP 40T, and PVP 40T +SLS systems, respectively. The surface area of these samples changed from 7.43 to 6.27, 5.88 to 5.87, and 5.91 to 5.72  $\text{m}^2/\text{g}$  for the PVP K-15, PVP 40T, and PVP 40T +SLS systems, respectively. The dissolution rate did not change in the thermal cycling stress test because the key properties of these drug powders, especially the particle size and surface area, did not change with time. As an example, the dissolution profile of danazol stabilized with the PVP 40T + SLS binary system is shown in Figure 4.5. Under 2-week thermal cycling stress test, high potency danazol dry powders with PVP K-15, PVP 40T or PVP 40T + SLS as stabilizing

excipients were very stable when desiccant was used to prevent the particle from moisture.

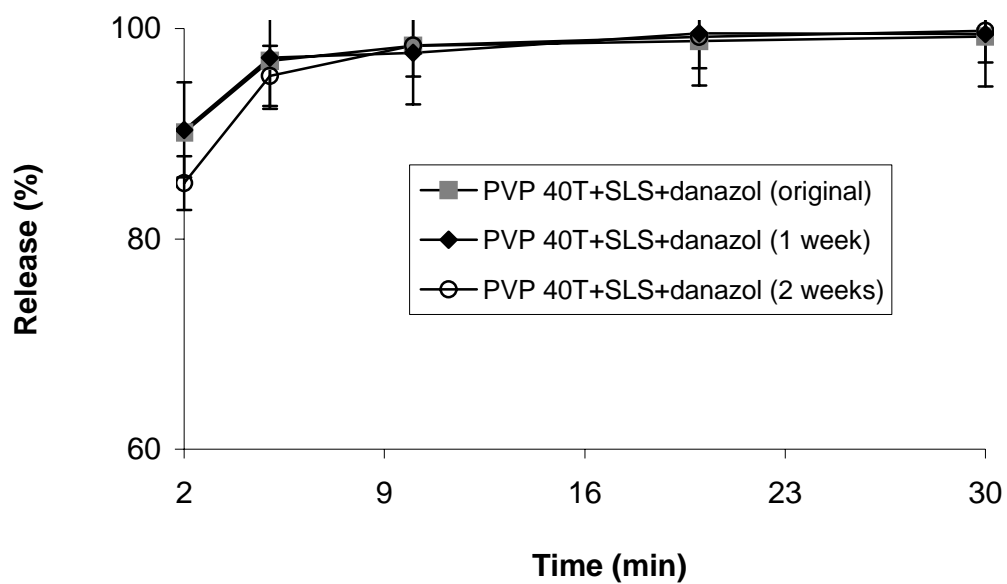


Figure 4.5. Dissolution profile of system danazol +PVP 40T+SLS during 2-week thermal cycling stress test

#### 4.4 CONCLUSIONS

High dissolution rates were obtained for danazol produced by EPAS with PVP 40T, PVP K-15 or PVP 40T together with SLS as stabilizers. The high dissolution rates, e.g. 90% in 2 min with a drug-to-surfactant ratio of 9:1, are remarkable given the high potencies, that is the very low amounts of excipients. Since only about 5% of the surfactant required for forming the EPAS suspensions is adsorbed onto the particles, the rest may be removed after centrifugation. After removal of the free surfactant and drying, the particles may be redispersed in pure water without any growth in particle size or loss in surface area. The dissolution rates were high only for surfactants with an adsorption of 10% w/w or more during the EPAS spray. The dissolution rates were high for surfactants that produced particles smaller than 15  $\mu\text{m}$  with surface areas greater than 5  $\text{m}^2/\text{g}$  and much lower for the other systems with larger particles and smaller surface areas. The high surfactant adsorption levels were required to prevent particle agglomeration and growth. These results indicate that the small particle size and large surface area of the surfactant-coated particles, with reduction in crystallinity less than 20%, was enough to produce high dissolution rates. Not only is the surface area,  $S$ , much higher for the EPAS particles, but this much larger surface area is accessible to water given the hydrophilic surfactant coating on the particle surface. The high surface area was evident in the nanostructured aggregates shown in the ESEN micrographs. In a 2-week thermal cycling stress test with desiccant, the powders were very stable as the dissolution rate, crystallinity, particle size and surface area changed only a minimal amount with time. The ability to engineer stable particles with high potencies and high dissolution rates with EPAS presents new opportunities in the development of commercial formulations for water insoluble drugs.

#### 4.5 REFERENCES

- (1) Choudhury, S.; Nelson, K. F. *Int J Pharm* **1992**, 85, 175-180.
- (2) Kushida, I.; Ichikawa, M.; Asakawa, N. *J Pharm Sci* **2002**, 91, 258-266.
- (3) Lee, E. J.; Lee, S. W.; Choi, H. G.; Kim, C. K. *Int J Pharm* **2001**, 218, 125-131.
- (4) Grant, D. J.; Higuchi, T. *Solubility behavior of organic compounds*; New York: Wiley, 1990.
- (5) Oh, D.; Curl, R. L.; Amidon, G. L. *Pharm Res* **1993**, 10, 264-270.
- (6) Liversidge, G., G.; Cundy, K. C. *Int J Pharm* **1995**, 125, 91-97.
- (7) Reddy, R. K.; Khalil, S. A.; Gonda, M. W. *J Pharm Sci* **1976**, 65, 115-118.
- (8) Torchilin, V. P. *J Controlled Release* **2001**, 73, 137-172.
- (9) Bakatselou, V.; Oppenheim, R. C.; Dressman, J. B. *Pharm Res* **1991**, 8, 1461-1469.
- (10) Zhang, X.; Burt, H. M.; Mangold, G.; Dexter, D.; VonHoff, D.; Mayer, L.; Hunter, W. L. *Anticancer Drug* **1997**, 8, 696-701.
- (11) Liversidge, G. G.; Cundy, K. C.; Bishop, J. F.; Czekai, D. A.: U. S., 1991.
- (12) Pace, S. N.; Pace, G. W.; Parikh, I.; Mishra, A. K. *Pharm Technol* **1999**, 23, 116-134.
- (13) Aiache, J. M.; Beyssac, E. In *Encyclopedia of Pharmaceutical Technology*; Ewarbrick J, B. J., Ed.; New York: Marcel Dekker, 1994; Vol. 12, pp 389-420.
- (14) Illig, K. J.; Mueller, R. L.; Ostrander, K. D.; Swanson, J. R. *Pharm Technol* **1996**, 20, 78-88.
- (15) Young, T. J.; Mawson, S. M.; Johnston, K. P. *Biotechnol Prog* **2000**, 16, 402-407.
- (16) Arias, M. J.; Gines, J. M.; Moyano, J. R.; Perez-Martinez, J. I.; Rabasco, A. M. *Int J Pharm* **1995**, 123, 25-31.
- (17) Margarit, M. V.; Rodriguez, I. C.; Cerezo, A. *Int J Pharm* **1994**, 108, 101-107.
- (18) Rowley, G.; Pearson, J. T.; Hussian, M. S.; Hartup, D. E.; Jones, B. E. *J Pharm Pharmacol* **1985b**, 37, 112P.

- (19) Brown, S.; Rowley, G.; Pearson, J. T. *Int J Pharm* **1998**, *165*, 227-237.
- (20) Chen, X.; Young, T. J.; Sarkari, M.; Williams, R. O.; Johnston, K. P. *Int J Pharm* **2002**, *242*, 3-14.
- (21) Sarkari, M.; Brown, J.; Chen, X.; Swinnea, S.; Williams, R. O.; Johnston, K. P. *Int J Pharm* **2002**, *243*, 17-31.
- (22) Lyklema, J. *Fundamentals of interface and colloid science, Vol II: solid-liquid interfaces.*; New York: Academic Press, 1991.
- (23) Dijt, J. C.; Cohen, S. M. A.; Hofman, J. E.; Fleer, G. J. *Colloids and Surfaces* **1990**, *51*, 141-158.
- (24) Wingrave, J. A. *Oxide Surfaces*; Marcel Dekker: New York, 2001.
- (25) De Gennes, P. G. *Adv Colloid Interface Sci* **1987**, *27*, 189-209.
- (26) Tripp, C. P.; Hair, M. L. *Langmuir* **1996**, *12*, 3952-3956.
- (27) Uekama, K.; Ikegami, K.; Wang, Z.; Horiuchi, Y.; Hirayama, F. *J Pharm Pharmacol* **1992**, *44*, 73-78.
- (28) Hocking, M. B.; Klimchuk, K. A.; Lowen, S. *Journal of Macromolecular Science: Polymer Reviews* **1999**, *39*, 177-203.
- (29) Esumi, K.; Iitaka, M.; Torigoe, K. *Journal of Colloid and Interface Science* **2002**, *232*, 71-75.
- (30) Laibinis, P. E.; Whitesides, G. M. *J Am Chem Soc* **1992**, *114*, 1900-1905.
- (31) Mawson, S.; Yates, M. Z.; O'Neill, M. L.; Johnston, K. P. *Langmuir* **1997**, *13*, 1519-1528.



## CHAPTER 5

### **Flocculation of Suspensions Formed by Antisolvent Precipitation to Produce Redispersible Naproxen Nanocrystals**

#### **5.1 INTRODUCTION**

It is estimated that more than 1/3 of the compounds being developed by the pharmaceutical industry are poorly water soluble.<sup>1,2</sup> The bioavailability of class II poorly water soluble drugs is often dependent upon the dissolution rate of the drug in the gastrointestinal tract.<sup>3</sup> Dissolution rates may be increased by reducing the particle size to increase the surface area, and by coating drug particles with hydrophilic surfactants to enhance wetting and solvation. Ultra fine particles can be readily dissolved and are easily absorbed due to their small size and, consequently, high specific surface area.<sup>4-6</sup> The model drug of choice in this study, Naproxen, *d*-2-(6-methoxy-2-naphthyl)propionic acid,  $\text{CH}_3\text{OC}_{10}\text{H}_6\text{CH}(\text{CH}_3)\text{CO}_2\text{H}$ , is an anti-inflammatory compound with a low water solubility of 15 mg/L.<sup>7</sup>

Antisolvent precipitation is a widely used process to prepare inorganic and organic particles. A number of recent studies have utilized antisolvent precipitation to produce nanoparticles of poorly water soluble drugs.<sup>8-11</sup> In this process, a poorly water soluble drug with or without surfactant(s) are dissolved in a water miscible organic solvent, including methanol, ethanol, tetrahydrofuran (THF) and acetonitrile etc. The organic solution is then mixed with an “antisolvent”, usually an aqueous solution containing a surfactant (s) by a confined impinging jets (CIJ) mixer,<sup>10</sup> sonication,<sup>9</sup> or just pouring the antisolvent into organic drug solution.<sup>8</sup> Supercritical fluid antisolvents can be used to achieve a great deal of control over particle morphology.<sup>12-15</sup> Upon mixing, the supersaturated solution leads to nucleation and growth of drug particles, which may

be stabilized by surfactants. With sufficient supersaturation, and arrested growth by surfactant stabilization, it becomes possible to form suspensions of submicron particles in the aqueous solution.

Several drying techniques have been used to recover the drug nanoparticles from aqueous suspensions produced by antisolvent precipitation. Ketoconazole, itraconazole and ibuprofen micronized particles were spray dried.<sup>8</sup> Budesonide particles with a size range from 1 to 10  $\mu\text{m}$  were filtered with 0.8  $\mu\text{m}$ -pore-size polycarbonate membranes.<sup>9</sup> A wiped film evaporator was used to strip the organic solvent, and then spray drying was used for drying the suspension.<sup>11</sup>

The objective of this study was to recover nanoparticles of poorly water soluble drugs produced by antisolvent precipitation at low temperatures from 0 to 22°C by flocculation and filtration and to examine their properties. Temperature is shown to have a large effect on the particle size distribution in the suspension. The particles were separated from the solvent by flocculation with concentrated salt solution, to collapse the steric stabilizers, followed by filtration and vacuum drying. The surfactant composition and structure, and the type and concentration of salt in the drug suspension were optimized to produce large, loose flocs which could be redispersed into pure water readily after filtration and drying. The increase in drug potency upon filtration and the reproducibility in the composition and yield of the powder are examined. Another goal was to achieve particles sizes after redispersion similar to those in the original suspensions prior to flocculation. The dissolution rate of naproxen powder produced by flocculation was compared with that of suspensions dried by lyophilization and that of bulk naproxen. X-ray diffraction was used to investigate the crystallinity of naproxen. Optical microscopy and SEM were used to characterize the morphologies of the naproxen

flocs in the suspension and after drying. The concentration of residual salt in the dried samples was measured by conductivity and shown to be far below the toxic limit.

Compared to other solvent removal techniques, the use of flocculation and filtration offers several advantages. The flocs may be filtered much more rapidly and efficiently than the original nanoparticle suspension. Rapid filtration reduces the time for the growth of the primary particles in the concentrated precipitate. Particle growth is a potential problem in this step as the stabilizers are no longer solvated. The filtration can be operated at low temperatures much more easily than in the case of spray drying and other solvent evaporation techniques. Otherwise drying at high temperatures may lead to undesirable particle growth.<sup>11</sup> Separation by filtration avoids challenges in evaporation, for example for solvents such as ethanol that form azeotropes with water. Whereas it may take days for lyophilization, the time for flocculation and filtration was on the order of minutes. Finally, the potency of the drug can be increased in the filtration step since the dispersed particle phase contains a higher fraction of drug than the continuous phase.

## **5.2 EXPERIMENTAL**

### **5.2.1 Materials**

Naproxen, polyvinylpyrrolidone (PVP K-15,  $M_w = 10,000$ ) and poly(ethylene oxide-*b*-propylene oxide-*b*-ethylene oxide) (Pluronic F127) with a nominal molecular weight of 12,500 and a PEO/PPO ratio of 2:1 by weight were purchased from Spectrum Chemical Mfg. Corp. (Gardena, CA). Sodium sulfate (anhydrous) and sodium carbonate (anhydrous) were obtained from Fisher Scientific Company (Fair lawn, NJ). Sodium phosphate tribasic dodecahydrate was from EM Science (Gibbstown, NJ). HPLC grade acetonitrile and methanol was obtained from EM Industrial Inc (Gibbstown, NJ).

### 5.2.2 Antisolvent precipitation

The antisolvent apparatus is shown in Figure 5.1. The naproxen solution in methanol or ethanol was fed by a HPLC pump through a 1 m long 1/16 in. o.d.  $\times$  0.030 in. i.d. stainless steel tube. The organic solution was sprayed in the shape of a cylindrical column without atomization through the stainless steel tubing into precooled aqueous surfactant solution. The aqueous surfactant solution was contained in a 250 ml glass cylinder submerged in a temperature controlled water/ethylene glycol bath controlled to 3°C. The stainless steel tube was submerged approximately 4 cm under the surface of the aqueous solution. To enhance the mixing between organic phase and aqueous phase, a magnetic stir bar was placed inside the glass cylinder and stirred at a fixed rate to form a vortex. Unless specified elsewhere, 7% w/v naproxen with or without surfactant was dissolved into methanol. The organic solution was then sprayed into 50 ml aqueous solution at 5 ml/min for 1.4 min to yield a suspension concentration of 10 mg/ml. After spraying for a required time to produce the desired suspension concentration, the suspension was analyzed within 5 min to determine the particle size by static light scattering with Malvern Mastersizer-S (Malvern Instruments Ltd., U. K.). The suspension was sonicated in the Mastersizer to break up the aggregates until stable particle size distribution was obtained. The particle size of the same suspension was also measured after 5 min sonication with a powerful sonicator (Beckman, Model TJ-6, USA) in an ice/water bath at an output control of 7 and 30% duty cycle.

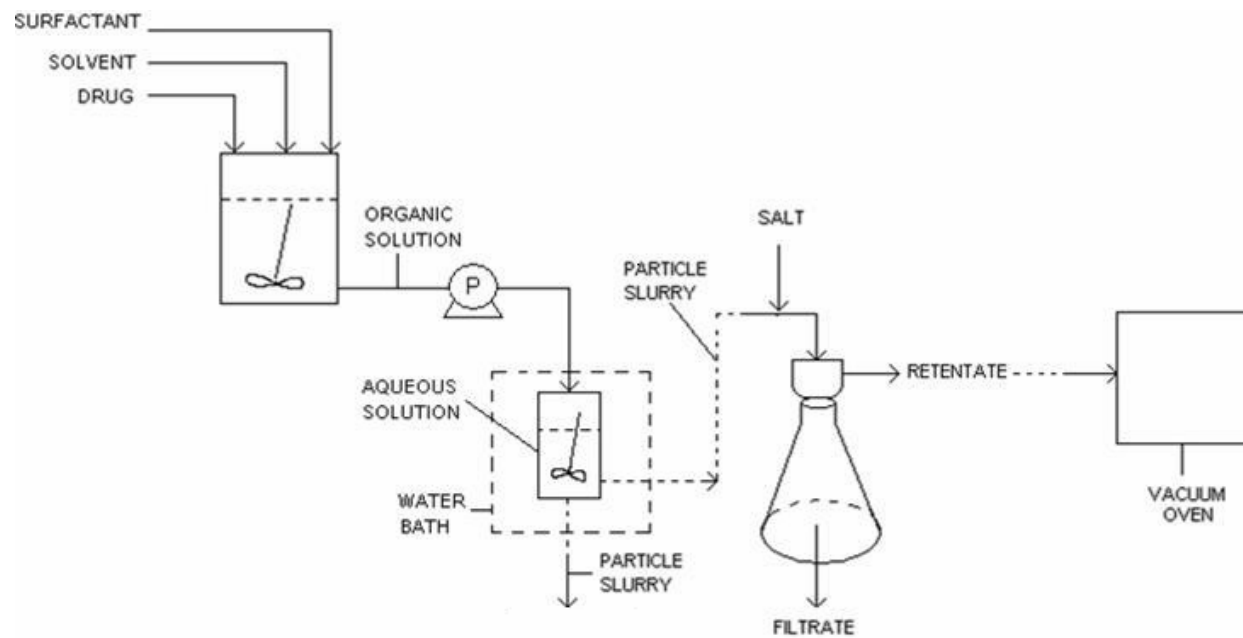


Figure 5.1. Process for producing pharmaceutical powder by antisolvent precipitating, flocculation with salt, filtration and vacuum drying.

### **5.2.3 Recovery of naproxen nanoparticles by salt flocculation followed by filtration and vacuum drying**

After particle size measurement, another suspension produced at exactly the same experimental conditions was sonicated in an ice/water bath at an output control of 7 and 30% duty cycle for 5 min. Then, a given volume of 20% w/v sodium sulfate was added into the suspension and mixed thoroughly with a spatula. The suspension was left at room temperature for 3 min to form large flocs. The flocs were filtered with P2 filter paper (Fisher Scientific, Fair lawn, NJ) under vacuum (-27 in. Hg). Gentle stirring was necessary in the first 3 min of filtration to prevent forming dense precipitate cake which would increase resistance to filtration and result in a long filtration time. The filtration was continued for 10 s after no more water droplets were formed at the tip of the ceramic funnel. The precipitate was placed into a vacuum oven and dried overnight at room temperature at a vacuum of -30 in. Hg. To check the reproducibility of this process, for each formulation, triplicate samples were prepared.

The precipitate weight was determined after vacuum drying. A known amount of this dry powder, about 5 mg, was dissolved into 50 ml acetonitrile/water mixture, 50:50 (v:v). The potency of naproxen was determined by measuring the naproxen concentration by HPLC (Shimadzu, LC-10AT VP, Japan). The salt concentration was determined from the electrical conductivity as described below. The surfactant composition in the final powder was calculated by difference given the total precipitate weight, the drug potency and the salt concentration. The drug recovery was calculated from the HPLC measurement and the total amount of drug fed to the suspension in the antisolvent process. The surfactant recovery was calculated with the same method, given the surfactant composition in the dry powder. Wide angle X-ray scattering was employed to detect the crystallinity of naproxen. CuK  $\alpha_1$  radiation with a wavelength of 1.54054 Å

at 40 kV and 20 mA from a Philips PW 1720 X-ray generator (Philips Analytical Inc., Natick, MA) was used. The samples were well-mixed to minimize the effects of preferred orientation. A Philips goniometer was used to measure the reflected intensity at a  $2\theta$  angle between 5 and  $45^\circ$  with a step size of  $0.05^\circ$  and a dwell time of 1 s.

#### **5.2.4 Particle size**

Particle size distributions based on volume fraction were measured for the original antisolvent suspension prior to flocculation and for the dried powders after redispersion and sonication with laser light scattering (Mastersizer-S, Malvern Instruments Ltd., U. K.). Approximately 5 ml of the suspension with a concentration of 10 mg drug/ml water was diluted with 500 ml distilled water, to produce a light obscuration in the desired range of 10-30%. The amount of drug in the water was several folds above the solubility limit. In control experiments, samples were stirred in the Mastersizer for up to 10 min, and there was very little change in the particle size distribution. To study the redispersibility of the dry powders, about 100 mg dry powder was suspended into 500 ml distilled water to produce an obscuration in the range 10-30%. After 1 min, the particle size distribution was measured. Ultrasound was used in the measurement to break up the aggregated particles. The uncertainty in mean particle size for different sprays at the same experimental conditions was about 10 to 15%.

#### **5.2.5 Measurement of residual salt concentration in flocculated samples by conductivity**

The residual concentration of sodium sulfate was measured by conductivity. The conductivities of a series of standard concentration of sodium sulfate solutions in acetonitrile/water mixture (v:v= 50:50) were measured with a conductivity probe with cell constant of 1/cm (Model 3252, YSI Inc., Oh.). For salt concentrations ranging from 0.003 to 0.05 mg/ml, a linear standard line was obtained with a correlation coefficient of

0.9999. A small amount, about 5 mg, of dried naproxen powder was dissolved in the same acetonitrile/water mixture to yield a salt concentration in the linear range of the standard curve to determine the conductivity.

#### **5.2.6 Morphology of the flocs in the suspension and after drying**

Optical microscopy and scanning electron microscopy (SEM) were used to characterize the morphology of the naproxen flocs in the suspension and in the dried powder. A drop of antisolvent suspension flocculated with sodium sulfate solution was placed onto a microscope slide (25×75 mm, Erie Scientific Co. Portsmouth, N.H) and carefully covered with a microspore cover glass (22×22 mm, Fisher Scientific, Pittsburg, PA). The morphology of naproxen flocs in the suspension was examined with an optical microscope (Axioskop 2 plus, Cal Zeiss Vision GmbH, Germany). Another suspension produced with the same experimental conditions was filtered with a P2 filter paper under vacuum for 11 min. The dried powders were mounted on an aluminum cylinder using double adhesive carbon conductive tabs (Ted Pella, Inc.) and coated with Au for 25 s using a Pelco Model 3 sputter-coater under an Ar atmosphere. A Hitachi S-4500 scanning electron microscope (SEM) (Hitachi Instruments Inc., Irvine, CA) at an accelerating voltage of 10 kV with a secondary electron detector was used to obtain digital images of the samples.

#### **5.2.7 Dissolution test**

The dissolution of naproxen powder was tested in pure water using a USP Apparatus II (Vankel 7000, Vankel Technology Grul, Cary, NC) at 50 rpm. All dissolution tests were conducted at sink conditions, in this case at 15% of its solubility in water. Antisolvent powders containing approximately 2 mg naproxen were added to 900 ml pure water at 37°C. Aliquots of the dissolution medium (5 ml) were sampled at 2, 5,



10, 20 and 30 min. The aliquots were filtered through 0.45  $\mu\text{m}$  syringe filters and 2 ml of each sample was diluted with 0.1 ml acetonitrile before analysis. Naproxen concentrations were measured using HPLC (Shimadzu, LC-10AT VP, Japan). Dissolutions were repeated two to three times for the powder and the average deviations are reported in the dissolution figures.

## **5.3 RESULTS AND DISCUSSION**

### **5.3.1 Effect of temperature on drug particle size in antisolvent precipitation**

The effect of temperature on the particle size distribution in the aqueous suspension produced by antisolvent precipitation was determined. 5% w/v naproxen and 2% w/v Pluronic F127 in ethanol solution was sprayed into 50 ml 3% w/v PVP K-15 at flow rate of 1 ml/min for 5 min. The final suspension concentration was 5 mg/ml. The organic solution was at room temperature. As shown in Figure 5.2, the mean particle size doubled from 270 nm at 0°C to 540 nm at 30°C. At temperatures higher than 30°C, the mean particle size increased markedly and reached 9.3  $\mu\text{m}$  at 60°C. This temperature behavior was also observed for ketoconazole. When 4% w/v ketoconazole and 2% w/v Pluronic F127 in methanol solution was sprayed into 50 ml 3% w/v PVP K-15 at flow rate of 1 ml/min for 20 min, to form a suspension concentration of 16 mg/ml, the mean particle size of ketoconazole increased from 350 nm at 4.6°C to 9.1  $\mu\text{m}$  at 23.8°C. Several factors may lead to larger particles at high temperature including degree of supersaturation, crystal growth rate and Ostwald ripening. The solubility of both drugs in the organic-water mixture increases with temperature. Thus, for a given drug concentration in the feed, the supersaturation decreases with temperature. The lower supersaturation lowers the nucleation rate. The smaller number of nuclei may be expected to produce larger particles for a given drug concentration in the final

suspension. Also, the diffusion rate of drug molecules to the surface of the growing particles and the kinetics of addition of drug molecules to the surface increase with temperature. Furthermore, Ostwald ripening or diffusion of molecules from smaller crystals to larger crystals is also favored by higher solubility at higher temperature. Based on these experiments, all other experiments in this paper were performed at room temperature and below.

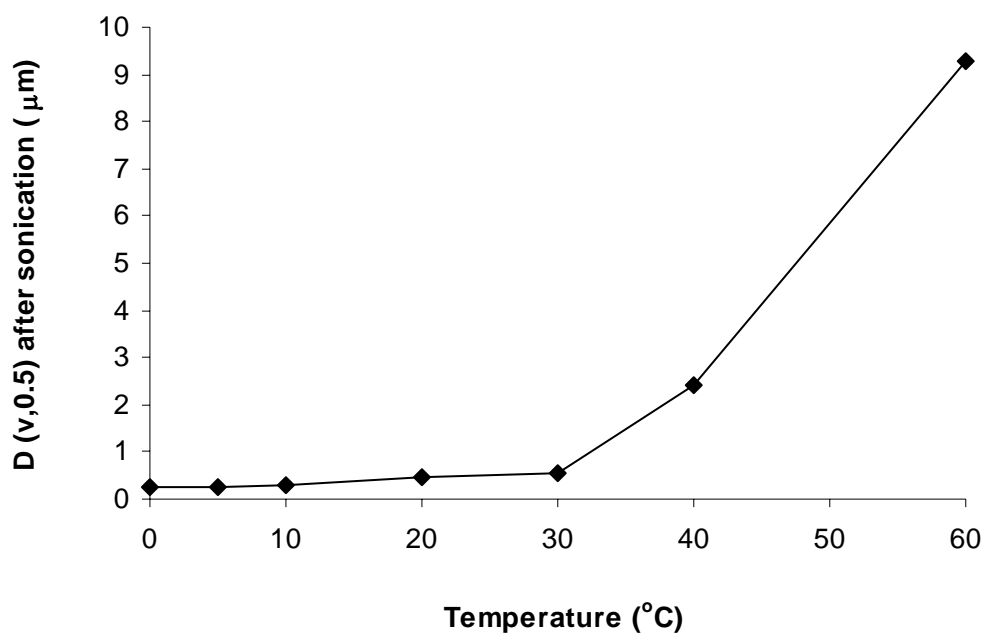


Figure 5.2. Temperature effect on particle size of naproxen suspensions produced by antisolvent precipitation. Organic phase: 5% w/v naproxen+ 2% w/v Pluronic F127 in ethanol; aqueous phase: 50 ml 3% w/v PVP K-15; flow rate  $Q=1$  ml/min;  $t=5$  min; suspension concentration= 5 mg/ml.

### 5.3.2 Compositions of the Formulations

As shown in Table 5.1, four systems were studied. In system A, only 10% w/v PVP K-15 was used in organic phase and there was no surfactant in the aqueous phase. This system was designed for long-term stability since PVP K-15 has a high glass transition temperature which is helpful for drug stability by decreasing the mobility of drug molecules. In system B, 10% w/v Pluronic F127 ( $\text{HO}(\text{CH}_2\text{CH}_2\text{O})_{98}(\text{CH}_2\text{C}(\text{CH}_3)\text{CHO})_{67}(\text{CH}_2\text{CH}_2\text{O})_{98}\text{H}$ ) was used in the organic phase, as it has been shown to be an effective stabilizer<sup>16, 17</sup> and 3% w/v PVP K-15 was included in the aqueous phase to raise the  $T_g$  of the final powder. To attempt to raise the potency of the drug, in system C the Pluronic F127 concentration was reduced to 5% w/v and in system D, the PVP K-15 concentration was reduced to 1% w/v. The overall drug/Pluronic F127/PVP K-15 ratios in the final suspension based on the amounts fed are also given. The total solid weight was 1.22 g for system A, 2.72 g for system B, 2.36 g for system C and 1.36 g for system D. The total drug potencies (weight of drug/total weight) if all fed materials ended up in the solid were 41.2% for system A, 18.5% for system B, 21.3% for system C and 37.0% for system D.

Table 5.1. System investigated

Sys.	Organic phase	Aqueous phase	Drug/Pluronic/ PVP ratio in the suspension	Total solid weight (g)	Total drug potency (%)
A	10% PVP K-15	Pure water	1/0/1.4	1.22	41.2
B	10% Pluronic F127	3% PVP K-15	1/1.4/3	2.72	18.5
C	5% Pluronic F127	3% PVP K-15	1/0.7/3	2.36	21.3
D	5% Pluronic F127	1% PVP K-15	1/0.7/1	1.36	37.0

### 5.3.3 Particle size of naproxen in aqueous suspensions

As shown in Table 5.2 and 5.3, aggregated naproxen nanoparticles were produced during antisolvent precipitation at both 22 and 3°C. With only PVP K-15 in the organic phase and pure water in the aqueous phase (System A, overall drug/Pluronic F127/PVP K-15 ratio= 1/0/1.4), the particle sizes were large in the original suspensions after spraying at either 22°C or 3°C. Even after sonication in the Mastersizer, the mean particle size was still undesirably large, as shown in Table 5.2. After the original suspensions were stirred with a magnetic stir bar for 20 h at room temperature and then sonicated, the mean particle sizes became extremely small, well below 0.4 µm at both temperatures. More surfactants may adsorb to the particles during stirring and aid breakup of the aggregates.

In order to attempt to reduce the aggregation of the particles at 3°C, 5% w/v Pluronic F127 was added to the aqueous phase. The mean particle size of the original suspension was 15.9 µm. After 6 min sonication in the Mastersizer, the mean particle

size decreased to 0.29  $\mu\text{m}$ . In this case the aggregates broke up without the need to stir the solution for 20 h. Since the copolymer Pluronic F127 has hydrophobic moieties which adsorb onto hydrophobic drug particle surfaces, the adsorption of Pluronic F127 with PVP K-15 provided greater steric repulsion and looser aggregates. The looser aggregates may be broken up more easily by sonication.

The particle sizes for the other formulations were determined as shown in Table 5.3. The results for suspensions prior to flocculation are shown in the second and third columns. In order to avoid the need for stirring for long periods of time to break up aggregates, the organic phase stabilizer was changed to Pluronic F127 for all of the systems in Table 5.1 except the first one. In addition, PVP K-15 was utilized in the aqueous phase to achieve a sufficiently high  $T_g$  for the final powder. For system B and C, the mean particle sizes were extremely small, below 0.5  $\mu\text{m}$ , in the original suspension even without sonication. After sonication, the particle size decreased only a small amount given that the particles were already very small. However, when the PVP K-15 concentration in the aqueous phase was lowered to 1% w/v in system D, the mean particle size of the original suspension increased to 9.8  $\mu\text{m}$ . These aggregates were broken up readily upon sonication. After sonication the mean particle size was 0.29  $\mu\text{m}$  for systems B-D, although the  $D(v, 0.9)$  was 7.0  $\mu\text{m}$  for system D. Without sonication, a higher concentration of 3% w/v PVP K-15 in the aqueous phase was helpful in forming the nanosuspension. In system B and C, the overall concentration of PVP K-15 was much higher than that of Pluronic F127, unlike the case for system D. The higher overall stabilizer concentration may have been required to provide enough steric stabilization to prevent aggregation of naproxen nanoparticles.

Table 5.2. Particle size of naproxen suspensions produced by antisolvent precipitation vs. time for system A without any added salt. Organic phase: 7% w/v naproxen+ 10% w/v PVP K-15 in methanol.

Temperature		T=22°C			T=3°C	
suspension	D(v,0.1/0.5/0.9) w/o sonication (µm)	D(v,0.1/0.5/0.9) after sonication with Mastersizer (µm)	Son. time (min)	D(v,0.1/0.5/0.9) w/o sonication (µm)	D(v,0.1/0.5/0.9) after sonication with Mastersizer (µm)	Son. time (min)
Aqueous phase: pure water						
Original suspension	7.5/15.9/28.4	2.4/5.3/7.2	7	6.2/12.6/153.1	2.3/4.5/6.3	15
After 20 hours stirring at room temperature	4.5/6.4/11.0	0.15/0.36/2.1	3	6.1/12.1/19.7	0.11/0.29/0.88	5
Aqueous phase: 5% w/v Pluronic F127						
Original suspension				6.9/15.9/42.4	0.10/0.29/3.3	6

Table 5.3. Particle size of naproxen in the original suspension before and after sonication, and after flocculation, filtration, vacuum drying and redispersion into pure water.

Sys.	D(v,0.1/0.5/0.9) in the original suspension ( $\mu\text{m}$ )	D(v,0.1/0.5/0.9) after 5 min sonication ( $\mu\text{m}$ )	V of salt (ml)	C <sub>salt</sub> in susp. (M)	D(v,0.1/0.5/0.9) after redispersion into water ( $\mu\text{m}$ )	D(v,0.1/0.5/0.9) after redispersion and sonication ( $\mu\text{m}$ )	t <sub>son.</sub> (min)	Release in 2 min (%)
A	4.5/6.4/11.0	0.15/0.36/2.1	175	1.10	16.5/91.6/243.0	0.12/0.32/3.24	3	27.3
A			200	1.13	29.4/155.7/447.1	0.22/2.02/11.6	6	25.5
B	0.14/0.48/95.2	0.11/0.29/1.01	100	0.94	0.10/0.30/6.8	0.10/0.27/3.07	1	95.4
B			125	1.01	0.11/0.31/1.87	0.11/0.28 /1.13	1	96.4
B			150	1.06	0.23/0.48/19.3	0.11/0.32/7.72	1	74.8
C	0.11/0.30/3.8	0.12/0.29/0.68	125	1.01	0.11/0.31/2.57	0.10/0.25/0.79	1	94.9
D	0.14/9.8/173.9	0.10/0.29/6.95	125	1.01	0.28/2.65/22.3	0.19/0.38/4.10	2	49.5

### 5.3.4 Polymer-salt cloud point concentrations and flocculation of naproxen nanoparticles with various salts

Sterically stabilized dispersions may be flocculated by reducing the solvency of the dispersion medium for the stabilizing moieties to induce the onset of instability. Pelton<sup>18</sup> reported that the critical flocculation temperature (CFT) corresponds to the cloud point temperature of the stabilizing polymer. A few reports have described the influence of inorganic salts on the cloud point behavior of Pluronics<sup>19-21</sup> and PVP.<sup>22-24</sup> As shown in Figure 5.3, the cloud point temperatures of PVP 44, 000 and Pluronic F127 decreased linearly with increasing concentrations of sodium sulfate. At a given temperature, the polymer precipitates as the salt concentration increases. In Figure 5.3, the concentration of PVP was 0.74% w/v on the basis of a partial specific volume of 0.952 cm<sup>3</sup>/g for PVP.<sup>25</sup> The concentration of Pluronic F127 was 5 mg/ml or 0.5% w/v. PVP contains N-C=O units on the lactam rings that hydrogen bond with water as observed with viscometric measurements<sup>26</sup> and spectrophotometric studies.<sup>27</sup> The decrease of the Huggins constant with the addition of inorganic salt into PVP aqueous solution indicates a loss in water-PVP H-bonding and thus in PVP hydration leading to precipitation.<sup>22</sup> For the same reasons, salt also precipitates PEO homopolymers<sup>28-31</sup> and of PEO-containing nonionic surfactants such as Pluronics.<sup>19-21</sup>

The reciprocal of cloud point temperatures,  $1/T_{cp}$  of two fractionated and two unfractionated PVP samples have been shown to be linear in  $1/\overline{M}_w^{1/2}$ .<sup>24</sup> With a lower molecular weight of 10, 000, more sodium sulfate is required to precipitate the PVP K-15 used in this study than the PVP 44, 000 shown in Figure 5.3.<sup>23</sup>

The stabilizing moieties collapse at the onset of the cloud point where the solvent is worse than a  $\theta$ -solvent, as a result of the large number of interacting segments.<sup>32</sup> Steric repulsion becomes weak and the stabilizing chains interact with each other leading



to flocculation as the Brownian collisions between particles become sticky. Some free surfactant might also precipitate out from the solution and interact with flocculating particles. Since the particle size of coated naproxen was typically larger than 200 nm and the molecular weight of stabilizing polymers was not more than 12, 500, the van der Waals attraction between the particles is also important in addition to attraction between polymer segments.<sup>32</sup> If the flocs are sufficiently large, the drug particles may easily be recovered from the solution by filtration.

To more fully understand the salinity of flocculation, the critical flocculation salinity was measured for a 1.26% w/v concentration of either PVP K-15 or Pluronic F127. The solvent was a mixture of methanol (12.6%, v/v) and water (87.4%, v/v) with the same composition as the system A suspension. A concentration of 1.06 M salt was needed to precipitate PVP from solution at room temperature in the methanol/water mixture while only 0.98 M was needed without any methanol. For pure Pluronic F127, 0.71 M salt concentration was needed for solution with methanol while 0.58 M was needed without methanol. Apparently, at same concentration and temperature, Pluronic F127 was precipitated much more easily with sodium sulfate than PVP K-15 which is consistent with Figure 5.3. Less salt is needed to flocculate Pluronic F127 than PVP ( $M_w = 44,000$ ) at 25°C from pure water without methanol. This difference is expected to be even larger for PVP K-15 since a greater salt concentration is required to precipitate the lower molecular weight.<sup>23</sup> The critical flocculation salinities, despite the presence of methanol are in the same order expected from the cloud points. Methanol also raises the cloud point temperature for poloxamine 908, a copolymer containing polyethylene oxide moieties.<sup>33</sup>

A much lower salt concentration is required for a divalent sulfate to precipitate these polymers relative to a monovalent anion.<sup>19, 22</sup> Three multivalent inorganic salts

which are known to produce a large reduction in the cloud point temperature of PVP<sup>22</sup> and Pluronic F127,<sup>19</sup> sodium carbonate, sodium sulfate and sodium phosphate, were used to attempt to flocculate the nanoparticles. Large flocs were formed with sodium sulfate which were readily filtered. 20% w/v sodium carbonate and 10% w/v sodium phosphate were also tested for flocculation. In each case, when a small volume of the salt solution was added to the suspension to produce a molarity less than 0.04 M, a clear solution was formed as the naproxen particles dissolved. When 0.4 ml sodium carbonate or 1 ml sodium phosphate solution was added into 25 ml of the suspension, the pH of the solution increased to 11.3 for CO<sub>3</sub><sup>2-</sup> and 11.9 for PO<sub>4</sub><sup>3-</sup> due to the acid-base hydrolysis. The solubility of naproxen increases from 0.0159 mg/ml in pure water to 196.7 mg/ml at a pH higher than 8,<sup>34</sup> which is well above the pK<sub>a</sub> of naproxen. This solubility is much higher than the naproxen concentration in the suspension, consistent with our observation of dissolution. Based on these results all of the flocculation experiments utilized sodium sulfate.

### 5.3.5 Dissolution rate

The dissolution rates of the dried naproxen powders are shown in Figure 5.4 (a) for system B and for a series of formulations in Figure 5.4 (b). The dissolution rates were highly reproducible as shown by the error bars which represent the average deviation, defined by  $\frac{1}{n} \sum |x - \bar{x}|$ . The dissolution rates were very high for systems B and C, and significantly slower for systems A and D. As shown in Figure 5.4 (a), approximately 100% naproxen was released in 2 min for the suspension dried by lyophilization. For samples flocculated with 100 ml or 125 ml salt solution, the dissolution rates of naproxen were only slightly slower than for the lyophilized ones. The flocculated sample of system B was stored with desiccant under vacuum at room temperature. After 1 month,

the dissolution rate of this sample did not change, as shown in Figure 5.4 (b). The differences in these dissolution rates will now be analyzed in terms of the particle size distributions.

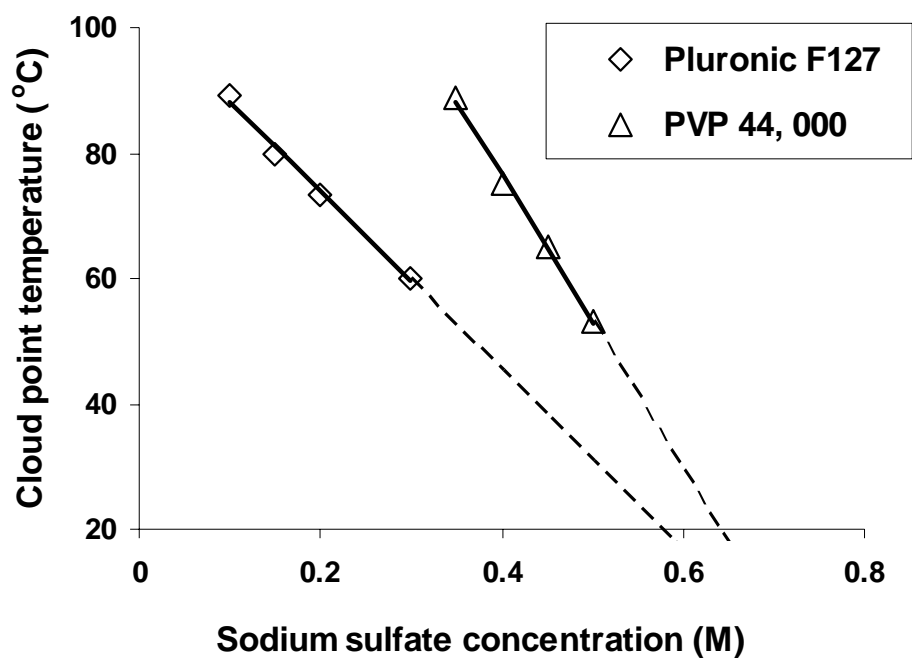


Figure 5.3. Cloud point temperature of PVP<sup>22</sup> and Pluronic F127<sup>19</sup> at various sodium sulfate concentrations in water. The data were obtained and extrapolated from Salamova, et al.<sup>22</sup> and Pandit et al.<sup>19</sup>

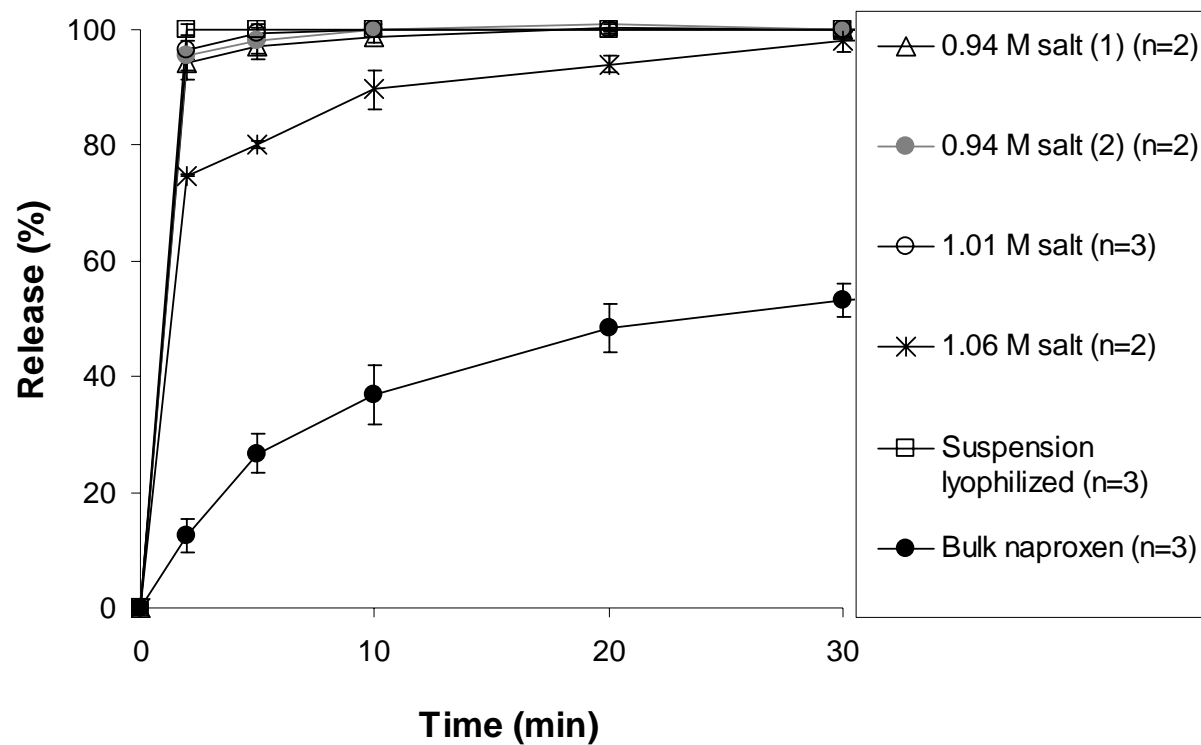


Figure 5.4 (a). Effect of salt concentration on dissolution rate of flocculated, filtered and vacuum dried naproxen nanoparticles produced by antisolvent precipitation (system B). Conditions were the same as Table 5.3 and 5.4. As marked, the suspension was lyophilized in one case

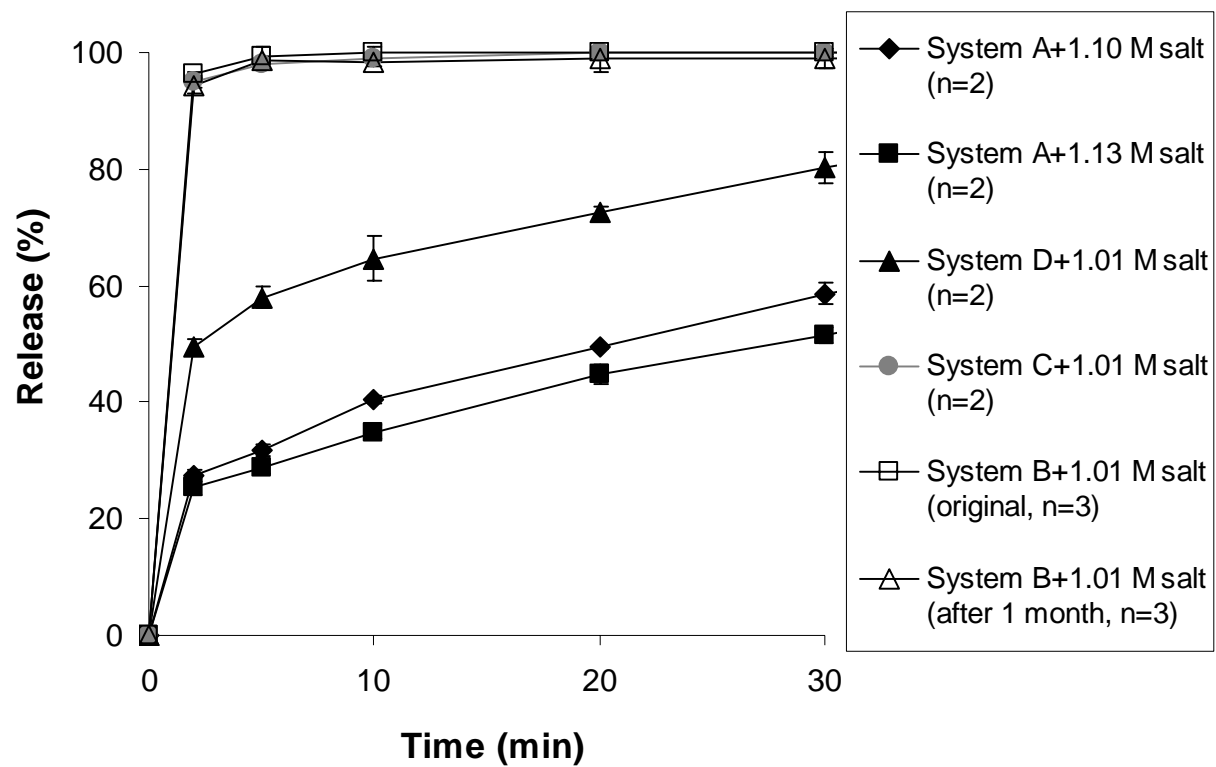


Figure 5.4 (b). Effect of stabilizers on dissolution rate of flocculated, filtered and vacuum dried naproxen nanoparticles produced by antisolvent precipitation. Conditions were the same as Table 5.3 and 5.4.

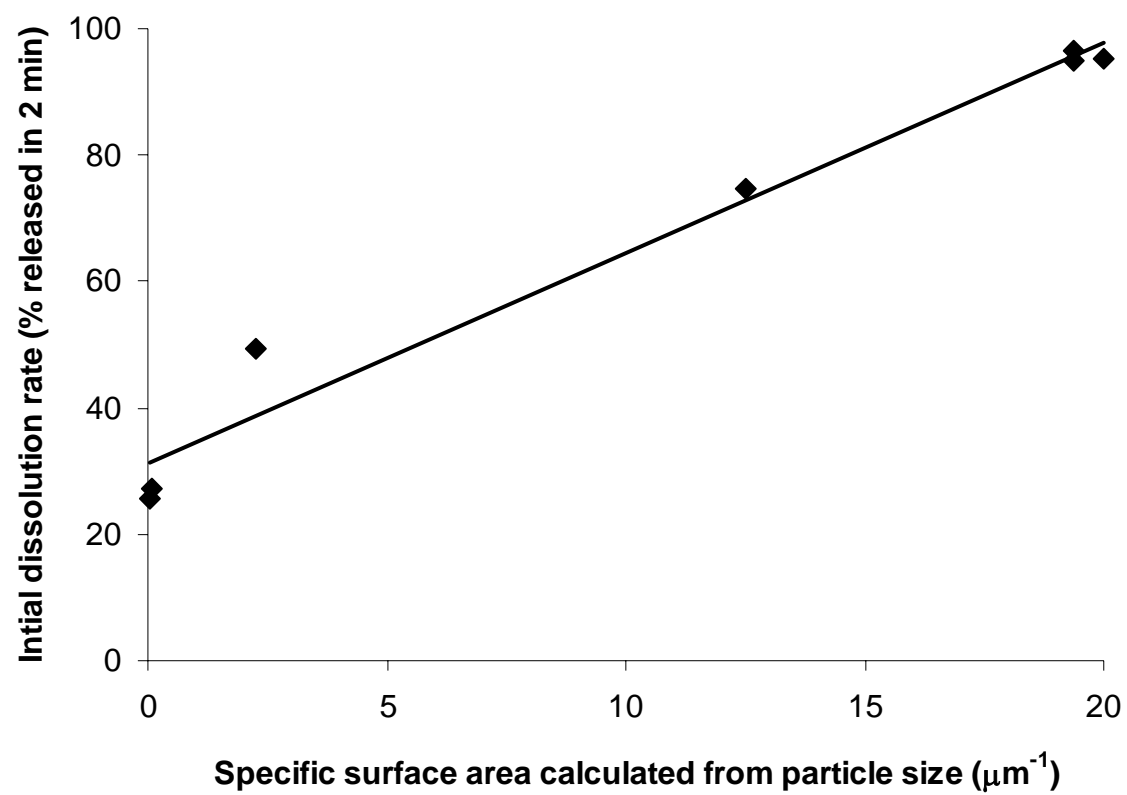


Figure 5.4 (c). Correlation between initial dissolution rate and specific surface area of flocculated, filtered and vacuum dried naproxen particles ( $R^2 = 0.97$ ).

### **5.3.6 Particle redispersibility into water after flocculation followed by filtration and vacuum drying**

The dry powder was redispersed into pure water, and the particle sizes are shown in the sixth and seventh columns of Table 5.3. For system A flocculated with a salt concentration of 1.10 or 1.13 M, the dried naproxen particles formed a very coarse suspension upon stirring without sonication. The mean particle size of the dried particles was 91.6  $\mu\text{m}$  without sonication at 1.10 M salt concentration, but decreased to 0.32  $\mu\text{m}$  after 3 min sonication. With a higher salt concentration of 1.13 M, the mean particle size of naproxen decreased from 155  $\mu\text{m}$  without sonication to 2.02  $\mu\text{m}$  after 6 min sonication. Because the mean particle size was only 0.29  $\mu\text{m}$  after flocculation and filtration but before drying, the particle growth must have taken place during the drying step. The slow dissolution rates in system A are consistent with the large particle sizes upon redispersion without sonication.

In order to study the reversibility of flocculation, a suspension flocculated at 1.13 M salt concentration was filtered with a 0.45  $\mu\text{m}$  Whatman® nylon membrane filter paper (Whatman International Ltd. Maidstone, England) for 43 min. The particle size of redispersed naproxen after drying was 17.1  $\mu\text{m}$  after sonication. Apparently, if the particles are allowed to remain flocculated for tens of minutes or more, redispersion is no longer complete. Perhaps slow diffusion of the stabilizer away from the stress zones that are created by the close approach of the particles leads to irreversible aggregation.<sup>32</sup>

For system B, with either 0.94 or 1.01 M salt, the dried particles could be redispersed into water readily with particle sizes similar to the original suspensions. Consequently the dissolution rates were extremely rapid with 96% release in two min. As the concentration was increased to 1.06 M, the mean size of redispersed particles increased modestly to 0.48  $\mu\text{m}$  with a high  $D(v, 0.9)$  of 19.3  $\mu\text{m}$ . Likewise, the

dissolution rate decreased to 75% in two min. Here, 1 min sonication was needed to reduce the particle size to the value prior to flocculation. Higher salt concentrations appeared to produce tighter flocs after drying, requiring sonication to fully break them up, whereas sonication was not needed for the lower salt concentrations.

For system C, particles flocculated at 1.01 M salt concentration could be redispersed easily after drying to achieve a similar particle size as in the original dispersion. Consequently, the dissolution rate was extremely fast as in the case for the two lowest salinities in system B. However, for system D, with a low PVP K-15 concentration in the aqueous phase, the mean particle size of the redispersed dried powders without sonication was extremely large, 2.7  $\mu\text{m}$ . The size decreased most of the way to the value prior to flocculation after 2 min sonication. The dissolution rate was much slower than in systems B and C. Therefore, the dissolution rate is more closely related to the aggregate size than the size of the particles after sonication.

For all of the examples in Table 5.3, the dissolution rate was correlated closely with the particle size of the redispersed powder without sonication. Assuming spherical particles, the specific surface area of naproxen particles was calculated by,  $S = 6/D$ , where  $D$  is the average diameter of the particles from the Mastersizer, shown in the sixth column of Table 5.3. As shown in Figure 5.4 (c), a straight line with a correlation coefficient of 0.97 was obtained between initial dissolution rate (% released in 2 min) and specific surface area of naproxen particles after redispersion. This correlation is consistent with Noyes-Whitney equation, where the dissolution rate is proportional to the specific surface area of drug particles.



### **5.3.7 Reproducibility of salt flocculation process on precipitate weight, drug potency, salt concentration, surfactant concentration, drug and surfactant yield**

The filtration time and properties of the precipitate including naproxen potency (drug/total solids, w/w), drug yield (fraction in precipitate versus total amount fed), surfactant yield (fraction in precipitate) and filtration selectivity ((g precipitate drug/g filtrate drug) / (g precipitate surfactant/g filtrate surfactant)) for four systems flocculated with various concentrations of sodium sulfate are shown in Table 5.4. Compared to the overall naproxen potencies in Table 5.1 for the suspensions, the naproxen potencies in the precipitate were higher, since some free or nonadsorbed surfactant ended up in the filtrate. For system A, even at salt concentration of 1.10 M, the resulting flocs were not stable. Stirring or pouring broke up the fragile flocs. Thus, the precipitate weight was not reproducible, relative to the other systems. The poor flocculation was due to a salinity too close to the critical flocculation salinity, 1.06 M with 12.6% v/v methanol in the suspension. When salt concentration was increased to 1.13 M, larger flocs formed and consequently the drug and surfactant yields increased. The naproxen potencies were similar for both salinities and were well above the overall potency in the suspension.

For system B, a control was performed in which the suspension was filtered without adding any salt. Without flocculation by salt, only 0.050 g precipitate was recovered as the particles were too small for the filter. At salt concentration of 0.47 M, only a small amount of flocculation occurred, and the drug particles plugged up the filter paper in 5 min. As the salt concentration increased from 0.94 to 1.01 to 1.06 M, the drug and surfactant yields increased significantly. A drug yield higher than 92% was obtained at a salt concentration higher than 1.4 times of the critical flocculation salinity of Pluronic F127. The naproxen potency decreased a small amount with salinity and was about double the overall potency. The relative deviation (average deviation/mean value) of the

precipitate weight decreased from 5.5% with 0.94 M salt to 0.9% with 1.01 or 1.06 M salt. The increase of reproducibility of precipitate weight and drug yield with salt concentration likely indicates more stable, stronger and larger aggregates that could be filtered more effectively. An increase in aggregate size with an increase in the distance above the cloud point temperature has also been observed for clay particles stabilized with PEO formed at higher temperature above the cloud point.<sup>30</sup> The increase in the flocculation efficiency was attributed to an increase in the tendency for the PEO to phase separate and adsorb onto the clay particles.<sup>30</sup>

As the Pluronic 127 concentration was lowered 2 fold in system C relative to system B for a given salinity, the potency increased from 36.7 to 54.1%, yet the dissolution rate remained extremely high. The potency was over 2.5 times that of the overall potency in the suspension. The drug yield increased to 97.6% while the surfactant yield decreased significantly. Furthermore, the particle size changed very little. Given these beneficial results, the PVP K-15 concentration was reduced by a factor 3 in system D relative to system C and the drug yield increased to nearly 100%. The concentrations of drug and surfactant were similar, while the salt concentration decreased to 6.4%.

The selectivity for drug particles over surfactants ( $\text{g precipitate drug/g filtrate drug}$ ) / ( $\text{g precipitate surfactant/g filtrate surfactant}$ ) in the filtration process was very high and usually quite reproducible as shown is the last column of Table 5.4. The high deviation for system C was due to high drug yield, and thus the very small amount of drug in the filtrate. The excellent reproducibility in nearly all of the properties in Table 5.4 for most systems makes the flocculation/filtration concept of practical interest.

Based on dissolution rate and drug recovery, systems B and C flocculated at 1.01 M salt concentration may be expected to produce the highest drug bioavailability. The recommended daily dose of naproxen in adults for rheumatoid arthritis, osteoarthritis, and

ankylosing spondylitis is 500-1000 mg.<sup>35</sup> According to the ratio of sodium sulfate to naproxen in systems B or system C, the daily dose of sodium sulfate from these powders would be 81-286 mg. This amount is much less than the commercial daily dose from OCL<sup>®</sup>, a saline laxative (Abbott), in which 1.29 g sodium sulfate was used.<sup>36</sup> Thus flocculation of naproxen nanoparticles with sodium sulfate is applicable in the pharmaceutical industry based on toxicity.

Table 5.4. Properties of the precipitate after vacuum drying including selectivity for drug vs. surfactant

System	C <sub>salt</sub> in susp. (M)	Filtration time (min)	Precip. weight (g)	Drug Potency (%)	Salt conc. (% w/w)	Surf. conc. (% w/w)	Drug yield (%)	Surf. yield (%)	selectivity for filtration
A	1.10	8.6	0.5083±0.0994 (n=3)	69.0±0.2 (n=3)	25.2±0.3 (n=3)	5.8±0.4 (n=3)	70.2±14.0 (n=3)	4.4±0.2 (n=3)	94.5±73.9
A	1.13	7.7	0.6552±0.0030 (n=2)	66.3±0.7 (n=2)	19.6±0.7 (n=2)	14.1±1.4 (n=3)	86.9±1.3 (n=3)	12.9±1.2 (n=3)	45.5±6.8
B	0.94	16.5	1.0768±0.0596 (n=3)	38.2±0.8 (n=3)	10.6±1.4 (n=3)	51.2±1.1 (n=3)	79.7±1.4 (n=3)	24.1±0.9 (n=3)	12.4±0.5
B	1.01	11	1.2523±0.0113 (n=4)	36.7±0.7 (n=4)	10.5±0.5 (n=4)	52.9±0.5 (n=3)	91.8±1.4 (n=3)	29.9±0.3 (n=3)	28.8±8.5
B	1.06	11.5	1.4825±0.0139 (n=3)	31.8±0.7 (n=3)	9.3±0.5 (n=3)	58.9±1.0 (n=3)	94.1±1.7 (n=3)	39.4±1.0 (n=3)	28.9±12.3
C	1.01	12	0.9021±0.0017 (n=2)	54.1±0.5 (n=2)	8.8±0.0 (n=2)	37.1±0.7 (n=2)	97.6±1.5 (n=2)	18.0±0.3 (n=2)	316.1±206.5
D	1.01	14	0.8930	55.7±0.5 (n=2)	6.4±0.2 (n=2)	37.9 (n=2)	99.4 (n=2)	39.6 (n=2)	256.8

### **5.3.8 Morphology of flocculated naproxen nanoparticles by optical microscope and SEM**

The morphology of naproxen nanoparticle flocs of system B flocculated at 1.01 M salt concentration in the suspension and after drying is shown in Figure 5.5 (a) and (b). As shown in Figure 5.5 (a), naproxen flocs with sizes ranging from 5  $\mu\text{m}$  to 150  $\mu\text{m}$  were formed in the suspension. These flocs were larger than the 2  $\mu\text{m}$  limit for P2 filter paper and thus more than 90% of the naproxen was recovered. As shown in Figure 5.5 (b) (left panel), a floc with size larger than 30  $\mu\text{m}$  was formed during flocculation and drying. This particle, however, was composed of primary nanoparticles of approximately 300 nm, shown on the right, consistent with the size measured by light scattering.

### **5.3.9 X-ray diffraction**

X-ray diffraction was used to analyze the crystallinity of the dry powders. As shown in Figure 5.6, the highest naproxen peaks coincided with those of bulk Pluronic F127. The naproxen peaks were much smaller and broader in the physical mixtures of the various formulations as well in the dried powders produced by antisolvent precipitation. However, the naproxen peaks at  $2\theta = 22.6^\circ$  and  $2\theta = 23.9^\circ$ , especially in the high potency samples produced by flocculation, were evident. Thus, crystalline naproxen was formed whether the suspension was dried by lyophilization or flocculation followed by filtration and vacuum drying. The presence of sodium sulfate in the final powder is also apparent in the diffraction pattern.

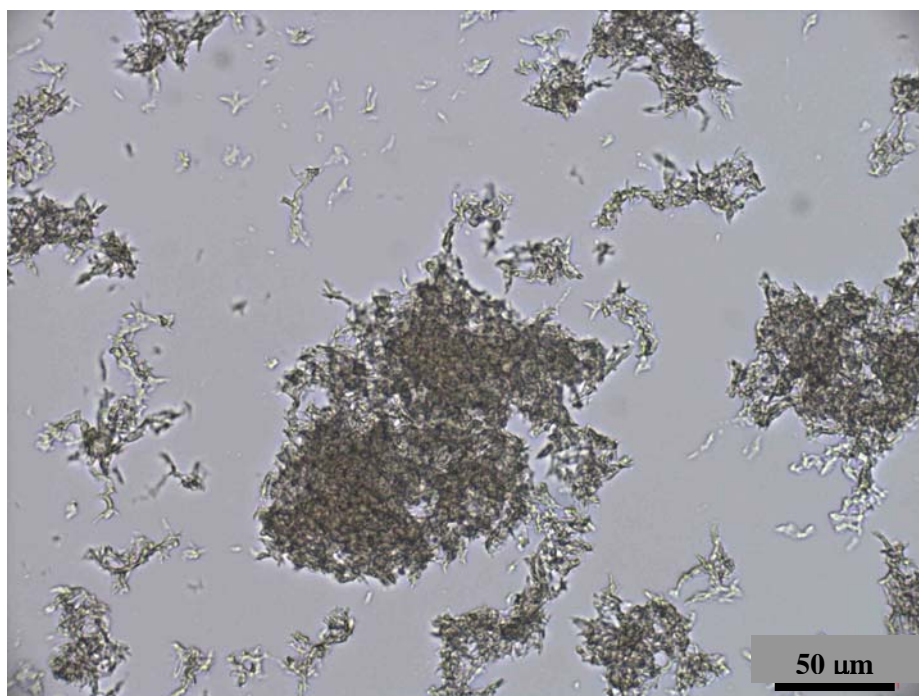


Figure 5.5 (a). Microscopic pictures of naproxen flocs of system B in suspension at salt concentration of 1.01M.

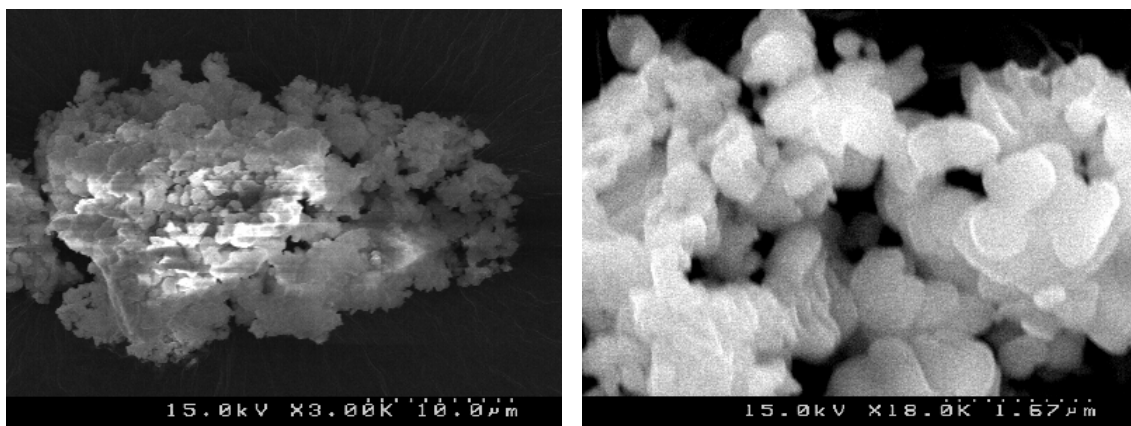


Figure 5.5 (b). SEM pictures of naproxen flocs after filtration and vacuum drying. Same sample as Figure 5.5 (a).

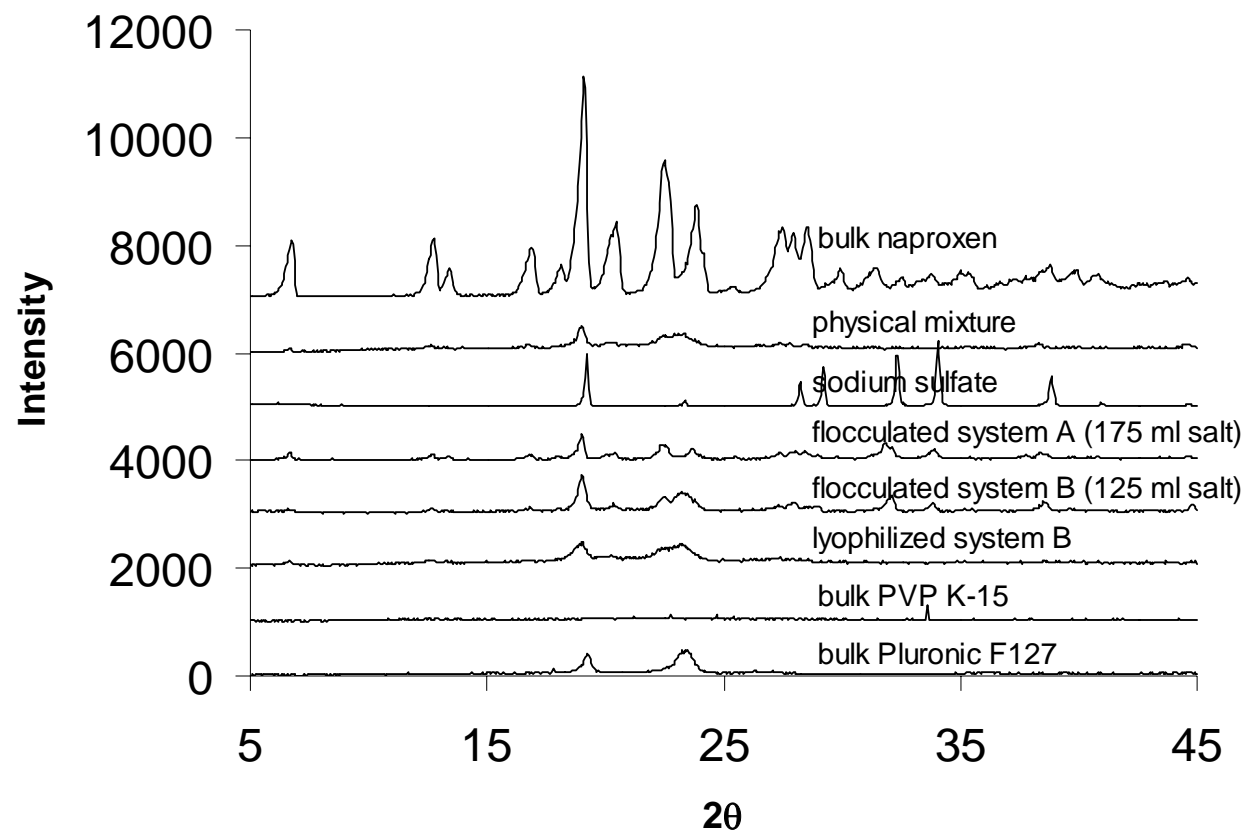


Figure 5.6. X-ray diffraction of flocculated, filtered and vacuum dried naproxen particles produced by antisolvent precipitation. One of the suspensions without flocculation was dried by lyophilization as marked. Conditions were the same as Table 5.3 and 5.4.

## 5.4 CONCLUSIONS

Crystalline naproxen powders composed of submicron primary particles produced by antisolvent precipitation were successfully recovered from aqueous suspensions by flocculation with sodium sulfate followed by filtration and vacuum drying. The flocculation was reversible as the particle size upon redispersion in water under various conditions was comparable to the original particle size in the aqueous suspension prior to flocculation. Less salt was needed for flocculation when the stabilizer was Pluronic F127, where the hydrophilic group was ethylene oxide, than for PVP K-15, where it was N-C=O units on lactam rings, consistent with the trend for cloud point phase equilibria curves. The dissolution rate of dried, flocculated naproxen particles coated with stabilizers was very high when the size of the nanoparticles upon redispersion was on the order of only 300 nm. The size measured by light scattering was consistent with the primary particle size in the powders measured by SEM. The redispersibility of the dried powders was successful for a minimum salt concentration and the proper composition and concentration of the stabilizer. The dissolution rate was linearly correlated with the specific surface area calculated from the average particle diameter after redispersion. Extremely rapid dissolution, up to 95% of the powder in two min, was achieved for 300 nm particles. The salt concentration could be optimized to control the flocculation to balance the drug yield versus potency with excellent reproducibilities in each of 1-2%. The drug potencies of flocculated samples were enhanced by up to 61% relative to the initial value by the filtration step. The yield of the drug in the powder was typically 92 to 99% and the drug potency varied by only 1 to 2%. The residual sodium sulfate concentration in the dried powders, typically 10% or less was far below toxic limits based on the recommended dose of naproxen. The flocculation/filtration process simplifies



drying to obtain powder relative to lyophilization. It also produces smaller particles upon redispersion of the powder than would be expected in spray drying, where the particle sizes are usually above one micron.

## 5.5. REFERENCE

- (1) Radtke, M. *New drugs* **2001**, 3, 62-68.
- (2) Lipinski, C. *Am. Pharm. Rev.* **2002**, 5, 82-85.
- (3) Oh D, C., RL, Amidon GL *Pharm Res* **1993**, 10, 264-270.
- (4) Chen, X.; Vaughn, J. M.; Yacaman, M. J.; Williams, R. O.; Johnston, K. P. *J. Pharm. Sci.* **2004**, 93, 1867-1878.
- (5) Rogers, T. L.; Nelson, A. C.; Sarkari, M.; Young, T. J.; Johnston, K. P.; Williams, R. O. *Pharm Res* **2003**, 20, 485-493.
- (6) Sarkari, M.; Brown, J.; Chen, X.; Swinnea, S.; Williams, R. O.; Johnston, K. P. *Int J Pharm* **2002**, 243, 17-31.
- (7) Pozarnsky, G. A.; Matijevic, E. *Colloids and Surfaces A: Physicochemical and Engineering Aspects* **1997**, 125, 47-52.
- (8) Rasenack, N.; Muller, B. W. *Pharm Res* **2002**, 19, 1894-1900.
- (9) Ruch, F.; E., M. *Journal of Colloid and Interface Science* **2000**, 229, 207-211.
- (10) Johnson, B. K.; Prud'homme, R. K. *Polymeric Materials: Science & Engineering* **2003**, 89, 744-745.
- (11) Elder, E. J.; Hitt, J. E.; Rogers, T. L.; Tucker, C. J.; Saghir, S.; Svenson, S.; Evans, J. C. *Polymeric Materials Science and Engineering* **2003**, 89, 741.
- (12) Randolph, T. W.; Randolph, A. D.; Mebes, M.; Yeung, S. *Biotechnology Progress* **1993**, 9, 429-435.
- (13) Dixon, D. J.; Johnston, K. P.; Bodmeier, R. A. *AIChE Journal* **1993**, 39, 127-139.
- (14) Yeo, S. D.; Lim, G. B.; Debenedetti, P. G.; Bernstein, H. *Biotechnology and Bioengineering* **1993**, 41, 341-346.
- (15) Palakodaty, S.; York, P. *Pharm. Res.* **1999**, 16, 976-985.
- (16) Chen, X.; Lo, C. Y.; Sarkari, M.; Williams, R. O.; Johnston, K. P. **In preparation.**
- (17) Chen, X.; Young, T. J.; Sarkari, M.; Williams, R. O.; Johnston, K. P. *Int J Pharm* **2002**, 242, 3-14.

- (18) Pelton, R. H. *Journal of Polymer Science, Part A: Polymer Chemistry* **1988**, 26, 9-18.
- (19) Pandit, N.; Trygstad, T.; Croy, S.; Bohorquez, M.; Koch, C. *Journal of Colloid and Interface Science* **2000**, 222, 213-220.
- (20) Bahadur, P.; Li, P.; Almgren, M.; Brown, W. *Langmuir* **1992**, 8, 1903-1907.
- (21) Bahadur, P.; Pandya, K.; Almgren, M.; Li, P.; Stilbs, P. *Colloid and Polymer Science* **1993**, 271, 657-667.
- (22) Salamova, U. U.; Rzaev, Z. M. O. *Polymer* **1996**, 37, 2415-2421.
- (23) Sekikawa, H.; Hori, R.; Arita, T.; Ito, K.; Nakano, M. *Chem. Pharm. Bull.* **1978**, 26, 2489-2496.
- (24) Güner, A.; Ataman, M. *Colloid & Polymer Science* **1994**, 272, 175-180.
- (25) Pleštil, J.; al., e. *Macromol. Chem. Phys.* **2001**, 202, 553-563.
- (26) Guven, O.; Eltan, E. *Makromolekulare Chemie* **1981**, 11, 3129-3134.
- (27) Turker, L.; Guner, A.; Yigit, F.; Guven, O. *Colloid and Polymer Science* **1990**, 268, 337-344.
- (28) Khoultaev, K. K. H.; Kerekes, R. J.; Englezos, P. *The Canadian Journal of Chemical Engineering* **1997**, 75, 161-166.
- (29) Khoultaev, K. K. H.; Kerekes, R. J.; Englezos, P. *AIChE Journal* **1997**, 43, 2353-2358.
- (30) Pang, P.; Englezos, P. *Fluid Phase Equilibria* **2002**, 194-197, 1059-1066.
- (31) Pang, P.; Englezos, P. *Colloids and Surfaces A: Physicochemical and Engineering Aspects* **2002**, 204, 23-30.
- (32) Napper, D. H. *Polymeric stabilization of colloidal dispersions*; Academic Press: New York, 1983.
- (33) Na, G. C.; Yuan, B. O.; Stevens, H. J.; Weekley, B. S.; Rajagopalan, N. *Pharm Res* **1999**, 16, 562-568.
- (34) Chowhan, Z. T. *Journal of Pharmaceutical Science* **1978**, 67, 1257-1260.
- (35) Fuller, M. A.; Sajatovic, M. *Drug information handbook for psychiatry 1999-2000*; Lexi-Comp: Hudson, OH, 1999.

- (36) *Electronic orange book : approved drug products with therapeutic equivalence evaluations.*; U.S. Dept. of Health and Human Services, Public Health Service, Food and Drug Administration, Center for Drug Evaluation and Research, Office of Information Technology, Division of Data Management and Services.: Rockville, Md.

## CHAPTER 6

### Conclusions and Recommendations for Further Study

#### 6.1. CONCLUSIONS

##### 6.1.1 Preparation of Cyclosporine A Nanoparticles by Evaporation Precipitation into Aqueous Solution (EPAS)

The rapid evaporation of the heated organic solution in EPAS results in fast nucleation leading to amorphous nanoparticle suspensions. A variety of hydrophilic stabilizers were found to diffuse to the surface of the growing particles rapidly enough to prevent growth of the nanoparticles. Nanoparticle suspensions with low drug crystallinity were formed for cyclosporine A with L- $\alpha$ -phosphatidylcholine vesicles, low molecular weight ethoxylated nonionic surfactants, and high molecular weight homopolymers. The drug concentrations were as high as 35 mg/ml, and drug/surfactant ratios reached unity. Both of these values are far in excess of the values obtained for solvation of this drug in micelles or vesicle bilayers.<sup>1, 2</sup> For the two solvents studied, diethyl ether and dichloromethane, the difference in particle size is related to Ostwald ripening and/or steric interactions between surfactant coated drug particles, and in the case of L- $\alpha$ -phosphatidylcholine, to the effect of solvent on the vesicle stability. The particle sizes were larger for the high molecular weight homopolymer stabilizers versus the low molecular weight ethoxylated surfactants. It is likely that the slower diffusion for the former allowed more time for particle growth. For a given drug/surfactant ratio, particle size decreased with increasing surfactant concentration, despite the increase in the concentration of the suspension. An increase in temperature speeds up evaporation

and nucleation leading to smaller particles, except in the cases where it is detrimental to steric stabilization, as was found for ethoxylated surfactants.

#### **6.1.2 Ketoprofen Nanoparticle Gels Formed by Evaporative Precipitation into Aqueous Solution (EPAS)**

Aqueous ~50 nm gels of a poorly-water soluble drug, ketoprofen, were produced by evaporative precipitation into aqueous solution (EPAS) followed by cooling. In only two minutes, 98% of this wet gel dissolved. In addition, 94% of the ketoprofen dissolved from suspensions with lower surfactant concentration, which were dried by lyophilization. The size of the particles in the gel changed only a small amount over one month reaching only 115 nm. The addition of electrostatic repulsion, due to ketoprofen ionization, to complement steric stabilization led to much smaller particles than normally produced by EPAS. Furthermore, the particles were amorphous, whereas crystalline particles are normally formed. The favorable interactions between ketoprofen and Pluronic F127 led to amorphous particles for low Pluronic F127 concentrations. Stable ketoprofen particles with a mean particle size of 135 nm, measured by dynamic light scattering, were formed with only 0.1% w/v Pluronic F127 and with an exceptionally high drug-to-surfactant ratio of 10:1. Here the concentration was well below the gelation concentration. For higher Pluronic concentrations, these interactions induced gelation and produced unusually smaller particles, as small as 50 nm. When the drug concentration in the organic phase increased from 20% to 70% w/v, the particle size of ketoprofen decreased from 401 to 122 nm at suspension concentration of 30 mg/ml due to higher supersaturation. The rapidly dissolving wet gels, with relatively low viscosities, are of interest in transdermal and parenteral delivery; furthermore, the gels may be dried for oral delivery.

### **6.1.3 Rapid Dissolution of High Potency Danazol Particles Produced by Evaporative Precipitation into Aqueous Solution**

High dissolution rates were obtained for danazol produced by EPAS with PVP 40T, PVP K-15 or PVP 40T together with SLS as stabilizers. The high dissolution rates, e.g. 90% in 2 min with a drug-to-surfactant ratio of 9:1, are remarkable given the high potencies, that is the very low amounts of excipients. Since only about 5% of the surfactant required for forming the EPAS suspensions is adsorbed onto the particles, the rest may be removed after centrifugation. After removal of the free surfactant and drying, the particles may be redispersed in pure water without any growth in particle size or loss in surface area. The dissolution rates were high only for surfactants with an adsorption of 10% w/w or more during the EPAS spray. The dissolution rates were high for surfactants that produced particles smaller than 15  $\mu\text{m}$  with surface areas greater than 5  $\text{m}^2/\text{g}$  and much lower for the other systems with larger particles and smaller surface areas. The high surfactant adsorption levels were required to prevent particle agglomeration and growth. These results indicate that the small particle size and large surface area of the surfactant-coated particles, with reduction in crystallinity less than 20%, was enough to produce high dissolution rates. Not only is the surface area,  $S$ , much higher for the EPAS particles, but this much larger surface area is accessible to water given the hydrophilic surfactant coating on the particle surface. The high surface area was evident in the nanostructured aggregates shown in the ESEN micrographs. In a 2-week thermal cycling stress test with desiccant, the powders were very stable as the dissolution rate, crystallinity, particle size and surface area changed only a minimal amount with time. The ability to engineer stable particles with high potencies and high dissolution rates with EPAS presents new opportunities in the development of commercial formulations for water insoluble drugs.

#### **6.1.4 Flocculation of Suspensions Formed by Antisolvent Precipitation to Produce Redispersible Naproxen Nanocrystals**

Crystalline naproxen powders composed of submicron primary particles produced by antisolvent precipitation were successfully recovered from aqueous suspensions by flocculation with sodium sulfate followed by filtration and vacuum drying. The flocculation was reversible as the particle size upon redispersion in water under various conditions was comparable to the original particle size in the aqueous suspension prior to flocculation. Less salt was needed for flocculation when the stabilizer was Pluronic F127, where the hydrophilic group was ethylene oxide, than for PVP K-15, where it was N-C=O units on lactam rings, consistent with the trend for cloud point phase equilibria curves. The dissolution rate of dried, flocculated naproxen particles coated with stabilizers was very high when the size of the nanoparticles upon redispersion was on the order of only 300 nm. The size measured by light scattering was consistent with the primary particle size in the powders measured by SEM. The redispersibility of the dried powders was successful for a minimum salt concentration and the proper composition and concentration of the stabilizer. The dissolution rate was linearly correlated with the specific surface area calculated from the average particle diameter after redispersion. Extremely rapid dissolution, up to 95% of the powder in two min, was achieved for 300 nm particles. The salt concentration could be optimized to control the flocculation to balance the drug yield versus potency with excellent reproducibilities in each of 1-2%. The drug potencies of flocculated samples were enhanced by up to 61% relative to the initial value by the filtration step. The yield of the drug in the powder was typically 92 to 99% and the drug potency varied by only 1 to 2%. The residual sodium sulfate concentration in the dried powders, typically 10% or less was far below toxic limits based on the recommended dose of naproxen. The flocculation/filtration process simplifies



drying to obtain powder relative to lyophilization. It also produces smaller particles upon redispersion of the powder than would be expected in spray drying, where the particle sizes are usually above one micron.

## **6.2 RECOMMENDATIONS**

It is recommended that other means such as NMR to be applied to test the ketoprofen-Pluronic F127 interaction in water. It is also recommended that hydrophobic silica with similar particle size of ketoprofen, ~50 nm to be dispersed into 5% w/v Pluronic F127 aqueous solution and the viscosity of the suspension to be measured and compared with ketoprofen-Pluronic F127 gel.

It is recommended that the concept of high potency by centrifugation or filtration to get rid of free surfactant to be generalized to antisolvent precipitation. The surfactant adsorption in antisolvent precipitation, the dissolution rate and long term stability of high potency drug particles from antisolvent precipitation to be investigated.

It is recommended that the adsorption of various surfactants onto naproxen drug particles during antisolvent precipitation and after to be measured and compared with other drugs with higher LogP. It is also recommended that the concentrations of remaining surfactants, Pluronic F127 and PVP K-15, after salt flocculation and filtration to be quantitatively measured.

It is recommended that the particle size of drug particle in antisolvent precipitation to be controlled by manipulating the mixing time of organic solution and aqueous antisolvent, the nucleation and growth rate of drug particles, and the surfactant adsorption rate.

It is also recommended that the crystal growth of drug particles produced by antisolvent precipitation during organic solvent stripping to be minimized by choosing suitable temperature.

### 6.3 REFERENCES

- (1) Young, T. J.; Johnston, K. P.; Pace, G. W.; Mishra, A. K. *AAPS PharmSciTech* **2004**, 5.
- (2) Young, T. J.; Mawson, S. M.; Johnston, K. P. *Biotechnol. Prog.* **2000**, 402-407.

## Appendix

### **Rapid Dissolution of High Potency Itraconazole Particles Produced by Evaporative Precipitation into Aqueous Solution**

#### **A.1 INTRODUCTION**

Itraconazole is a water-insoluble active pharmaceutical ingredient (API) used to treat systemic fungal infections. These fungal infections are a major cause of morbidity and mortality in immunocompromised patients. Itraconazole inhibits the fungal enzymes that produce ergosterol, an important component of the fungal cell wall. For oral delivery, high dissolution rates are required to drive sufficient permeation through the intestines to achieve the desired bioavailability. Currently available antifungal products, including amphotericin B, liposomal amphotericin B, flucytosine, and the azole antifungal agents (e.g. fluconazole, ketoconazole and itraconazole) have poor oral bioavailabilities which limit their use. Itraconazole is a weakly basic API (pKa= 3.7) possessing an extremely low water solubility of 0.472 ng/ml, which impedes its bioavailability.<sup>1</sup> The dissolution rate of an API into an aqueous solution depends upon the diffusion coefficient,  $D$ , the surface area,  $S$ , the local equilibrium concentration of API in the diffusion layer surrounding the particle,  $C_s$ , and the diffusion layer thickness,  $h$ , as follows:

$$\frac{dm}{dt} = \frac{DS}{h}(C_s - C)$$

where  $C$  is the concentration of the API in dissolution media at time  $t$ . The surface area  $S$  may be increased by reducing the particle size, by increasing the porosity and by enhancing wetting of the particles by the dissolution media. Wetting may be enhanced

with hydrophilic excipients that are surface active at the API-aqueous interface.<sup>2</sup> The value of  $C_s$  may also be enhanced by trapping the API in metastable crystalline or amorphous states with higher free energies than the lowest energy equilibrium crystalline state. The metastable states may produce a higher local value of  $C_s$ .

Various techniques have been used to improve the bioavailability of poorly soluble APIs including the use of surfactants to enhance wetting,<sup>3, 4</sup> mechanical milling to reduce particle size<sup>5</sup> and the formation of solid dispersions.<sup>6</sup> Widely used mechanical techniques based on high shear or impactation, including microfluidization and milling can be limited by unfavorable yields due to solid losses, high polydispersity in particle size, shear-induced particle denaturation, long processing time, high energy requirements and the need for separating the product and processing agent.<sup>7-10</sup> To overcome many of these limitations, various approaches are being developed to form particles from solution in semi-continuous spray processes, for example spray drying, precipitation with a compressed fluid antisolvent and.<sup>11, 12</sup>

Evaporative precipitation into aqueous solution (EPAS) is a new process that produces submicron to micron-sized hydrophobic API particles stabilized by surfactants and dispersed in an aqueous medium.<sup>13-15</sup> As shown in Figure A.1, API dissolved with or without surfactant (s) in organic solvent, for example, dichloromethane or diethyl ether, is sprayed through an atomizer into a hydrophilic surfactant aqueous phase. The organic phase is heated prior to atomization while the temperature of the aqueous solution is controlled at a temperature above the boiling point of the organic solvent but below the thermal decomposition temperature of the API. The rapid evaporation of the organic solvent produces high supersaturation and rapid precipitation of the API in the form of suspended particles that are stabilized by a variety of surfactants present in either or both the organic and aqueous phases. The surfactants adsorb onto the API surface and prevent

particle growth during the spray process. EPAS produces systems with a high API-to-surfactant ratio or payload relative to formulations in which the API is dissolved in micelles or liposomes.<sup>5, 13-15</sup>

Chen et al.<sup>13</sup> developed a concept to produce high potency APIs with API-to-surfactant ratios greater than 13, corresponding to potencies (wt API/wt API + wt surfactant) as high as 93%. Typical potencies for APIs dissolved in micelles or vesicles are lower by an order of magnitude or more. Aqueous dispersions formed by EPAS were centrifuged to remove the non-adsorbed or free surfactant. The desirable orientation of the small amount of adsorbed surfactant on the surface of the particles, which were produced by EPAS, led to stable particles with high wettability and dissolution rates. Because the hydrophilic segment of the surfactant stabilizes the aqueous dispersions, it is also oriented properly to produce high dissolution rates with very large API-to-surfactant ratios with a minimal amount of surfactant. For danazol stabilized by polyvinyl pyrrolidone (PVP) alone or with sodium lauryl sulfate (SLS), high surface areas on the order of 5 m<sup>2</sup>/g produced high dissolution rates.

The objective of this study was to demonstrate that high potency itraconazole particles with rapid dissolution rates may be produced by the EPAS process followed by centrifugation and vacuum drying. We chose to look at a considerably more challenging API, itraconazole, versus the previous study with danazol.<sup>13</sup> The extreme hydrophobicity for itraconazole is reflected in the octanol/water partition coefficient (LogP) of 5.66 versus 4.21 for danazol. Consequently, dissolution rates are extremely slow for bulk itraconazole without surfactant stabilization. The experimental variables included the type of nozzle, surfactant concentration in the organic phase and the stabilization mechanism of various surfactants (API concentration was fixed). A micrometering valve nozzle and a conical nozzle were investigated to determine the effects of the intensity of

atomization. The dissolution rate was analyzed as a function of the particle size in the original EPAS dispersion, surface area, and crystallinity to provide an understanding of the mechanism of enhanced dissolution rates.

## **A.2 EXPERIMENTAL**

### **A.2.1 Materials**

Itraconazole was purchased from Spectrum Chemicals & Laboratory Products Corporation (Gardena, CA). Pluronic F127 (BASF, Mount Olive, NJ), Polyvinylpyrrolidone (PVP K-15,  $M_w = 10,000$  and PVP 40T,  $M_w = 40,000$ ) (Sigma, St. Louis, MO), Myrj 52 (Sigma, MO), sodium lauryl sulfate (Sigma, MO) and deoxycholic acid (Sigma, St. Louis, MO) were used as received. HPLC grade acetonitrile was from EM Science (Gibbstown, NJ) and spectro grade dichloromethane was from Fisher Scientific Co. (Houston, TX).

### **A.2.2 Evaporative precipitation into aqueous solution (EPAS)**

The EPAS apparatus resembled an earlier version<sup>13-15</sup> and is shown in Figure A.1. The organic itraconazole solution in dichloromethane was fed by an HPLC pump through a 3 m long 1/16 in. o.d.  $\times$  0.030 in. i.d. stainless steel coiled tube contained within a 1-1/2" OD  $\times$  24" long plastic water jacket (Alltech, Deerfield, IL). Water was circulated through the jacket with a Julabo MP temperature controller (Julabo USA Inc., Allentown, PA). The aqueous solution was contained in a 125 ml separatory funnel submerged in a temperature-controlled water bath. The nozzle was submerged approximately 4 cm below the surface of the aqueous solution the water. The nozzle was insulated to the point where it entered the aqueous solution. To suppress and drain the foam produced by the organic vapor, air was blown downwards on top of the foam into the separatory funnel through three 1/16 in. o.d.  $\times$  0.030 in. i.d. stainless steel tubes. The surfactant in

the organic phase in all cases was Pluronic F127 while the surfactant in the aqueous phase was present with a concentration of 1% w/v in each case. After spraying for a required time to produce the desired API-to-surfactant ratio, the dispersion was recovered and analyzed within 30 min to determine the particle size as described below.

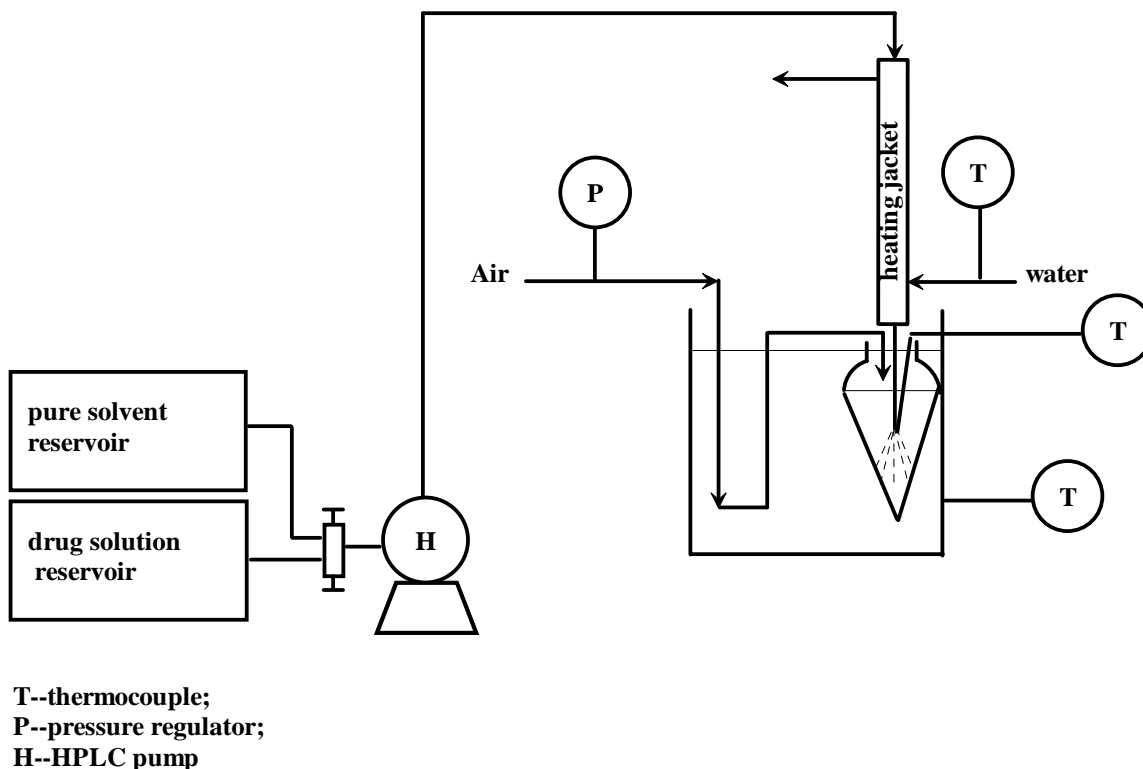


Figure A.1. Apparatus for evaporative precipitation into aqueous solution (EPAS)

Two nozzles were used in EPAS. The micrometering valve nozzle was an assembly that is part of a supercritical fluid extraction apparatus (5 mm o.d.  $\times$  136 mm long, ISCO, Lincoln, NE). The tip of the valve stem was located at the bottom of the nozzle well below the level of the aqueous solution. Atomization was achieved by adjusting the valve manually to maintain a pressure drop of  $\sim$  3500-4500 psi for a flow

rate of 1 to 3 ml/min. The conical nozzle was made from a 10 in. long, 1/16 in. o.d. × 0.030 in. i.d. stainless steel tube. The tube was cut with a wire cutter to produce an elliptical conical thin slit orifice. The tapered section of the tube was only 0.5 mm long. The tip was filed until the desired pressure drop was achieved for a given flow rate of organic solvent into air.<sup>14, 16</sup> When the solution was later sprayed into aqueous solution, the spray looked similar to the photograph reported earlier.<sup>14</sup>

### **A.2.3 High potency itraconazole powder by centrifugation**

Solutions comprising 2% w/v itraconazole with 3% w/v Pluronic F127 and 2% w/v itraconazole with 2% w/v Pluronic F127 were prepared in dichloromethane for the experiments with the conical nozzle and micrometering valve nozzle, respectively. The solution was sprayed at a flow rate of 1 ml/min unless otherwise specified into 50 ml aqueous solution containing 1% w/v surfactant or a surfactant mixture at 1:1 w/w ratio with a total concentration of 1% w/v, if two surfactants were used. The temperatures of both the heating jacket and water bath were 75°C and the pressure drop was 3500-4500 psi. After 25 min of spraying, dispersion with an API-to-surfactant ratio of 0.4 (conical nozzle) or 0.5 (micrometering valve nozzle), and an API concentration of 10 mg/ml water was recovered. The dispersions were centrifuged (BECKMAN, Model TJ-6) at 3500 rpm for 30 min. The supernatants were decanted and the precipitates were placed into a vacuum oven and dried at 40°C, and -30 in Hg overnight. The potency was determined by dissolving a known amount, about 10 mg, dry powder into 50 ml acetonitrile/water mixture (v:v = 70:30) and measuring itraconazole concentration by HPLC (Shimadzu, LC-600, Japan).



#### **A.2.4 Crystallinity and surface area measurement**

Wide angle X-ray scattering was employed to detect the crystallinity of itraconazole.  $\text{CuK}\alpha_1$  radiation with a wavelength of 1.54054 Å at 40 kV and 20 mA from a Philips PW 1720 X-ray generator (Philips Analytical Inc., Natick, MA) was used. The samples were well-mixed to minimize the effects of preferred orientation. A Philips goniometer was used to measure the reflected intensity at a  $2\theta$  angle between 3 and 45° with a step size of 0.05° and a dwell time of 1 s. Specific surface area was measured using a NOVA-2000 instrument (Quantachrome Corporation, Boynton Beach, FL). A known amount of powder (~0.1 g) was loaded into a Quantachrome sample cell and degassed for at least 3 h prior to analysis. Nitrogen was used as the absorbate. The degassed sample weight was used for surface area determination.

#### **A.2.5 Dissolution test**

After centrifugation and vacuum drying, ~10 mg of dry powder was placed into a USP II dissolution assembly at a stir rate of 75 rpm for 1 h in pH 1.6 aqueous solution that contained 0.5% w/v sodium lauryl sulfate and 0.1 M hydrochloric acid. Aliquots of the dissolution medium (5 ml) were sampled at 2, 5, 10, 20, 30 and 60 min. The aliquots were filtered through 0.45 µm syringe filters and 2 ml aliquots of each sample were diluted with 0.1 ml acetonitrile before analysis. Itraconazole concentrations were measured by HPLC (SHIMADZU, LC-600, Japan).

#### **A.2.6 Particle size**

Particle size distributions, based on volume fraction, of the original EPAS dispersion were measured by static light scattering with a Malvern Mastersizer-S (Malvern Instruments Inc., Southborough, MA). A 5 ml aliquot of dispersion containing 10 mg API/ml concentration in water, was diluted with 500 ml distilled water to produce

a light obscuration in the range of 10-30%. The solution was sonicated until the mean particle size of the dispersion reached a constant value. In a control experiment, 0.2 g bulk itraconazole was dispersed in 100 ml 3% w/v non micelle-forming PVP K-15 aqueous solution overnight under vigorous stirring, since it is very hydrophobic and difficult to disperse in pure water. 20 ml bulk itraconazole suspension was diluted with 500 ml pure water to measure the particle size of bulk itraconazole by Malvern. Ultrasound was used in the measurement to break up the agglomerated particles.

### **A.3 RESULTS AND DISCUSSION**

The results are presented below for the micrometering valve nozzle and the conical nozzle. The smaller particles for the conical nozzle were shown to be consistent with a finer spray and greater degree of atomization.

#### **A.3.1 Micrometering valve nozzle: particle size and dissolution rate**

The effect of several surfactants as stabilizers in the aqueous phase was investigated with the micrometering valve nozzle. Without Pluronic F127 in the organic phase, surfactant in the aqueous phase alone could not stabilize the itraconazole particles. The API particles floated on top of the aqueous phase due to poor surfactant adsorption. With the addition of 2% w/v Pluronic F127 in the organic phase, stable itraconazole suspensions were formed by EPAS. The organic solutions containing 2% w/v Pluronic F127 and 2% w/v itraconazole were sprayed into 50 ml of 1 % w/v surfactant aqueous solution at a flow rate of 1 ml/min unless specified otherwise. The spray time was 25 min. For each EPAS sample, the pressure drop across the nozzle was maintained at ~ 3600 psi for each spray. Visual observation of the EPAS spray indicated that the angle of the jet was narrower and the droplets appeared to be larger in comparison with those

produced with the conical nozzle. Samples were analyzed to determine the particle size and dissolution rate of the surfactant stabilized itraconazole particles.

The particle sizes produced with the surfactants are shown in Table A.1. After sonication, the mean diameters of the particles in dispersion were dependent on the structure of the aqueous surfactant and the flow rate of organic phase. When the flow rate of organic phase was increased from 2 ml/min to 3 ml/min, itraconazole particle size increased from 9.4  $\mu\text{m}$  to 13.8  $\mu\text{m}$ . Despite the large particle size, Figure A.2 shows that the release rate after 5 min with PVP K-15 and Pluronic F127 was 36.1% compared to 7.5% from the bulk itraconazole, a slight improvement in API dissolution. The dissolution rate enhancement for the itraconazole particles after EPAS illustrates the importance of wetting of the API particle surface due to the hydrophilic surfactants. Experiments were performed with anionic surfactants, sodium lauryl sulfate and deoxycholic acid, but the dissolution rates were poor due to incompatibility of the surfactants and the acid dissolution media. For all of the surfactants, the poor atomization with this nozzle produced particles that were too large with too little surface area. In order to produce powder with a faster dissolution rate, all the experiments below were performed with a conical nozzle that produced more intense atomization.

Table A.1. Mean particle size  $D(v, 0.5)$  of itraconazole particles in the EPAS suspension for various organic phase flow rates with the micrometering valve nozzle. Experimental conditions were the same as in Figure A.2.

Aqueous surfactant	$D(v, 0.5)$ ( $\mu\text{m}$ )
PVP K-15 (Q= 2 ml/min)	18.6
PVP 40T (Q= 2 ml/min)	9.4
PVP40T (Q= 3 ml/min)	13.8
DCA (Q=1 ml/min)	11.5
SLS (Q=1 ml/min)	19.2
PVP 40T+SLS (Q=1 ml/min)	16.9

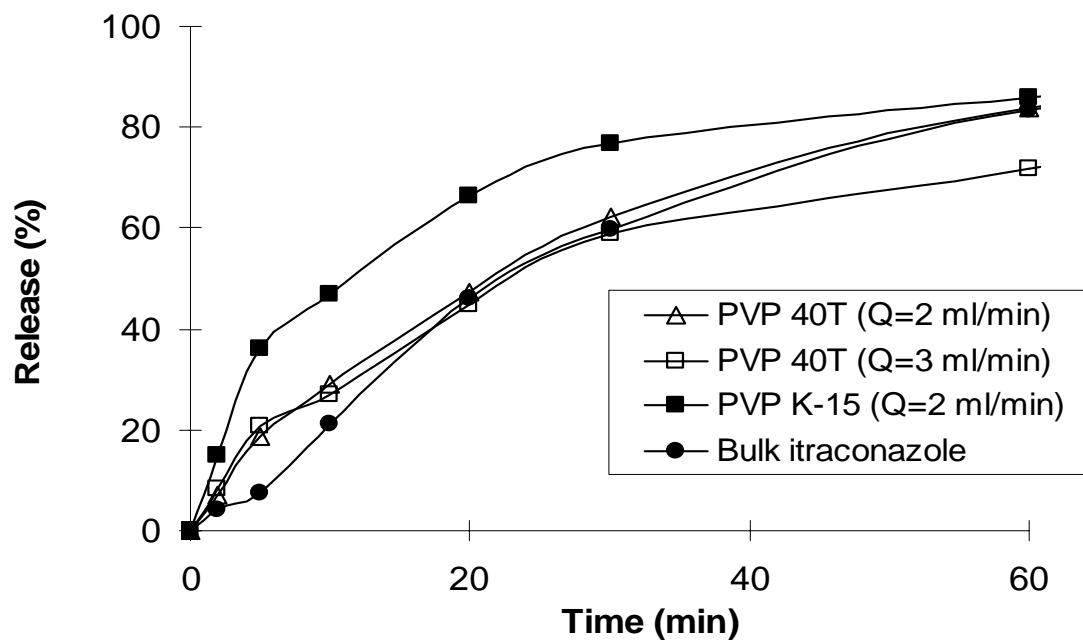


Figure A.2. Dissolution rates for dried EPAS itraconazole particles produced with the micrometering valve at various organic flow rates and aqueous surfactant concentration of 1% w/v.

### **A.3.2 Conical nozzle**

Experiments with the micrometering valve nozzle showed that adding Pluronic F127 in the organic phase and decreasing the flow rate of organic phase led to itraconazole suspensions with smaller particle size. Therefore, for the experiments with the conical nozzle, more Pluronic F127 was added into the organic phase and the flow rate was decreased to 1 ml/min. Additional nonionic surfactants were studied with the conical nozzle due to the unsuccessful results with the micrometering valve nozzle for ionic surfactants. A concentration of 3% w/v Pluronic F127 was used in the organic phase with the conical nozzle to stabilize the particles for an aqueous solution concentration of 1% w/v of various surfactants. The solution containing 3% w/v Pluronic F127 and 2% w/v itraconazole was sprayed into 50 ml aqueous solution at a flow rate of 1 ml/min for 25 min. The appearance and angle of the atomized jet were comparable to those reported earlier.<sup>14</sup> Visually, the spray appeared to be composed of finer droplets than for the micrometering valve nozzle above, consistent with the finer orifice.

#### ***A.3.2.1 Dissolution rate***

As shown in Figure A.3, the dissolution rate of the high potency powder after centrifugation was strongly dependent on the type of surfactant. It was much higher for PVP K-15 than the other surfactants. In 10 min, 35, 60, 70 and 90% itraconazole was dissolved with PVP 40T, Myrj 52, Pluronic F127 and PVP K-15 as the surfactants, respectively. For each surfactant, the dissolution rate was substantially higher than for the bulk itraconazole. The properties of the EPAS dispersions and powders after centrifugation were measured to understand their dissolution properties.

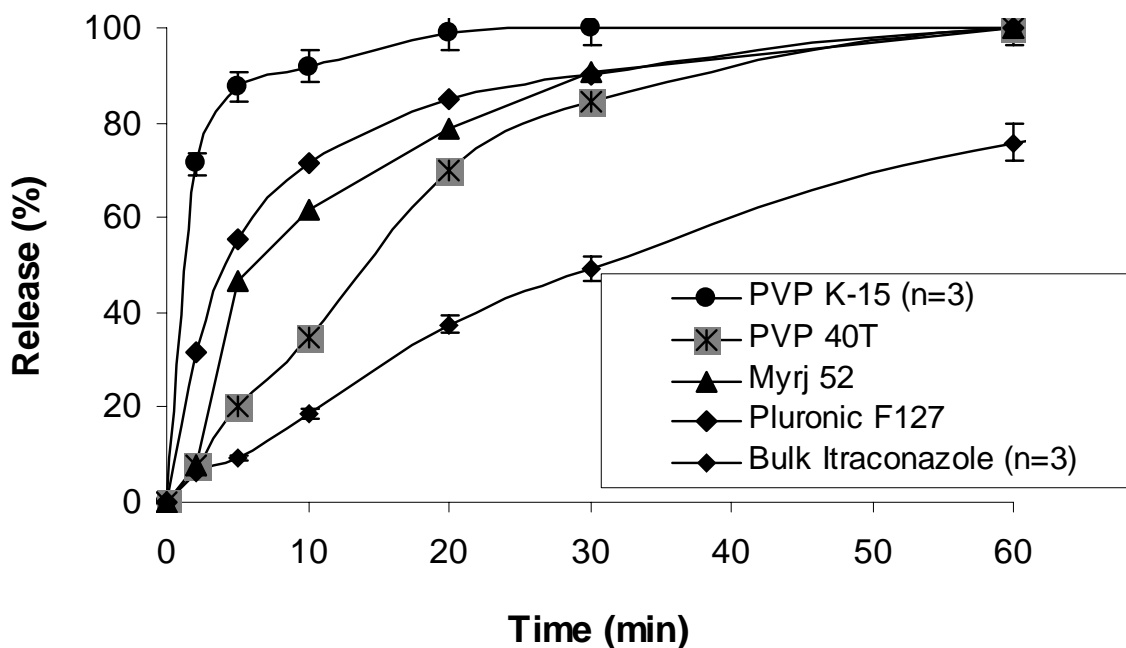


Figure A.3. Dissolution rates for dried EPAS itraconazole particles produced with conical nozzle for various aqueous surfactants at a concentration of 1 % w/v and organic flow rate of 1 ml/min.

#### A.3.2.2 Particle size and surface area

For the EPAS dispersions without centrifugation, Table A.2 shows the mean particle diameters based on volume, the particle size distributions of EPAS suspensions and surface areas, itraconazole potencies of dried EPAS particles. Itraconazole coated with PVP K-15 yielded the smallest mean diameter, 8.7  $\mu\text{m}$ , with small particle in nanometer range,  $D(v, 0.1) = 0.9 \mu\text{m}$  and high surface area, as high as 9.38  $\text{m}^2/\text{g}$ . The calculated surface area for monodisperse spheres with a similar particle diameter would be 1.04  $\text{m}^2/\text{g}$ . The much larger surface area for the powders in Table A.2 suggests that the particles were not uniform spheres but were aggregates composed of smaller primary particles. Therefore, the increase of surface area must be due to factors other than the

average particle size of the aggregates measured by light scattering. In addition, particles with smallest particles in the distribution contribute high surface area. In the dissolution rate experiments, not only was the surface area, 9.38 m<sup>2</sup>/g, higher for these particles, but this much larger surface area was accessible for wetting by the dissolution media given the hydrophilic surfactant coating on the particle surface.

Table A.2. Mean particle size D (v, 0.5), and particle size distribution of itraconazole in EPAS suspension formed with the conical nozzle; and surface area and potency of itraconazole in dried EPAS powder. Experimental conditions were the same as in Figure A.3.

EPAS itraconazole system	D (v, 0.5) (μm)	D (v,0.1), D(v,0.9) (μm)	Potency of itraconazole (% w/w)	Surface area (m <sup>2</sup> /g)
Bulk itraconazole	3.10	1.5, 6.6		5.13
PVP K-15	8.7	0.9, 55.4	78.9	9.38
PVP 40T	15.2	3.2, 39.5	72.5	3.28
Myrj 52	18.7	3.4, 48.0	68.8	3.17
Pluronic F127	10.6	4.2, 26.6	47.3	3.87



The average particle diameters were 10.6, 18.6 and 15.2  $\mu\text{m}$  for Pluronic F127, Myrj 52 and PVP 40T systems respectively. The dissolution rates for these systems, with larger particle sizes and surface areas, on the order of 3  $\text{m}^2/\text{g}$ , were significantly lower than for the PVP K-15 system. Even though these systems had larger particle size and lower surface areas compared to the bulk itraconazole,  $D(v, 0.9) = 3.1 \mu\text{m}$  and  $S = 5.13 \text{ m}^2/\text{g}$ , they still exhibited better dissolution profiles compared to the bulk API. Thus the increase in accessible surface area to the dissolution medium resulting from the hydrophilic surfactant coating on the particle surfaces was a key property that enhanced the dissolution rate. This correlation between the dissolution rate and the surface area was also observed for the earlier study with danazol.<sup>13</sup>

A significant fraction of the surfactant was free and not adsorbed; thus the potency increased markedly after removing the free surfactant for all systems investigated. The API-to-surfactant ratio for PVP K-15 was 9.3 times higher after centrifugation versus the fed amount with itraconazole potency increased from 28.6% to 78.9% after centrifugation. The observation of the highest dissolution rate for itraconazole coated with PVP K-15 is consistent with the higher surface area, smaller particle size. The higher surface area suggests that the surfactant adsorbed more quickly onto the growing itraconazole particles than for the other surfactants to retard particle growth. Relative to PVP 40 T, the diffusion rate of lower molecular weight PVP K-15 is faster, leading to faster adsorption kinetics. A higher level of adsorption for PVP K-15 versus PVP 40 T was confirmed explicitly in the EPAS study of danazol.<sup>13</sup>

Slower API dissolution for Pluronic F 127 was also observed for danazol and was attributed to a lower degree of adsorption reflecting slower adsorption dynamics. Fundamental studies indicate that slow adsorption dynamics for this type of block copolymer on solid surfaces results from rearrangements of the blocks on the surface.<sup>17</sup>

For PVP homopolymers, these rearrangements between two types of blocks are not needed leading to faster adsorption and thus faster release. Myrj 52 ( $\text{CH}_3(\text{CH}_2)_{16}(\text{OCH}_2\text{CH}_2)_{40}\text{OH}$ ) has a shorter PEO (40) chain than Pluronic F127 ( $\text{HO}(\text{CH}_2\text{CH}_2\text{O})_{98}(\text{CH}_2\text{C}(\text{CH}_3)\text{HO})_{67}(\text{CH}_2\text{CH}_2\text{O})_{98}\text{H}$ ). It is possible that this shorter PEO chain provided less satisfactory steric stabilization, leading to larger particle size.

The quality of each EPAS spray depends on the size (diameter) and geometry of the nozzle, and the physical properties of the dispersed and the continuous phases.<sup>18</sup> To investigate the effect of the geometry of the conical nozzle on the particle size, three conical nozzles were produced. After cutting the tubing, the tips were filed to produce different size cones. The pressure drops for the three nozzles to produce a flow rate of 1 ml/min were 4500, 3600 and 3000 psi. The mean particle size was similar in each case, in the range of 7.6-8.7  $\mu\text{m}$ . The variations in dissolution rate were within experimental error. Therefore, the slight difference in atomization for the three nozzles was not enough to influence the particle size and dissolution rate. In these experiments both the organic dispersed phase (2% w/v itraconazole, 3% w/v F127 in dichloromethane solvent) and the continuous phase (1% w/v PVP K-15 aqueous solution) were kept identical.

#### **A.3.2.3 Crystallinity**

Figure A.4, illustrates the X-ray diffraction profiles of itraconazole contained in the dry powders. The crystalline peak positions were the same as for the bulk itraconazole. The  $\alpha$ -peak heights of itraconazole in different surfactant systems at  $2\theta = 20.5^\circ$  are also listed in Figure A.4. The crystallinity was found to be similar to that of the bulk itraconazole after correction for the presence of the surfactants in the dry powder. It was assumed that the itraconazole peak height was linear in concentration for a fixed weight. Thus enhanced dissolution rates may be achieved with high surface area crystalline particles.

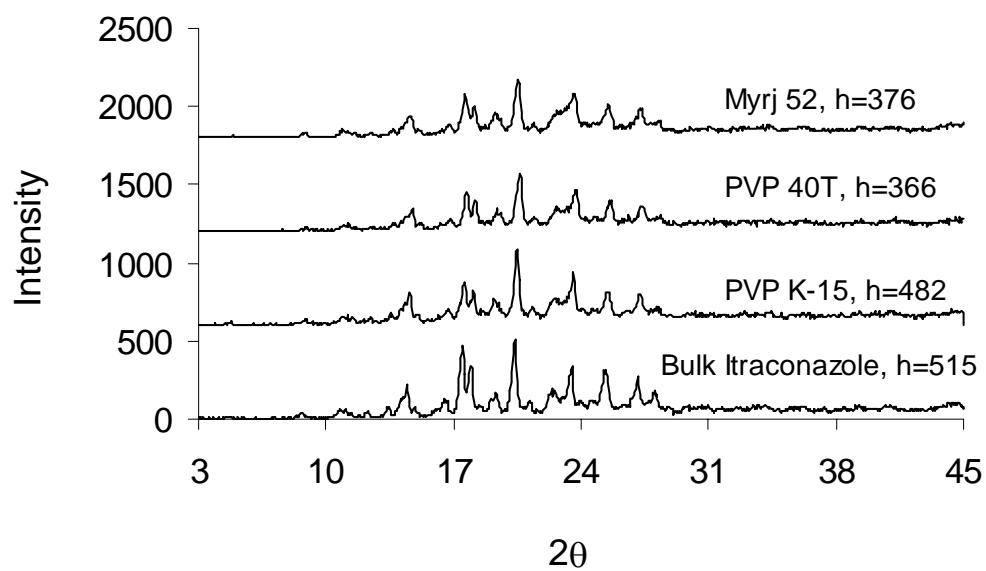


Figure A.4. X-ray diffraction pattern and  $\alpha$  peak height,  $h$ , at  $2\theta = 20.5^\circ$  of dried EAPS itraconazole powders produced with the conical nozzle.

#### **A.4 CONCLUSIONS**

EPAS followed by removal of free surfactant produced high surface area particles with high potencies up to 79% and rapid dissolution rates. A significant fraction of the surfactant was free and not adsorbed; thus the potency increased markedly after removing the free surfactant. The hydrophilic segment of the surfactant stabilizes the aqueous dispersions formed in the EPAS sprays. This segment extends outwards from the particle surface and facilitates wetting and thus high dissolution rates. In essence, the EPAS process orients the surfactant in an optimal architecture for subsequent high dissolution rates in aqueous media. The dissolution rate was highest for PVP K-15 as the surfactant in the aqueous phase, 90% dissolved in 10 minutes, consistent with the highest surface area for this system. The surface areas reached 9.38 m<sup>2</sup>/g despite the high potencies and thus the relatively small amounts of adsorbed surfactant. The high dissolution rates and high potencies are desirable for the goal of achieving high bioavailabilities of poorly water soluble drugs.

## A.5 REFERENCES

- (1) Peeters, J.; Neeskens, P.; Tollenaere, J. P.; Van Remoortere, P.; Brewster, M. E. *Journal of Pharmaceutical Sciences* 2002, 91, 1414-1422.
- (2) Reddy, R. K.; Khalil, S. A.; Gonda, M. W. *J Pharm Sci* 1976, 65, 115-118.
- (3) Brown, S.; Rowley, G.; Pearson, J. T. *Int J Pharm* 1998, 165, 227-237.
- (4) Rowley, G.; Pearson, J. T.; Hussian, M. S.; Hartup, D. E.; Jones, B. E. *J Pharm Pharmacol* 1985b, 37, 112P.
- (5) Pace, S. N.; Pace, G. W.; Parikh, I.; Mishra, A. K. *Pharm Technol* 1999, 23, 116-134.
- (6) Jung, J. Y.; Yoo, S. D.; Lee, S. H.; Kim, D. S. Y.; Lee, K. H. *Int J Pharm* 1999, 187, 209-218.
- (7) Rubinstein, M. H.; Gould, P. *Drug Dev. Ind. Pharm.* 1987, 13, 81-92.
- (8) Byers, J. E.; Peck, G. E. *Drug Dev. Ind. Pharm.* 1990, 16, 1761-1779.
- (9) Illig, K. J.; Mueller, R. L.; Ostrander, K. D.; Swanson, J. R. *Pharm Technol* 1996, 20, 78-88.
- (10) Aiache, J. M.; Beyssac, E. *Powder as dosage forms*; Marcel Dekker: New York, 1994.
- (11) Dixon, D. J.; Johnston, K. P.; Bodmeier, R. A. *AIChE Journal* 1993, 39, 127-139.
- (12) Rogers, T. L.; Johnston, K. P.; Williams, R. O. *Drug Development and Industrial Pharmacy* 2001 Nov, 27, 1003-1015.
- (13) Chen, X.; Williams, R. O.; Johnston, K. P. *J. Pharm. Sci.* 2004, 93, 1867-1878.
- (14) Chen, X.; Young, T. J.; Sarkari, M.; Williams, R. O.; Johnston, K. P. *Int J Pharm* 2002, 242, 3-14.
- (15) Sarkari, M.; Brown, J.; Chen, X.; Swinnea, S.; Williams, R. O.; Johnston, K. P. *Int J Pharm* 2002, 243, 17-31.
- (16) Young, T. J.; Mawson, S. M.; Johnston, K. P. *Biotechnol Prog* 2000, 16, 402-407.
- (17) Tripp, C. P.; Hair, M. L. *Langmuir* 1996, 12, 3952-3956.
- (18) Lefebvre, A. H. *Atomization and Sprays*; Taylor&Francis, 1989.

## Bibliography

- (1) *Federal Register: International Committee on Harmonization, Quality Guidance Q3C*, 1997.
- (2) *The Merck Index: an encyclopedia of chemicals, drugs, and biologicals*; Merck & CO., Inc.: Rahway, 1996.
- (3) *Pharmaceutical practice*; Churchill Livingstone: New York, 1990.
- (4) *Electronic orange book: approved drug products with therapeutic equivalence evaluations.*; U.S. Dept. of Health and Human Services, Public Health Service, Food and Drug Administration, Center for Drug Evaluation and Research, Office of Information Technology, Division of Data Management and Services.: Rockville, Md.
- (5) Aiache, J. M.; Beyssac, E. *Powder as dosage forms*; Marcel Dekker: New York, 1994.
- (6) Alessi, P.; Cortesi, A.; Kikic, I.; Foster, N. R.; Macnaughton, S. J.; Colombo, I. *Ind. Eng. Chem. Res.* **1996**, 35, 4718-4726.
- (7) Amidon, G. L.; Lennernäs, H.; Shah, V. P.; Crison, J. R. *Pharm. Res* **1995**, 12, 413-420.
- (8) Ansel, H. C.; Allen, L. V.; Popovich, N. G. *Pharmaceutical dosage forms and drug delivery systems*, 7th ed. ed.; Lippincott-Williams & Wilkins: Philadelphia, PA, 1999.
- (9) Arias, M. J.; Gines, J. M.; Moyano, J. R.; Perez-Martinez, J. I.; Rabasco, A. M. *Int J Pharm* **1995**, 123, 25-31.
- (10) Bahadur, P.; Li, P.; Almgren, M.; Brown, W. *Langmuir* **1992**, 8, 1903-1907.
- (11) Bahadur, P.; Pandya, K.; Almgren, M.; Li, P.; Stilbs, P. *Colloid and Polymer Science* **1993**, 271, 657-667.
- (12) Bakatselou, V.; Oppenheim, R. C.; Dressman, J. B. *Pharm Res* **1991**, 8, 1461-1469.
- (13) Blankschtein, D.; Thurston, G. M.; Benedek, G. B. *J. Chem. Phys.* **1986**, 85, 7268-7288.
- (14) Bodmeier, R.; Chen, H. *Journal of Controlled Release* **1990**, 12, 223-233.

- (15) Broadhead, J.; Rouan, S. K. E.; Rhodes, C. T. *Drug Dev. Ind. Pharm.* **1992**, 18, 1169-1206.
- (16) Brown, S.; Rowley, G.; Pearson, J. T. *Int J Pharm* **1998**, 165, 227-237.
- (17) Brown, W.; Schillen, K.; Almgren, M. *Journal of physical chemistry* **1991**, 95, 1850-1858.
- (18) Byers, J. E.; Peck, G. E. *Drug Dev. Ind. Pharm.* **1990**, 16, 1761-1779.
- (19) Cathrein, E.; Stein, H.; Stoller, H. J.; Viardot, K.: EP, 1991.
- (20) Cevc, G. *Advanced Drug Delivery Reviews* **2004**, 56, 675-711.
- (21) Chattopadhyay, P.; Gupta, R. B. *Ind. Eng. Chem. Res.* **2001**, 40, 3530-3539.
- (22) Chen, X. *Drug. Del. Sci. Techn.* **to appear**.
- (23) Chen, X.; Lo, C. Y.; Sarkari, M.; Williams, R. O.; Johnston, K. P. **In preparation**.
- (24) Chen, X.; Vaughn, J. M.; Yacaman, M. J.; Williams, R. O.; Johnston, K. P. *J. Pharm. Sci.* **2004**, 93, 1867-1878.
- (25) Chen, X.; Young, T. J.; Sarkari, M.; Williams, R. O.; Johnston, K. P. *Int J Pharm* **2002**, 242, 3-14.
- (26) Choudhury, S.; Nelson, K. F. *Int J Pharm* **1992**, 85, 175-180.
- (27) Chowhan, Z. T. *Journal of Pharmaceutical Science* **1978**, 67, 1257-1260.
- (28) Cohn, D.; Sosnik, A.; Levy, A. *Biomaterials* **2003**, 24, 3707-3714.
- (29) Couvreur, P.; Puisieux, F. *Advanced Drug Delivery Reviews* **1993**, 10, 141-162.
- (30) Cussler, E. L. *Diffusion, Mass transfer in fluid systems*; Cambridge University Press: NY, 1986.
- (31) de Bruijn, V. G.; van den Broeke, J. P.; Leermakers, F. A. M.; Keurentjes, J. T. F. *Langmuir* **2002**, 18, 10467-10474.
- (32) De Gennes, P. G. *Adv Colloid Interface Sci* **1987**, 27, 189-209.
- (33) Dijt, J. C.; Cohen, S. M. A.; Hofman, J. E.; Fleer, G. J. *Colloids and Surfaces* **1990**, 51, 141-158.
- (34) Dixon, D. J.; Johnston, K. P.; Bodmeier, R. A. *AIChE Journal* **1993**, 39, 127-139.

- (35) Elder, E. J.; Hitt, J. E.; Rogers, T. L.; Tucker, C. J.; Saghir, S.; Svenson, S.; Evans, J. C. *Polymeric Materials Science and Engineering* **2003**, 89, 741.
- (36) Esumi, K.; Iitaka, M.; Torigoe, K. *Journal of Colloid and Interface Science* **2002**, 232, 71-75.
- (37) Fagerholm, U.; Borgstrom, L.; Ahrenstedt, O.; Lennernas, H. J. *Drug Targeting* **1995**, 3, 191-200.
- (38) Fuller, M. A.; Sajatovic, M. *Drug information handbook for psychiatry* 1999-2000; Lexi-Comp: Hudson, OH, 1999.
- (39) Ghaderi, R.; Artursson, P.; Carlfors, J. *Pharm. Res.* **1999**, 16, 676-681.
- (40) Gilbert, J. C.; Hadgraft, J.; Bye, A.; Brookes, L. G. *International Journal of Pharmaceutics* **1986**, 32, 223-228.
- (41) Grant, D. J.; Higuchi, T. *Solubility behavior of organic compounds*; New York: Wiley, 1990.
- (42) Gref, R.; Quellec, P.; Sanchez, A.; Calvo, P.; Dellacherie, E.; Alonso, M. J. *European Journal of Pharmaceutical and Biopharmaceutics* **2001**, 51, 111-118.
- (43) Güner, A.; Ataman, M. *Colloid & Polymer Science* **1994**, 272, 175-180.
- (44) Guven, O.; Eltan, E. *Makromolekulare Chemie* **1981**, 11, 3129-3134.
- (45) Hocking, M. B.; Klimchuk, K. A.; Lowen, S. *Journal of Macromolecular Science: Polymer Reviews* **1999**, 39, 177-203.
- (46) Horn, D.; Rieger, J. *Angew. Chem. Int. Ed.* **2001**, 40, 4330-4361.
- (47) Hu, J.; Johnston, K. P.; Williams, R. O. *European Journal of Pharmaceutical Sciences* **2003**, 20, 295-303.
- (48) Hu, J.; Johnston, K. P.; Williams, R. O. *Polymeric Materials: Science & Engineering* **2003**, 89, 743.
- (49) Hu, J.; Johnston, K. P.; Williams, R. O. *International journal of pharmaceutics* **2004**, 271, 145-154.
- (50) Hu, J.; Roger, T. L.; Brown, J.; Young, T. J.; Johnston, K. P.; Williams, R. O. *Pharmaceutical Research* **2002**, 19, 1278-1284.
- (51) Illig, K. J.; Mueller, R. L.; Ostrander, K. D.; Swanson, J. R. *Pharm Technol* **1996**, 20, 78-88.



- (52) Johnson, B. K., Princeton, 2003.
- (53) Johnson, B. K.; Prud'homme, R. K. *Polymeric Materials: Science & Engineering* **2003**, 89, 744-745.
- (54) Jung, J. Y.; Yoo, S. D.; Lee, S. H.; Kim, D. S. Y.; Lee, K. H. *Int J Pharm* **1999**, 187, 209-218.
- (55) Khoultaev, K. K. H.; Kerekes, R. J.; Englezos, P. *The Canadian Journal of Chemical Engineering* **1997**, 75, 161-166.
- (56) Khoultaev, K. K. H.; Kerekes, R. J.; Englezos, P. *AIChE Journal* **1997**, 43, 2353-2358.
- (57) Kushida, I.; Ichikawa, M.; Asakawa, N. *J Pharm Sci* **2002**, 91, 258-266.
- (58) Labhasetwar, V.; Song, C.; Humphrey, W.; Shebuski, R.; Levy, R. J. *Journal of Pharmaceutical Science* **1998**, 97, 1229-1234.
- (59) Laibinis, P. E.; Whitesides, G. M. *J Am Chem Soc* **1992**, 114, 1900-1905.
- (60) Lee, E. J.; Lee, S. W.; Choi, H. G.; Kim, C. K. *Int J Pharm* **2001**, 218, 125-131.
- (61) Lefebvre, A. H. *Atomization and Sprays*; Taylor&Francis, 1989.
- (62) Lengsfeld, C. S.; Delphanque, J. P.; Barocas, V. H.; Randolph, T. W. B. *J. Phys. Chem.* **2000**, 104, 2725-2735.
- (63) Lennernäs, H.; Ahrenstedt, O.; Hallgren, R.; Knutson, L.; Ryde, M.; Paalzow, L. K. *Pharm. Res* **1992**, 9, 1243-1255.
- (64) Lennernas, H.; Ahrenstedt, O.; Ungell, A. L. *Br. J.Clin. Pharmacol.* **1994**, 37, 589-596.
- (65) Lennernas, H.; Nilsson, D.; Aquilonius, S. M.; Ahrenstedt, O.; Knutson, L.; Paalzow, L. K. *Br. J.Clin. Pharmacol.* **1993**, 35, 243-250.
- (66) Lipinski, C. *Am.Pharm. Rev.* **2002**, 5, 82-85.
- (67) Liversidge, G., G.; Cundy, K. C. *Int J Pharm* **1995**, 125, 91-97.
- (68) Liversidge, G. G.; Cundy, K. C.; Bishop, J. F.; Czekai, D. A.: U. S., 1991.
- (69) Lyklema, J. *Fundamentals of interface and colloid science, Vol II: solid-liquid interfaces.*; New York: Academic Press, 1991.
- (70) Malmsten, M.; Lindman, B. *Macromolecules* **1993**, 26, 1282-1286.

- (71) Malmsten, M.; Lindman, B. *Macromolecules* **1992**, 25, 5440-5446.
- (72) Margarit, M. V.; Rodriguez, I. C.; Cerezo, A. *Int J Pharm* **1994**, 108, 101-107.
- (73) Martin, A. N. *Physical pharmacy: physical chemical principles in the pharmaceutical sciences*, 4th ed.; Lea & Febiger: Philadelphia, 1993.
- (74) Masters, K. *Spray Drying Handbook*, 3rd ed.; New York: John Wiley and Sons, 1979.
- (75) Mawson, S.; Yates, M. Z.; O'Neill, M. L.; Johnston, K. P. *Langmuir* **1997**, 13, 1519-1528.
- (76) Miyazaki, S.; Tobiyama, T.; Takada, M.; Attwood, D. *Journal of pharmacy and pharmacology* **1995**, 47, 455-457.
- (77) Mortensen, K.; Brown, W.; Norden, B. *Physical Review Letters* **1992**, 68, 2340-2343.
- (78) Müller, R. H.; Benita, S.; Böhm, B. *Emulsion and nanosuspensions for the formulation of poorly soluble drugs*; Medpharm: Stuttgart, 1998.
- (79) Na, G. C.; Yuan, B. O.; Stevens, H. J.; Weekley, B. S.; Rajagopalan, N. *Pharm Res* **1999**, 16, 562-568.
- (80) Napper, D. H. *Polymeric stabilization of colloidal dispersions*; Academic Press: New York, 1983.
- (81) Oh, D.; Curl, R. L.; Amidon, G. L. *Pharm Res* **1993**, 10, 264-270.
- (82) Paavola, A.; Yliruusi, J.; Rosenberg, P. *Journal of Controlled Release* **1998**, 52, 169-178.
- (83) Pace, S. N.; Pace, G. W.; Parikh, I.; Mishra, A. K. *Pharm Technol* **1999**, 23, 116-134.
- (84) Palakodaty, S.; York, P. *Pharm. Res.* **1999**, 16, 976-985.
- (85) Pandit, N.; Trygstad, T.; Croy, S.; Bohorquez, M.; Koch, C. *Journal of Colloid and Interface Science* **2000**, 222, 213-220.
- (86) Pang, P.; Englezos, P. *Fluid Phase Equilibria* **2002**, 194-197, 1059-1066.
- (87) Pang, P.; Englezos, P. *Colloids and Surfaces A: Physicochemical and Engineering Aspects* **2002**, 204, 23-30.

- (88) Peeters, J.; Neeskens, P.; Tollenaere, J. P.; Van Remoortere, P.; Brewster, M. E. *Journal of Pharmaceutical Sciences* **2002**, 91, 1414-1422.
- (89) Pelton, R. H. *Journal of Polymer Science, Part A: Polymer Chemistry* **1988**, 26, 9-18.
- (90) Peracchia, M. T.; Vauthier, C.; Desmaele, D.; Gulik, A.; Dedieu, J. C.; Demoy, M.; d'Angelo, J.; Couvreur, P. *Pharm. Res* **1998**, 15, 550-556.
- (91) Peters, D. *Journal of Materials Chemistry* **1996**, 6, 1605-1618.
- (92) Pleštil, J.; al., e. *Macromol. Chem. Phys.* **2001**, 202, 553-563.
- (93) Pozarnsky, G. A.; Matjevic, E. *Colloids Surf. A Physico. Chem. Eng. Asp.* **1997**, 125, 47-52.
- (94) Radtke, M. *New drugs* **2001**, 3, 62-68.
- (95) Randolph, T. W.; Randolph, A. D.; Mebes, M.; Yeung, S. *Biotechnology Progress* **1993**, 9, 429-435.
- (96) Rasenack, N.; Muller, B. W. *Pharm Res* **2002**, 19, 1894-1900.
- (97) Rasenack, N.; Müller, B. W. *Pharmaceutical Development and Technology* **2004**, 9, 1-13.
- (98) Reddy, R. K.; Khalil, S. A.; Gonda, M. W. *J Pharm Sci* **1976**, 65, 115-118.
- (99) Reverchon, E. J. *Supercritical Fluids* **1999**, 15, 1-21.
- (100) Rogers, T. L.; Nelsen, A. C.; Sarkari, M.; Young, T. J.; Johnston, K. P.; Williams, R. O. *Pharmaceutical Research* **2003**, 20, 485-493.
- (101) Rogers, T. L.; Hu, J.; Yu, Z.; Johnston, K. P.; Williams, R. O. *International Journal of Pharmaceutics* **2002**, 242, 93-100.
- (102) Rogers, T. L.; Johnston, K. P.; Williams, R. O. *Pharmaceutical Development and Technology* **2003**, 8, 187-197.
- (103) Rogers, T. L.; Johnston, K. P.; Williams, R. O. *Drug Development and Industrial Pharmacy* **2001 Nov**, 27, 1003-1015.
- (104) Rogers, T. L.; Nelsen, A. C.; Hu, J.; Brown, J. N.; Sarkari, M.; Young, T. J.; Johnston, K. P.; Williams, R. O. *European Journal of Pharmaceutics and Biopharmaceutics* **2002**, 54, 271-280.

- (105) Rogers, T. L.; Overhoff, K. A.; Shah, P.; Santiago, P.; Yacaman, M. J.; Johnston, K. P.; Williams, R. O. *European Journal of Pharmaceutics and Biopharmaceutics* **2003**, 55, 161-172.
- (106) Rowley, G.; Pearson, J. T.; Hussian, M. S.; Hartup, D. E.; Jones, B. E. *J Pharm Pharmacol* **1985b**, 37, 112P.
- (107) Rubinstein, M. H.; Gould, P. *Drug Dev. Ind. Pharm.* **1987**, 13, 81-92.
- (108) Ruch, F.; E., M. *Journal of Colloid and Interface Science* **2000**, 229, 207-211.
- (109) Salamova, U. U.; Rzaev, Z. M. O. *Polymer* **1996**, 37, 2415-2421.
- (110) Sarkari, M.; Brown, J.; Chen, X.; Swinnea, S.; Williams, R. O.; Johnston, K. P. *Int J Pharm* **2002**, 243, 17-31.
- (111) Sekikawa, H.; Hori, R.; Arita, T.; Ito, K.; Nakano, M. *Chem. Pharm. Bull.* **1978**, 26, 2489-2496.
- (112) Shama, J. O.; Zhang, Y.; Finlay, W. H.; Roaa, W. H.; Lobenberg, R. *International Journal of Pharmaceutics* **2004**, 269, 457-467.
- (113) Sjöström, B.; Bergenstöhl, B.; Lindberg, M.; Rasmuson, A. C. *J. Dispersion Science and Technology* **1994**, 15, 89-117.
- (114) Subramaniam, B.; Rajewski, R. A.; Snavely, K. *J. Pharm. Sci.* **1997**, 86, 885-890.
- (115) Thiering, R.; Dehghani, F.; Dillow, A.; Foster, N. R. *J. Chem. Technol. Biotechnol.* **2000**, 75, 42-53.
- (116) Torchilin, V. P. *J Controlled Release* **2001**, 73, 137-172.
- (117) Tripp, C. P.; Hair, M. L. *Langmuir* **1996**, 12, 3952-3956.
- (118) Turker, L.; Guner, A.; Yigit, F.; Guven, O. *Colloid and Polymer Science* **1990**, 268, 337-344.
- (119) Uekama, K.; Ikegami, K.; Wang, Z.; Horiuchi, Y.; Hirayama, F. *J Pharm Pharmacol* **1992**, 44, 73-78.
- (120) Wanka, G.; Hoffmann, H.; Ulbricht, W. *Colloid polymer science* **1990**, 268, 101-117.
- (121) Wei, G.; Xu, H.; Ding, P. T.; Li, S. M.; Zheng, J. M. *Journal of controlled release* **2002**, 83, 65-74.

- (122) Wingrave, J. A. *Oxide Surfaces*; Marcel Dekker: New York, 2001.
- (123) Yaws, C. L. *Chemical properties handbook: physical, thermodynamic, environmental, transport, safety, and health related properties for organic and inorganic chemicals*; New York : McGraw-Hill, 1999.
- (124) Yeo, S. D.; Lim, G. B.; Debenedetti, P. G.; Bernstein, H. *Biotechnology and Bioengineering* **1993**, 41, 341-346.
- (125) Young, T. J.; Johnston, K. P.; Pace, G. W.; Mishra, A. K. *AAPS PharmSciTech* **2004**, 5.
- (126) Young, T. J.; Mawson, S. M.; Johnston, K. P. *Biotechnol Prog* **2000**, 16, 402-407.
- (127) Zhang, X.; Burt, H. M.; Mangold, G.; Dexter, D.; VonHoff, D.; Mayer, L.; Hunter, W. L. *Anticancer Drug* **1997**, 8, 696-701.

## **Vita**

Xiaoxia Chen was born on November 20, 1974 in Dingbian County, Shaanxi Province, China to Zhiyi Chen and Jinfang Gao. She graduated from Dingbian High School, Shaanxi Province in 1991 and entered Tsinghua University in Beijing, China. She graduated in Chemical Engineering in June 1996. She then enrolled in the graduate program at Tsinghua University, and received her M.S. in Biochemical Engineering in June 1999. She then entered the University of Texas at Austin in August 1999, and received her Ph.D in Chemical Engineering in July 2004.

Permanent address: 1634 West 6<sup>th</sup> Street, Apt. A, TX 78703

This dissertation was typed by the author.